République Algérienne Démocratique et Populaire
Ministère de l'Enseignement Supérieur et de la Recherche Scientifique
Université A.MIRA-BEJAIA

Faculté des Sciences Exactes
Département Physique

Laboratoire de Physique Théorique.

THÈSE

EN VUE DE L'OBTENTION DU DIPLÔME DE DOCTORAT

Domaine : Science de la matière Filière : Physique

Spécialité : Physique Théorique

Présentée par
GUEBOUDJI Ahmed

Thème

Multi-messenger astrophysics for optimal exploitation of future gravitational wave observatories

Soutenue le : 09/12/2023 **Devant le Jury composé de :**

Nom et Prénom	**Grade**		
Mr GHARBI AbdeLhakim	**Professeur**	Univ. de Bejaia	Président
Mr AOUDIA Sofiane	**MCA**	Univ. de Bejaia	Rapporteur
Mr HAOUAT Salah	**Professeur**	Univ. de Jijel	Examinateur
Mme OULEBSIR Nadia	**MCA**	Univ. de Bejaia	Examinateur
Mr BELABBAS Abdelmoumene	**MCA**	Univ. de Bejaia	Examinateur

2023/2024

Contents

List of Figures

List of Tables

Acknowledgments

I would like to express my deep gratitude to my thesis supervisor, Professor Aoudia Sofiane, for his exceptional guidance, unwavering support, and invaluable insights throughout my research journey. His extensive knowledge and expertise in the field of theoretical physics have been instrumental in shaping the direction and focus of my research, and I am truly fortunate to have had the opportunity to work under his supervision.

I would also like to extend my heartfelt thanks to the members of my thesis committee, Mr GHARBI Abdehakim , Mr HAOUAT Salah, M OULEBSIR Nadia, and Mr BELABBAS Abdelmoumene, for their invaluable feedback and constructive criticism, which have significantly improved the quality of my research. Their diverse perspectives and expertise have been essential in broadening my understanding of the subject matter and refining my research methodology.

Moreover, I would like to express my appreciation to all the faculty members of the Laboratory of Theoretical Physics (Laboratoire de Physique Théorique LPT) for their support, encouragement, and unwavering commitment to academic excellence. The research environment at LPT has been conducive to my intellectual growth and development, and I have learned so much from the inspiring scholars and researchers in this esteemed institution.

Lastly, I extend heartfelt thanks to my family, friends, and colleagues for their unwavering support during this challenging yet rewarding journey. Special gratitude to my wife and the anticipation of welcoming our coming son OMAR, their love and encouragement have been invaluable sources of inspiration.

In conclusion, I would like to express my heartfelt appreciation to everyone who has contributed to my academic and personal growth. Your support and encouragement have been invaluable, and I am deeply grateful for everything you have done for me.

Abstract

This thesis provides a comprehensive overview of the field of gravitational waves and multi-messenger astrophysics, with an emphasis on optimizing telescope networks for detecting transient events. The history of gravitational wave research, sources of gravitational waves, and observatories used to detect them, such as LIGO and Virgo, are discussed. Multi-messenger astrophysics is introduced as a means to combine observations from different messengers to gain a more complete understanding of astrophysical phenomena. The National Aures Observatory and its RAMSES project are presented as an example of a telescope network aimed at detecting and localizing transient events. An assignment problem solution is introduced using the branch and bound method to optimize the observatory's telescope network. Finally, simulations exploring the efficiency of telescopes, the effect of the area surveyed on the number of telescopes required, and a strategy for determining the number of telescopes needed for observation are discussed.

Key-words multi-messenger, gravitational waves, Gamma Ray Bursts, RAMSES Project, National Aures Observatory, Branch and bound Method, TAROT Telescope.

Résumé

Cette thèse offre une vue d'ensemble complète du domaine des ondes gravitationnelles et de l'astrophysique multi-messagers, avec un accent sur l'optimisation des réseaux de télescopes pour la détection d'événements transitoires. L'histoire de la recherche sur les ondes gravitationnelles, les sources d'ondes gravitationnelles et les observatoires utilisés pour les détecter, tels que LIGO et Virgo, sont discutés. L'astrophysique multi-messagers est présentée comme un moyen de combiner les observations de différents messagers pour mieux comprendre les phénomènes astrophysiques. L'Observatoire National des Aurès et son projet RAMSES sont présentés comme exemple de réseau de télescopes visant à détecter et à localiser des événements transitoires. Une solution de problème d'assignation est introduite en utilisant la méthode de branchement et de bornes pour optimiser le réseau de télescopes de l'observatoire. Enfin, des simulations explorant l'efficacité des télescopes, l'effet de la zone analysée sur le nombre de télescopes requis, et une stratégie pour déterminer le nombre de télescopes nécessaires pour l'observation sont discutées.

Mots-clés multi-messager , ondes gravitationnelles, Sursauts Gamma, Projet RAMSES, Observatoire National des Aurès, Méthode Branch and Bound, Télescope TAROT.

Chapter 1

Introduction

From the earliest times, astronomy has always played a large part in the history of mankind. In addition to the contemplative point of view (who has never marveled at the beauty of the celestial vault on a summer night?), the study of the stars and their movement has a lot to do with the advancement of civilizations. We know for example that the Egyptian civilization of the time of the pharaohs had its own denomination of the constellations. A little later, the Greeks were the first to try to understand the mechanisms that govern the movement of the stars and the Sun. The latter was by its proximity the most studied, and became the pillar of the Mayan or Inca civilizations, peoples for whom the importance of astronomy has been confirmed by archaeological research. ecological. If astronomy has nowadays become a science far from the daily life of the majority of people, it has not always been so. For example, an excellent knowledge of the celestial vault was necessary for sailors of yesteryear to be able to navigate the open sea, which they managed to do brilliantly, long before the advent of GPS. Much of the knowledge that seems obvious to us today has been acquired by astronomy. The calendar is based on the time of revolution of the Earth around the Sun. And what about the first five days of the week whose etymology comes from the names of the stars of the solar system in Latin

The eye, even if it was for a long time the first instrument used to admire and understand the stars, very quickly found itself limited in observing the infinitely far. Galileo was the first to build an instrument in the 15th century to "see from afar", which he called a telescope. Parallel to this, the development of mathematics and physics led to other sensational discoveries, the culmination of which in the astronomy of the solar system is certainly the discovery of Neptune in 1846 by Galle. From then on, astronomical advances closely followed technological developments, mathematical theories, and discoveries in physics.

Spectacles and telescopes became the favored tools of astronomers, and made it possible to confirm through observations the great theories, such as Einstein's general relativity by the eclipse of the Sun. of 1916, but also to discover new ones, such as the recession of the galaxies by Hubble in 1929. But humanity did not stop there. In his thirst for knowledge he developed means to observe the sky other than by the only photons visible to the eye. The astronomy of other wavelengths began with radio astronomy in the 1960s, which among other things allowed the confirmation of the hypothesis of the expansion of the Universe, also known as the "Big Bang", by the detection of the cosmic radiation background at 3 K. Observations at other wavelengths were more problematic; Indeed, with the terrestrial atmosphere being opaque to a large part of the radiation, it was necessary to find the means to overcome it. Astronomers then began to send balloons equipped with instruments and detectors to a very high altitude (40 km), then came the turn of rockets, and finally satellites, allowing long-term observations. These beginnings were the beginning of infrared, ultraviolet, X, γ, and gravitational wave (GW) astronomy, which is the basis of my subject.

Thanks to satellites equipped with γ photon detectors, a new type of astrophysical phenomenon were discovered at the end of the 1960s, namely gamma-ray bursts. Gamma-ray bursts are very brief and intense flashes of very high-energy photons, ranging from kilo-electron Volt (keV) to Mega-electron Volt (MeV). These events are the most violent in the Universe after the Big Bang, with total energy emitted that can wait (10^{46} J) for a few seconds to a few minutes. Their frequency is about 2 per day in the whole sky. It is impossible to predict a gamma-ray burst, both temporally and spatially. The many bursts detected by the BATSE instrument in the 1990s showed on the one hand the existence of two types of bursts, long bursts whose durations extend from a few seconds to a few minutes, and short bursts, with much shorter durations, less than a second, and on the other hand the isotropic distribution of the bursts in the sky, the first indication of their cosmological origin. A gamma-ray burst is very often followed by a delayed emission in the other wavelengths, which is called afterglow. These afterglows were observed for the first time thanks to the precise and rapid localization of the burst of February 28, 1997, by the Beppo-SAX satellite, which led to the detection of a rapidly decreasing source X over time. While gravitational waves can be produced with a gamma-ray burst, especially a short gamma-ray burst (the most likely source)

Gravitational waves were first predicted by Albert Einstein's theory of general relativity over a century ago, in 1916. However, it took decades for the technology to catch up with the theory. The first attempts to directly detect gravitational waves were made in the 1960s, but they were unsuccessful.

It wasn't until 2015, when the Laser Interferometer Gravitational-Wave Observatory (LIGO) detected the first gravitational wave signal from the collision of two black holes, that the existence of these ripples in the fabric of space-time was finally confirmed. This detection marked the beginning of a new era in astrophysics, allowing scientists to study the universe in a way that was not possible before.

The discovery of gravitational waves was the culmination of years of research and development. LIGO itself was a massive undertaking, involving hundreds of scientists and engineers from around the world. The observatory consists of two facilities, one in Livingston, Louisiana, and one in Hanford, Washington, separated by 3000 km. Each facility has two perpendicular arms, each 4 km long, with lasers bouncing back and forth between mirrors to detect any changes in the length of the arms caused by passing gravitational waves. The detection of gravitational waves by LIGO and Virgo in 2015 ushered in a new era of astronomy, as the first direct detection of gravitational waves allowed for the study of astrophysical phenomena through a new messenger, leading to the development of multi-messenger astrophysics. Multi-messenger astrophysics is an exciting and rapidly developing field that has the potential to revolutionize our understanding of the universe. By combining observations from different messengers such as gravitational waves, electromagnetic radiation, neutrinos, and cosmic rays, scientists can study astrophysical phenomena in a more complete and detailed way than ever before.

For example, the detection of gravitational waves from merging black holes and neutron stars GW170817 by LIGO and Virgo has been followed by the detection of electromagnetic radiation GRB170817 from the same sources by various telescopes, allowing for a more comprehensive study of the events. This has led to breakthrough discoveries, such as the observation of the first kilonova associated with a neutron star merger, which was detected in both gravitational waves and electromagnetic radiation.

In addition to gravitational waves and electromagnetic radiation, neutrinos, and cosmic rays can also provide valuable information about astrophysical phenomena. Neutrinos are nearly mass-less particles that can travel through vast amounts of matter without being absorbed, allowing them to carry information from the most extreme and dense environments in the universe. Cosmic rays, on the other hand, are high-energy particles that can provide information about the acceleration mechanisms and magnetic fields in astrophysical sources.

The study of multi-messenger astrophysics requires the collaboration of scientists across different disciplines and the use of a variety of instruments and detectors. In recent years, there has been an increasing emphasis on building networks of observatories that can detect multiple messengers from the same astrophysical events. These networks, such as the Gamma-

ray Coordinates Network (GCN), provide real-time alerts of potential multi-messenger events, allowing for rapid follow-up observations and analysis.

Overall, multi-messenger astrophysics is an exciting and rapidly developing field that promises to provide new insights into the workings of the universe. By combining observations from different messengers, scientists can gain a more complete understanding of astrophysical phenomena and uncover new and unexpected discoveries. In this thesis, we explore the field of gravitational waves and their sources. We discuss the history of gravitational wave research, the various sources of gravitational waves, and the observatories used to detect them, such as LIGO and Virgo. We also delve into the exciting field of multi-messenger astrophysics, which combines multiple types of observations, such as gravitational waves, electromagnetic radiation, and neutrinos, to gain a deeper understanding of astrophysical phenomena.

Furthermore, we introduce the National Aures Observatory and its RAMSES project, which aims to detect and localize transient events, such as gamma-ray bursts and supernovae, using a network of telescopes. We also present an assignment problem solution using the branch and bound method to optimize the observatory's telescope network.

Finally, we discuss the results of our simulations, exploring the efficiency of telescopes, the effect of the area surveyed on the number of telescopes required, and building a strategy to determine the number of telescopes needed for observation after knowing the area to be surveyed.

Overall, this thesis presents a comprehensive overview of gravitational waves and multi-messenger astrophysics, with a focus on optimizing telescope networks to detect transient events.

Chapter 2

Gravitational Waves

2.1 History of GW

The notion of gravitational waves appears in the scientific literature as early as 1900 with Lorentz who imagines a gravitational field to propagate[1], Later, in 1905, Poincaré introduced the concept "gravity wave"[2]Although he defines waves that do not carry energy, his concept already conveys the idea that these waves travel at the speed of light.

It was not until 1916 that Einstein theoretically predicted the existence of gravitational waves by presenting them as solutions of his equations[3], To reach this conclusion, Einstein considers a perturbation of a flat space-time, thus linearizing his equations.

It was not until the 1950s that the physical nature of gravitational waves was established. Pirani shows the relationship between the Riemann tensor and the strain of the metric[4]. Considerations on the perturbation of a flat space-time become a special case of gravitational wave theory. Unlike other aspects of general relativity, the experimental validation of Einstein's predictions about the existence of gravitational waves took many years. We will see that the binary pulsar PSR1913 + 16 provided indirect evidence for the existence of gravitational radiation. But it wasn't until 100 years after Einstein's work that the first direct detection of gravitational waves was made in LIGO detector data in 2015, putting an end to all controversies over their existence for good.[5]

2.2 Weak field approximation

If we assume a weak field, that is to say, an almost flat space and without a source of the gravitational field, we can then consider the following metric:

$$g_{\mu\nu} = \eta_{\mu\nu} + h_{\mu\nu}$$

where $\eta_{\mu\nu}$ is the metric of a flat space (of Minkowski):

$$\eta_{\mu\nu} = \begin{pmatrix} -1 & 0 & 0 & 0 \\ 0 & 1 & 0 & 0 \\ 0 & 0 & 1 & 0 \\ 0 & 0 & 0 & 1 \end{pmatrix}$$

and $h_{\mu\nu} \ll 1$ is the perturbation of this metric.
By inserting this solution by linearizing the following Einstein equation.

$$R_{\mu\nu} - \frac{1}{2} g_{\mu\nu} R + \Lambda g_{\mu\nu} = \kappa T_{\mu\nu}$$

- $R_{\mu\nu}$is the Ricci tensor which represents the deformation of space-time;
- R is the scalar curvature which assigns to each point in space-time a simple real number characterizing the intrinsic curvature at that point;
- $g_{\mu\nu}$ is the metric tensor that defines the dot product of two vectors at each point in space;
- $\Lambda$is the cosmological constant added by Einstein in order to make his theory compatible with the idea that there is a static Universe. We will consider it here as zero.
- $\kappa$is Einstein's constant: $\kappa = \frac{8\pi G}{c^4}$;
- $T_{\mu\nu}$ is the energy-momentum tensor which represents the distribution of mass and energy in space-time.

we then obtain the following expression:

$$\Box \hbar_{\mu\nu} - \eta_{\mu\nu} \partial_\rho \partial_\sigma \hbar^{\rho\sigma} - \partial_\mu \partial_\rho \hbar^\rho_\nu - \partial_\nu \partial_\rho \hbar^\rho_\mu = -2\kappa T_{\mu\nu}$$

by defining: $\hbar_{\mu\nu} = h_{\mu\nu} - \frac{1}{2}\eta_{\mu\nu} h$ and $\Box$ d'Alembertian, $\Box = \partial^\mu \partial^\nu$.
Using the Lorenz gauge, defined by $\partial^\mu \hbar_{\mu\nu} = 0$, we can simplify the previous equation:

$$\Box \hbar_{\mu\nu} = -2\kappa T_{\mu\nu} \tag{2.2.1}$$

This equation is called the wave equation with reference to the general equation of wave physics. It describes the propagation of a wave in a medium.

Let us now place ourselves in a flat space empty of all matter ($T_{\mu\nu} = 0$).

the solutions of Equation (2.2.1) are known and take the following form:

$$\hbar_{\mu\nu} = \Re\left(A_{\mu\nu} e^{(ik_\rho x^\rho)}\right)$$

$\hbar_{\mu\nu}$ is the amplitude of the wave. $k_\rho = (\omega/c, \vec{k})$ is the wave vector whose norm is inversely proportional to the wavelength.

The dispersion relation of gravitational waves: $\omega^2 = c^2 \left|\vec{k}\right|^2$, indicates that the wave is traveling at the speed of light c.

In addition, the wave vector must satisfy the gauge conditions imposed above, the following equality must be verified:

$$k_\rho A^{\phi\rho} = 0 \tag{2.2.2}$$

Since $A_{\mu\nu}$ is a symmetric 4×4 matrix, it is composed of 10 independent elements. Equality (2.2.2) allows this number of elements to be reduced to 6. It is still possible to reduce this number by choosing a particular harmonic gauge, which is called a transverse and traceless gauge.

$$A^\mu_\mu = 0 \text{ traceless}$$
$$A^{0\mu} = 0 \text{ transverse}$$

This gauge further reduces the number of independent elements to 2. In the end, the amplitude takes the following form:

$$A_{\mu\nu} = \begin{pmatrix} 0 & 0 & 0 & 0 \\ 0 & A_{11} & A_{12} & 0 \\ 0 & A_{12} & -A_{11} & 0 \\ 0 & 0 & 0 & 0 \end{pmatrix}$$

From the form of the amplitude, we can deduce that a gravitational wave has two and only two polarizations. these two polarizations are called "+" and "×".

2.3 Gravitational wave sources

The most compact stars known are neutron stars and black holes. Cataclysmic phenomena including these compact objects can be of several types. In fact, these sources can be classified into three families:[6]

1. Continuous and stable sources over the observation time scale. Like, for example, the stochastic background which is the accumulation of all emissions since the beginning of the Universe or pulsars;

2. Transient sources lasting from a few milliseconds to a few seconds, such as the collapse of a star's core at the end of its life or the fusion of black holes;

3. Long-term transient sources ranging from a few tens of seconds to several minutes.

Before presenting these three categories and the sources they contain, let's first review the definition of compact objects.

2.3.1 compact objects

Compact objects are astronomical objects with extremely high densities and strong gravitational fields. These objects are typically remnants of massive stars that have undergone catastrophic events, such as supernova explosions. In astrophysics, compact objects are divided into two main categories: neutron stars and black holes.

2.3.1.1 Neutron stars NS

Following the death of a more massive star, above the Chandrasekhar limit, the energy reached by the electrons is such that the pressure of degeneration can no longer stop the gravitational collapse. The nuclear inverse beta decay processes are then favored, transforming the protons of matter into neutrons: the celestial object becomes a neutron star. This object has very intense magnetic fields (for the most intense $B = 10^{12}\text{to}10^{14}T$, called magnetar). In the extreme process of forming a neutron star, the forces involved cause the object in question to rotating rapidly. This object can produce a periodic electromagnetic signal ranging from the order of a millisecond to a few tens of seconds, called a pulsar. Pulsars and magnetars are generators of gravitational waves provided that an asymmetry is present in the form of the object.

2.3.1.2 black hole BH

A black hole is such a compact celestial object that the strength of its gravitational field prevents any form of matter or radiation from escaping. Such objects can neither emit nor scatter light and are therefore black, which in astronomy amounts to saying that they are optically invisible. The introduction of the concept of black holes began as part of Newton's universal gravitation in the late 18th century, particularly with the work of John Michell in 1784. The idea was to study objects whose mass was large enough that the speed of release was greater than the speed of light. When developing his metric [7], Schwarzschild found a singularity for objects with a radius equal to twice the mass (in reduced coordinates).

In 1963, Kerr modeled black holes with axial symmetry instead of spherical symmetry: they rotate along an axis and can be described by two parameters M and J, respectively mass and angular momentum [8]. From the point of view of gravitational waves, black holes are very good emitters: in fact, their ease in bending space-time makes them very good generators of high amplitude waves. Note also that in the absence of electromagnetic emissions, the only way to study black holes directly to detect the gravitational waves they emit when they merge.

2.3.2 Continuous gravitational wave sources

The detection of quasi-periodic sources requires data integration over long observation periods because the expected amplitude for the waves emitted by these sources are extremely low. Continuous gravitational wave sources are mainly neutron stars with very specific characteristics, such as their asymmetry, with or without matter.

Deformations of the crust of a neutron star generated by an elastic stress[9] or a magnetic field[10] are the main mechanisms of emission of gravitational waves for isolated systems. The waves generated have twice the rotational frequency of the neutron star and an amplitude proportional to the strain. The predictions made about the deformations are uncertain because they depend on the equation of the state of the neutron star.

Other mechanisms, independent of the deformation of the crust, associated with newly formed neutron stars make it possible to generate gravitational waves associated with instabilities of the normal modes of oscillation (r-modes [11] or f-modes[12]). These rapidly rotating neutron stars have a non-zero quadrupole moment. They can generate almost monochromatic gravitational waves.

2.3.2.1 Pulsar

A pulsar is a neutron star born from the gravitational collapse of a massive star that can be observed by electromagnetic "flashes" that swept the Earth at regular intervals. These rapidly rotating neutron stars have a non-zero quadrupole moment. They can generate almost monochromatic gravitational waves.

2.3.2.2 Stochastic background

A background of stochastic gravitational radiation is sought by current detectors. It has two different origins:

- astrophysics: from an incoherent superposition of gravitational waves emitted by all the transient and continuous sources from the separately undetectable origins.
- Cosmology: The Standard Model of Inflation predicts that 10 seconds after the Big Bang, during the decoupling of gravitons from the primordial plasma, an emission of gravitational waves has taken place. This period in the history of the Universe is only accessible through gravitational waves. The discovery of this stochastic background of gravitational waves would be proof of the veracity of the cosmological model of inflation.

2.3.2.3 R-modes

In the event that a newly born neutron star has a rapid rotation, instabilities called r-modes can appear. Gravitational radiation is then emitted while the instability is damped[13].

2.3.3 Transient gravitational wave sources

Transient gravitational wave sources are events or phenomena that produce gravitational waves, but only for a short period of time. These events typically involve violent or energetic processes, such as the collision of two black holes, the merger of two neutron stars, or the explosion of a supernova.

The detection of transient gravitational wave sources is a major area of research in modern astrophysics, as it provides important insights into the nature and behavior of some of the most extreme phenomena in the universe. Some of the most significant transient gravitational wave sources that have been detected so far include:

2.3.3.1 Binary system

Binary system; In 1974, the discovery of the binary pulsar named PSR B1913 + 16 by Hulse and Taylor (which won them the Nobel Prize in 1993 [14]), marked a turning point in the physics of gravitational waves. It is a binary pulsar, that is to say, it is composed of two elements: the pulsar that we detect and another invisible object for our instruments whose estimated mass is compatible with that of a neutron star. The two compact stars revolve around each other, emitting an almost monochromatic signal. As the system loses energy through gravitational radiation, the two stars come closer together by conserving energy. The waves emitted then increase in amplitude and frequency. In a little over 300 million years, the system will catastrophically converge toward the merger of the two compact bodies. The emitted gravitational wave will then have the form chirp.

The gravitational wave signal is of the form:

$$h(t) = A(t)\cos\phi(t) \tag{2.3.1}$$

2.3.3.2 Heartbroken Supernovae

The explosion of a supernova is an extremely bright event, as much as the host galaxy, and of very short duration, on the order of a fraction of a second. From a gravitational point of view, numerical simulations predict an energy emission of less than $10^{-6}M_{\odot}c^2$.

Due to this low amplitude of gravitational radiation, current detectors are only sensitive to nearby supernovae which makes the expected number relatively low (2-3 super nova/century/galaxy).

In addition, unlike transient sources seen so far, it is not possible to analytically predict the shape of the gravitational wave produced during a supernova. Although the general scenario could be verified, it is so complex that only numerical methods can be used to follow the evolution of the proto-neutron star until the explosion of the outer layers of matter.

2.3.3.3 Long-term transient sources

For most long-term transient sources, the mechanisms involved are associated with complex dynamics and hydrodynamic instabilities for which there is no analytical description.

However, there are many models that more or less realistically describe the emitted gravitational waves. including the following:

Accretion disk instability (ADI) Although the processes of creating a black hole are not fully understood, most models agree that obtaining a Kerr black hole is most likely,

Most models associate these black hole formation processes with an optical counterpart, in particular a gamma-ray burst (GRB).

Fallback accretion (FA) The death of a star usually results in the formation of a neutron star for the lighter ones, or a black hole for the heavier ones. However there is an intermediate case, depending on other parameters such as rotation, which results in the creation of an unstable neutron star, surrounded by a halo of matter which will accrete and fall into the object, thus collapsing the neutron star into a black hole. Because this phenomenon concerns a relativistic and asymmetric compact object, one would expect an emission of gravitational waves for the duration of the phenomenon which typically lasts between 30 s and 1000 s.

Magnetars When two neutron stars merge, the phenomenon can result in the creation of a black hole or a supermassive neutron star which will quickly collapse into either a black hole or a stable neutron star.[15], In this case, the amplification of the magnetic field during the fusion phase leads to the appearance of a magnetar inducing a quadrupole moment, which emits gravitational waves.

2.4 GW observatories

Gravitational wave observatories are specialized facilities designed to detect the extremely small ripples in the fabric of space-time that are produced by cosmic events, such as the merger of two black holes or the collision of two neutron stars. These observatories use advanced technology and sensitive instruments to detect the faint signals produced by these events.

2.4.1 Michelson interferometer

The Michelson interferometer is an optical device invented by Albert Abraham Michelson and Edward Morley produces interference by amplitude division. It essentially consists of two mirrors and a semi-reflecting blade. The two possible configurations of use are the air knife configuration and the air wedge configuration.

The Michelson interferometer consists of two mirrors M1 and M2 and a semi-reflecting plate called a separator. These three elements are orientable and M2 can be moved by translation (to adjust the distance noted d on the diagram).

On the diagram see Figure (2.4.1), which models a Michelson used as an air knife, the light source sends a ray (of intensity I) towards the separator blade. This ray is divided into two rays (blue and green) of intensity I / 2. M1 'represents the image of the mirror M1 by the separator, therefore symmetrical with respect to the latter; the blue dotted line, therefore, represents a virtual path equivalent to the real path of the light toward the mirror M1. The difference in length d of the arms of the interferometer induces a path difference between the two rays equal to 2d.

In the air knife configuration, if the inclination of the radius with respect to the normal of the blade (here 45 °) is equal to i, the path difference is equal to 2dcos i (in this case d2).

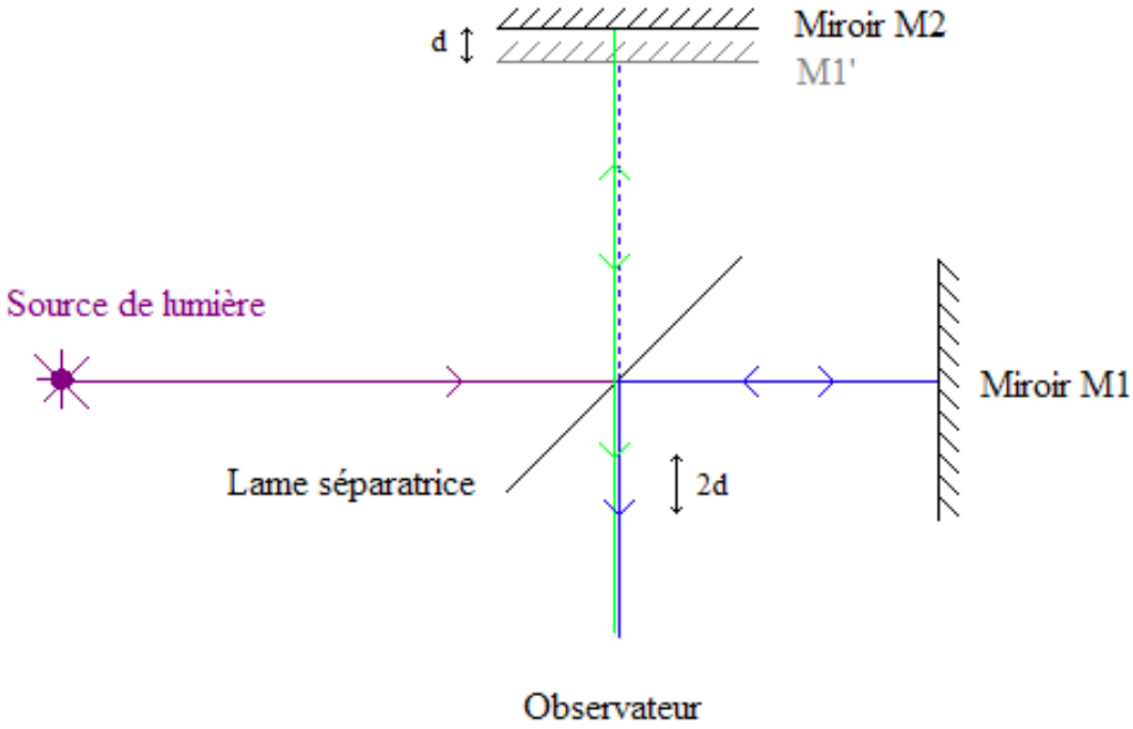

Figure 2.4.1: Michelson interferometer

2.4.2 Interferometric detector

The first prototype interferometer to test the technology was built by Forward in 1971 [16]. The technical foundations of current interferometers were laid by Weiss in 1972 [17]. However, it was not until the 1990s and some technological advances the first interferometric detector capable of detection was built. In the early 1970s, a project was brought to the United States, by Drever, Thorne, Weiss [18] and many others, leading to the creation of LIGO (Laser Interferometer for Gravitational waves Observatory) in 1974, the most expensive project of

the NSF (National Science Foundation). In Germany, Ruediger built a 10 m prototype, but German reunification in 89 put an end to the German project. Finally, in France and Italy, Brillet and Giazotto carry the Virgo project [19] approved in 1994.

After a decade of commissioning, improvements, and data collection, this first generation has given way to a new generation of detectors: advanced Virgo and advanced LIGO. These detectors, driven by considerable technological advances in terms of metrology, optics, and laser interferometry, resulted in the first detection of gravitational waves in September 2015.

2.4.3 Detection principle

To witness the passage of a gravitational wave, we must consider several points in space-time. These points associated with falling masses will see their relative distance change under the effect of the wave as shown in Figure 2.4.2 [20]. It is this relative distance that we are trying to measure precisely.

The whole difficulty comes from what we put behind the word "precise". Indeed, we have seen that the amplitude of gravitational waves is very small because space-time is very rigid. If we take free-falling masses spaced 1 m apart, we must be able to measure distance variations of the order of $10^{-21}m$. Only laser interferometry can measure variations in the distance that approach it. To reach $10^{-21}m$, however, modifications must be made to the Michelson interferometer.

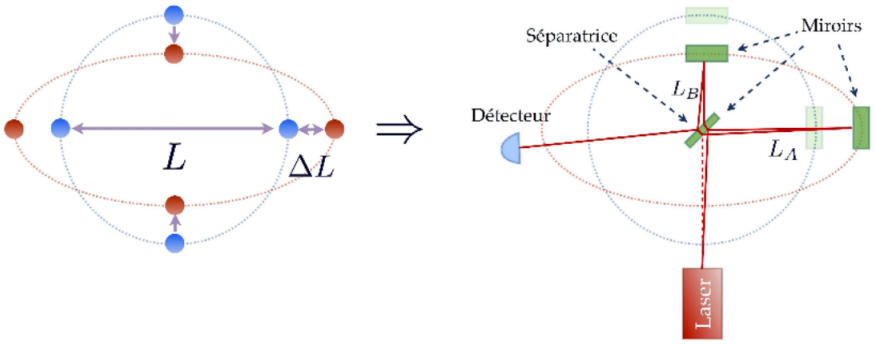

Figure 2.4.2: Principle of interferometric detection: two of the test masses from the thought experiment illustrated at left are replaced by mirrors in the figure on the right, forming an interferometer with a separator in the center .

2.4.4 LIGO

The Laser Interferometer Gravitational-Wave Observatory, abbreviated LIGO, is a large-scale physics experiment aimed at directly detecting gravitational waves. On February 11, 2016, a direct observation of gravitational waves by LIGO dated September 14, 2015, resulted from the collision of two black holes (GW150914). LIGO's mission is to directly observe gravitational waves of cosmic origin. These waves were first predicted in 1916 by Einstein's general theory of relativity when the technology needed to detect them did not yet exist.

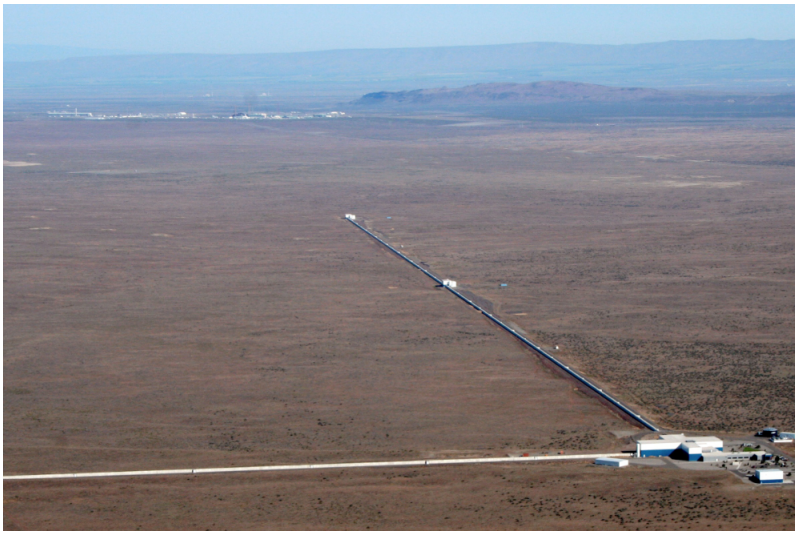

Figure 2.4.3: LIGO Hanford Observatory

2.4.5 VIRGO

The result of a Franco-Italian collaboration, the Virgo detector is one of the four-kilometer interferometers currently dedicated to the search for gravitational waves [21]. It was originally designed to be able to achieve sensitivity below 1021Hz to 300Hz, with a frequency band extending from 10Hz to 10kHz. The name Virgo comes from the initial sensitivity that should have made it possible to observe sources located in the Virgo cluster ($\sim$ 20 Mpc).

Figure 2.4.4: Virgo interferometer

2.4.5.1 advanced Virgo aVirgo

The advanced Virgo (aVirgo) project, funded by CNRS, INFN and NIKHEF was launched in 2011 [22]. aVirgo currently uses the original laser which can be driven to a power of $\sim$ 60W. A change of laser will achieve a final power of 100W. However, an increase in laser power results in an increase in noise from the radiation pressure. In order to counter this effect, new mirrors twice as heavy (42 kg) are installed. New polishing processes further improve the surface of mirrors as well as their reflection. Finally, a new coating is applied to the mirrors reducing optical losses as well as thermal noise. Suspended deflectors close to the mirrors are installed to trap the scattered light.

For advanced Virgo, the vacuum is improved from 10^{-7} mbar 10^{-9} mbar Several optical benches used for alignment are suspended and placed under a vacuum in order to gain sensitivity. After several months of commissioning, the aVirgo detector took data for the first time in August 2017 reaching a sensitivity of 30 Mpc 1 for a cycle tile of 85%. [23]

By advantageously completing the network formed by American detectors, it reduced the error in the location of events GW170814 and GW170817, which greatly favored the observation of an electromagnetic counterpart for GW170817.

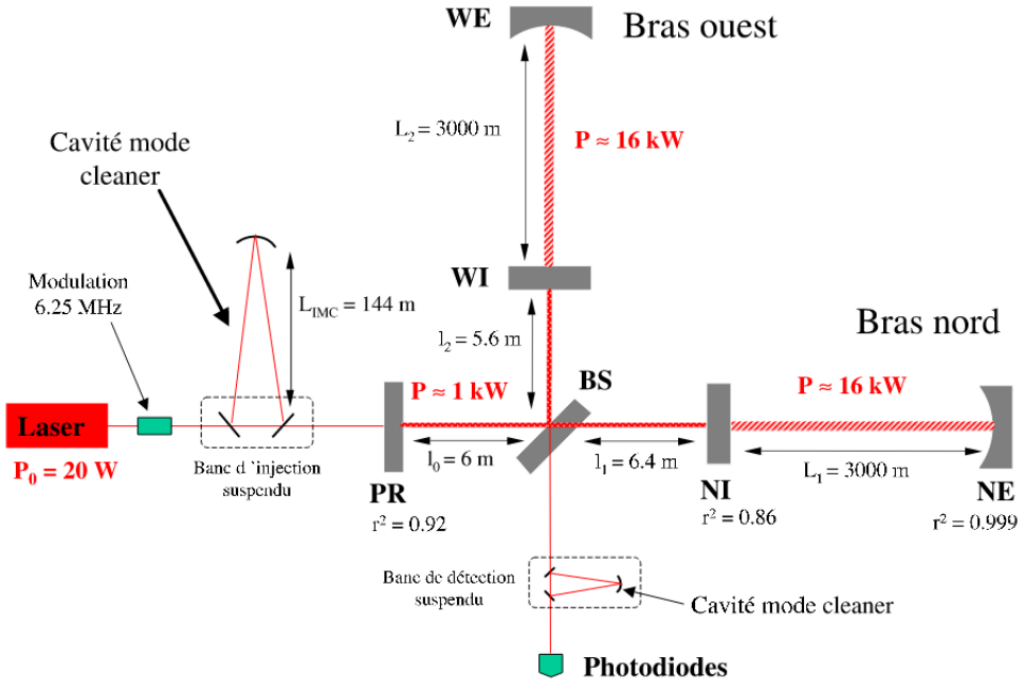

Figure 2.4.5: Schematic view of the Virgo optical device in its initial configuration.

2.4.6 Detector network

In 1992, the National Scientific Foundation (NSF) funded the Laser Interferometer Gravitational Wave Observation (LIGO) [18]. LIGO comprises two 4 km long detectors built in the United States at Hanford (WA) and Livingston (LA). Initially, Hanford's vacuum chamber contained two interferometers: one 4 km and one 2 km (half as sensitive). This should make it possible to reject environmental noise events having the same amplitude in the two detectors. Indeed, a true signal would have been twice as weak in the least sensitive detector. This idea turned out to be a bad idea, as having the two interferometers in the same vacuum chamber generated a lot of noise that could not be suppressed. As a result, the 2 km detector has been dismantled and will be recycled for the LIGO detector in India (IndIGO) which is under construction. LIGO took data from 2002 to 2010 and then stopped to carry out its update (advanced LIGO or aLIGO project) [5] which was put into service in September 2015.

The German-British collaboration GEO [24] built a 600 m interferometer near Hanover. Unlike Virgo and LIGO, GEO does not contain a Fabry-Perot cavity, but the arms are made up of delay lines [25]. This detector is still used as a prototype to develop and test advanced techniques which will then be installed in LIGO and Virgo.

The Japanese collaboration [26] is currently building the KAGRA detector, of the same

size as Virgo. The special feature of this detector is that it is underground, reducing much of the seismic noise. In addition, this detector will be partially cooled reducing the thermal noise of the suspensions of the mirrors. The first data taking should take place in 2019. It would advantageously complement the current network of detectors improving its efficiency, particularly in terms of locating sources.

India is also showing its willingness to participate in the development of gravitational astronomy and is funding the construction of an observatory in India that will house the second Hanford detector. Funding for the site for the installation of a LIGO-type interferometer is being finalized and the start of the project is scheduled for 2022 [27]. These observatories work together as a global network to detect gravitational waves and study the events that produce them. By analyzing the signals produced by these events, astrophysicists can gain important insights into the nature of the universe and the behavior of matter under extreme conditions.

2.4.7 Sensitivity and noise

To assess the performance of the detector, that is to say its sensitivity, we must compare its response to a gravitational wave to the noises that limit the measurement. There are many sources of noise from interferometric detectors due to their extreme sensitivity. However, they can be classified into three main categories:

- fundamental noises;
- transient noise from the environment;
- technological noise from detector components.

The characterization of the detector is an analysis in its own right which aims to understand the different noises encountered in the data, and to go back to their origin in order to subtract them from the data [28].

To characterize each noise source, we can rely on a theoretical prediction of their spectral density when it is available. By assuming that the noises add up, we can thus build the power spectral density which we can then compare directly to the measurement. The noise spectral density is the Fourier transform of the autocorrelation of the measured noise x (t): position sensitive detector PSD

$$PSD = \int_{-\infty}^{+\infty}\int_{-\infty}^{+\infty} x^*(t)x(t+\tau)e^{-i\omega t}dtd\tau$$

Figure 2.5 shows the sensitivity curve of aVirgo as well as the contributions of the main noises.

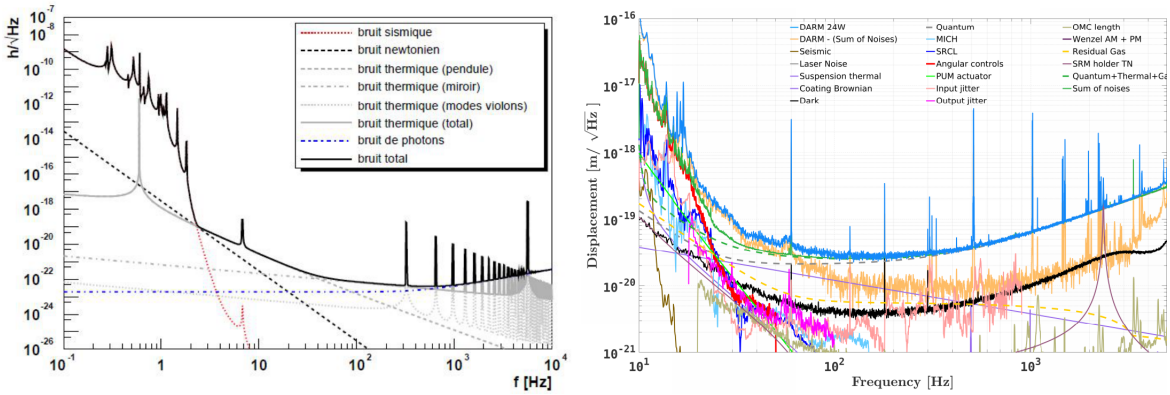

Figure 2.4.6: Components of the different noise sources contributing to the theoretical sensitivity (left). Noise components measured in L1 data during O2 (right).

2.4.8 LISA project

Laser Interferometer Space Antenna (LISA) is a future space mission of the European Space Agency (ESA) whose objective is to detect low frequency gravitational waves from space. LISA consists of a constellation of three satellites in heliocentric orbit forming an equilateral triangle 5 million kilometers apart, the three arms of which are linked by 6 laser beams.

LISA is the first space observatory of gravitational waves. between 0.1 mHz and 100 mHz,[29] unobservable by terrestrial interferometers due to their small size and seismic disturbances. Low-frequency gravitational waves are produced by very massive and very distant stars, such as supermassive black holes nestled in the center of galaxies.

The frequency band observed by LISA is considered to be the richest in gravitational waves. Thus the mission should make it possible to better understand the formation of binary stars in the Milky Way, to know the history of the Universe up to a redshift of the order of 20 (the first stars formed after the Big Bang) to test the theory of general relativity in strong gravitational fields and to observe the beginnings of the Universe using energies of the order of TeV.

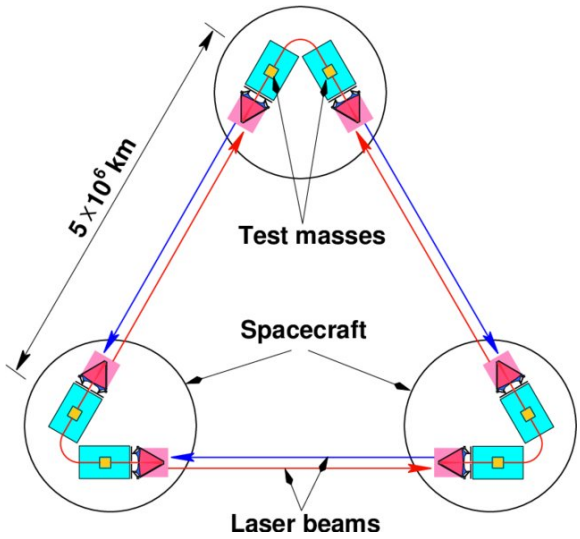

Figure 2.4.7: LISA space mission

2.5 Gravitational wave detections

If gravitational astronomy has been of real interest in recent years, it is because interferometric detectors for the first time perceived gravitational wave signals opening a new observation window for astrophysics.

2.5.1 Observation data collection (runs)

Gravitational wave observatories collect data in runs, which are periods of time during which the detectors are active and collecting data. Each run typically lasts for several months and is followed by a period of downtime during which the detectors are maintained and upgraded.

The data collected during a run is processed and analyzed by teams of scientists and researchers, who look for signals that may indicate the presence of gravitational waves. This analysis is a complex and computationally intensive process and typically involves comparing the data from multiple detectors to confirm the presence of a signal.

2.5.1.1 O1

After a series of major updates on the American aLIGO detectors, including a new mirror to recycle the signal, the increase in power from 20W to 100W and the use of new larger and heavier mirrors, improving from 3 to 5 times their sensitivity compared to the previous generation, the O1 run starts in 2015.

This O1 run is a transition run: its purpose is to check the functioning of the new pieces of detectors before installing new ones allowing to reach the nominal sensitivity of the advanced detectors, that is to say a factor of 3 in sensitivity compared to the initial generation.

During O1, a system for sending alerts was set up: online analyzes for the search for coalescence of compact objects and more generally for transient signals make it possible to detect an event in less than 10 minutes. An alert is then sent to a network of observers with whom a partnership has been signed. The alert specifies the nature and position of the source so that possible electromagnetic counterparts can be searched for. These alerts are not public and only partner groups can receive and export them.

2.5.1.2 O2

After O1, the increase in the laser power injected into the LIGO detectors created many difficulties which resulted in a little delay and a sensitivity slightly lower than that initially envisaged [30].

The run begins on November 25, 2016, with aLIGO detectors joined by aVirgo on August 1, 2017. It ends on August 25, 2017, with a sensitivity (range) of 30 Mpc for aVirgo, 60 Mpc for Hanford, and 100 Mpc for Livingston. With a useful cycle of about 60% for each detector, this run, of average duration (9 months), will however allow the discovery of the first coalescence of neutron stars.

2.5.1.3 O3

The third run (O3) began on 1 April 2019 [31]. On 6 January 2020, LIGO announced the detection of what appeared to be gravitational ripples from a collision of two neutron stars, recorded on 25 April 2019, by the LIGO Livingston detector. Unlike GW170817, this event did not result in any light being detected. Furthermore, this is the first published event for a single-observatory detection, given that the LIGO Hanford detector was temporarily offline at the time and the event was too faint to be visible in Virgo's data.

2.5.2 GW150914

Although the first observation run (O1) was a short transition run, it led to one of the greatest results of this decade: the first detection of gravitational waves emitted by the final plunge of two black holes (GW150914) that had occurred on September 14, 2015 [32].

This signal comes from the merger of two black holes of mass respectively $36^{+5}_{-4}M_{\odot}$ and $29^{+4}_{-4}M_{\odot}$ into a black hole of mass $62^{+4}_{-4}M_{\odot}$ letting escape an energy of no less than $3.0^{+0.5}_{-0.5}M_{\odot}c^2$ emitted in the form of gravitational waves. Sent 1.3 billion years ago, the signal only lasts a few hundred milliseconds.

Figure 2.5.1 shows the agreement between the theoretical predictions for this type of signal and the measurements made in the aLIGO data. Table 2.1 [32] summarizes the main characteristics of the event.

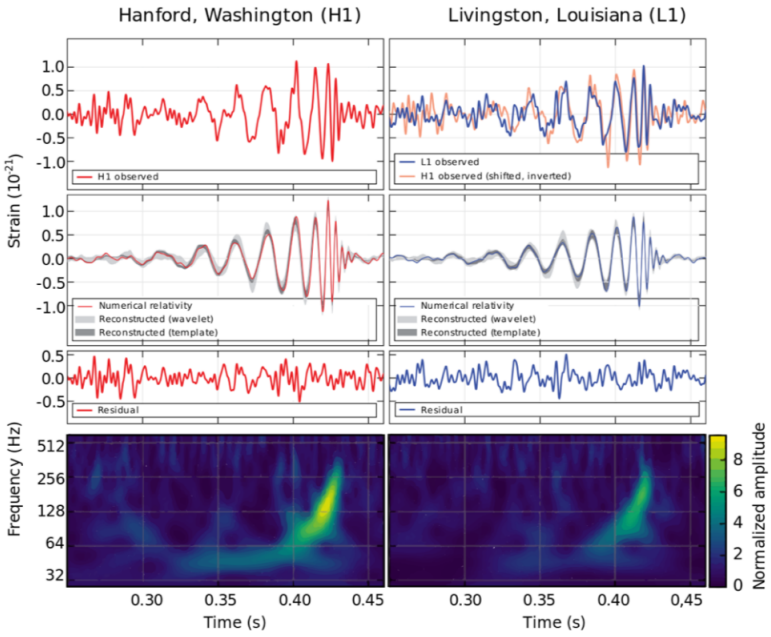

Figure 2.5.1: Signals of the first detection of gravitational waves. The first line represents the whitened data (high pass filter) of the two aLIGO detectors. The second line represents the signal calculated numerically within the framework of general relativity for this type of source as well as the signal reconstructed by two independent methods using the data. The third line represents the residual error between the reconstructed signal and the numerically calculated signal. The last line represents the time-frequency maps of the signal that can be seen with the naked eye.

Mass of the first black hole m_1	$36^{+5}_{-4}M_\odot$
Mass of the second black hole m_2	$29^{+4}_{-4}M_\odot$
Mass of final black hole M_f	$62^{+4}_{-4}M_\odot$
E_{rad}	$3.0^{+0.5}_{-0.5}M_\odot c^2$
Angular momentum of final black hole a_f	$0.67^{+0.05}_{-0.07}$
luminosity distance D_L	410^{+180}_{-160}
Redshift z	$0.09^{+0.03}_{-0.04}$

Table 2.1: Main parameters of the first event from the fusion of black holes detected on September 14, 2015

2.5.3 GW170814

On August 1, 2017, aVirgo joined the end of O2 for a common month of data taking. He thus participates in the detection of gravitational waves coming from the fusion of black holes, GW170814, August 14, 2017[33].

The presence of a third detector reduces the error associated with the location of the source. Figure 2.5.2 shows the 90% confidence interval of the sky location going from 180 deg^2 to 30 deg^2 using data from Virgo[33].

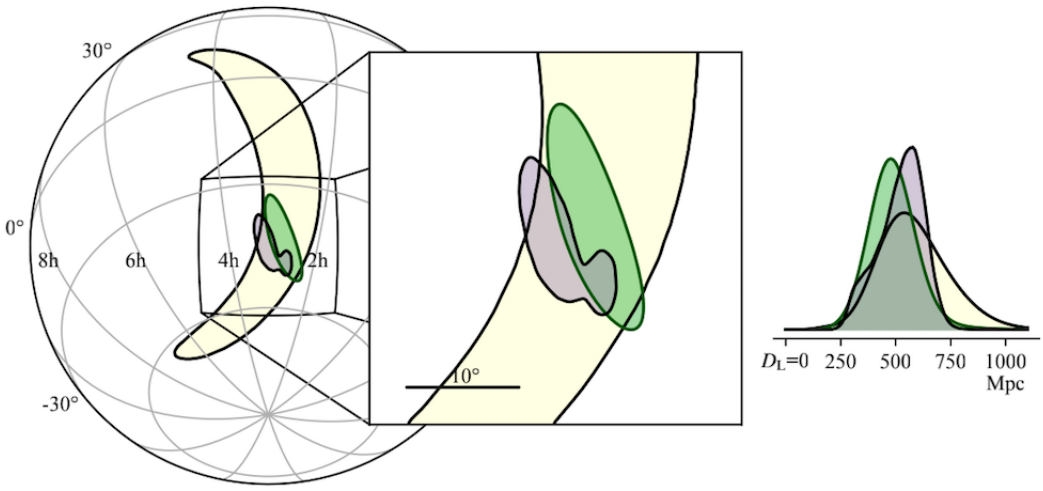

Figure 2.5.2: 90% confidence interval of the position of the black hole binary system fusion observed on August 14, 2017. The yellow zone represents this interval on the location of the source by considering only the two aLIGO detectors (Hanford & Livingston). The green and purple areas correspond to the 90% confidence interval of the location including the temporal information provided by aVirgo obtained with 2 different algorithms. We go from 180 deg^2 to only 28 deg^2.

2.5.4 GW170817

Three days after GW170814, a strong signal was observed by the Hanford detector consistent with a signal from the fusion of neutron stars. The particularity of this event is that it is associated with a GRB detected by the Fermi-GBM satellite. The event is not seen online in Livingston's data, however, so at the time of the event the detector horizon for this type of event was as follows:

- 107 Mpc for Hanford;
- 218 Mpc for Livingston;
- 58 Mpc for Virgo.

An alert was sent approximately 30 minutes after the event was detected with a first estimate of the position. A more precise window ($\approx 28\ deg^2$) was sent a few hours later. This alert was followed by many groups/telescopes and around 11h after detection, independent groups, Swope and DECam, identified an optical counterpart in NGC4993. The electromagnetic monitoring of this event made it possible to identify a residual emission signal characteristic of a kilonova [34, 35, 36, 37, 38, 39, 40, 41, 42].

The estimation of the parameters of the two neutron stars orbiting one another was done by means of the reconstruction of the gravitational wave signal, the masses of the two neutron stars are estimated: $m1 = 1.36 - 1.60\ M_\odot$ and m2 = $1.17 - 1.36\ M_\odot$. Uncertainty about the individual masses is important because of the degeneration of the models used for matched filtering. Conversely, chirp mass:

$$M = \frac{(m_1 m_2)^{3/5}}{(m_1 + m_2)^{1/5}},$$

is very well measured since the amplitude of the signal and the large number of cycles recorded by the detectors depends directly on M. GW170817 lasts a few hundred seconds and includes no less than 3000 cycles.

Table 2.2 [43] summarizes the main information about this event.

	Hypothesis $\|\chi_z\| \leq 0.05$	Hypothesis $\|\chi_z\| \leq 0.89$
Mass m_1	$1.36 - 1.60\ M_\odot$	$1.36 - 2.13\ M_\odot$
Mass m_2	$1.17 - 1.36\ M_\odot$.	$0.90 - 1.36\ M_\odot$
Chirp mass $\mathcal{M}$	$1.186^{+0.004}_{-0.002}\ M_\odot$	$1.187^{+0.004}_{-0.002}\ M_\odot$
Mass ratio m_2/m_1	$0.7 - 1.0$	$0.4 - 1.0$
Total mass m_{tot}	$2.74^{+0.04}_{-0.01}\ M_\odot$	$2.81^{+0.30}_{-0.08}\ M_\odot$
Energy emitted E_{rad} $(24Hz < f < 1kHz)$	$> 0.04\ M_\odot c^2$	$> 0.04\ M_\odot c^2$
luminosity distance D_L	$40\pm7Mpc$	$40\pm7Mpc$
Viewing angle θ	$< 56^\circ$	$< 56^\circ$
Viewing angle using the position of NGC4993	$< 28^\circ$	$< 28^\circ$

Table 2.2: Properties of GW170817 (90% confidence interval) estimated for two hypotheses of the angular moments of the initial objects (the first case considers that the objects have no angular momentum, the second case relaxes the constraint on the angular momentum.).

Chapter 3

Multi-messenger astrophysics MAA

MMA is astronomy that relies on the recording and interpretation of various signals from space[44]. The four messenger signals are gravitational waves, electromagnetic radiation, cosmic radiation, and particles, including neutrinos, as well as electrons, protons, etc, which are generated by various astrophysical processes[45], and allow obtaining various information about the sources in which they occur. The most famous event is a gateway to multi-messenger astronomy is GW170817, a Source with Over 4000 Messengers[46], the GRB 170817A gamma-ray burst was observed by the Fermi Gamma-ray Space Telescope and INTEGRALE, and its optical counterpart SSS17a was detected 11 hours later in the host galaxy NGC4993 at the Las Campanas Observatory[47], this observation was supplemented by other observations in optics by the Hubble Space Telescope and the Dark Energy Survey, in ultraviolet rays and by the Swift Gamma-Ray Burst Mission, in X-rays by the Chandra X-ray Observatory and in radio by the Karl G. Jansky very large array(VLA)[46].

3.1 Multi-messenger search strategies (combination of all messenger)

Based on how they use other messengers, search strategies for GW transients can be divided into four categories[48].

- All-sky searches, which do not rely on information from other messengers.(e.g. [49]).
- Externally-triggered searches, in which one looks for GW signals from sources that have been verified by other messengers. For example, using the location, time, and other parameters of detected GRBs, one can look for GW signals.(e.g. [50, 51]).

- Coherent multimessenger searches, in which multiple observatories of different messengers are used in a joint search to find sub-threshold signal candidates.(e.g. [52, 53]).
- Electromagnetic (EM) follow-up searches, in which GW signal candidates are used to initiate electromagnetic or other follow-up searches with other telescopes.(e.g. [54, 55]).

3.2 Neutrino counterpart

Many GW sources, especially GRBs, are expected to be abundant neutrino emitters[56, 57]. Based on two distinct emission mechanisms with two distinct energy ranges, astrophysical neutrino emission can be divided into two main sub-groups. Low-energy neutrinos (with energies of less than 100 MeV) are produced in the extremely hot, dense central regions of core-collapse supernovae, as well as likely GRBs. Shock-accelerated particles in relativistic outflows driven by the GRB's central engine are thought to emit high-energy neutrinos (with energies between 10 and 100 GeV) (e.g. [58]). Only low-energy astrophysical neutrinos and, in one case, supernova 1987A [59], have been confirmed so far.

One of the benefits of combining GW and neutrino searches [60] is that both GW and neutrino detectors (low and high energy) continuously observe the sky, recording signal candidates without the need to "point" the detector in a specific direction. Because the sky coverage for each messenger must overlap for a joint search, full sky coverage is especially important for multimessenger searches. Furthermore, whereas EM follow-up searches necessitate a fast response from EM telescopes, GW-neutrino observations can be carried out with a long latency without losing information[48].

IceCube Neutrino Observatory The IceCube Neutrino Observatory, or simply IceCube, is a neutrino observatory built at the South Pole. Its thousands of sensors are located under the Antarctic ice, spread over a cubic kilometer. IceCube is made up of 5,484 optical detectors called digital optical modules, each containing a photomultiplier tube (PMT) and a data acquisition the card that sends digital data to the acquisition station on the detector surface.

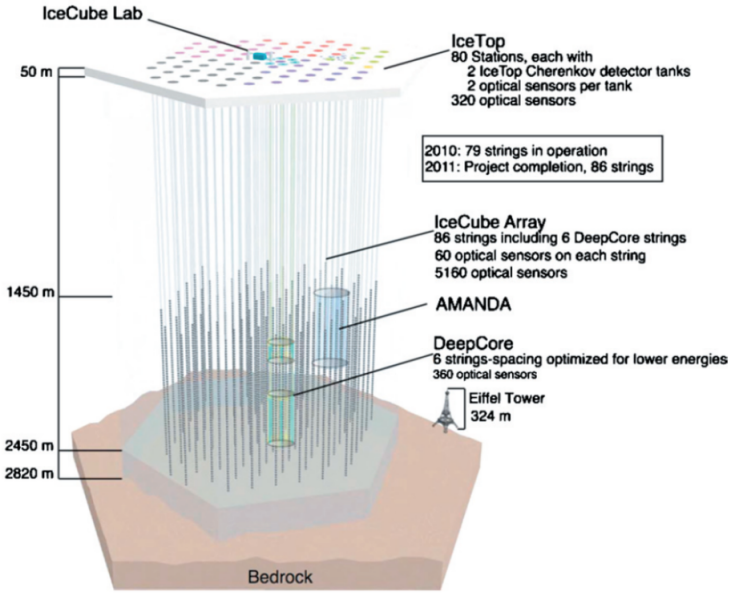

Figure 3.2.1: IceCube Neutrino Observatory

3.3 Electromagnetic follow-up

With the development of a global GW detector network, it became possible to reconstruct the direction of a GW signal candidate, albeit with a high degree of uncertainty. Such reconstruction allows GW signal candidates to be used in triggering electromagnetic (EM) followup observations, in which a telescope or satellite with a limited field of view is used to take observations in the GW signal candidate's assumed direction (i.e. a larger confidence region). There are a number of scientific benefits to such a follow-up search[48]:

- Because EM observations cannot cover the entire sky with high sensitivity in a continuous manner, GWs can be used to guide these telescopes in the right direction at the right time.

- The most interesting and powerful emission from an EM transient often occurs within the first seconds of its occurrence. Because GW emission is often expected to precede the onset of EM emission, telescopes may be able to begin follow-up observations at an early stage of emission, or even before the EM event begins.

- GW signal candidates are frequently too insignificant to be identified as extraterrestrial signals without a doubt. The presence of an EM follow-up event can greatly increase the significance of the joint observation, increasing the likelihood of detection.

- Information from the various messengers can enhance the information (and thus science) extracted from the source, similar to other multimessenger searches.

In 2009-2010 (S6-VSR2+3 science run), the first implementations of EM follow-up observations were made for the initial LIGO-Virgo detector network.[61]. After automatic and manual data quality validations, events with $\sim 1\mathrm{da}y^{-1}$ false alarm rates were chosen and sent out to telescopes. Because the reconstructed point spread function is typically large and irregularly shaped, probable directions were further narrowed down using a galaxy catalog. [62]. The remaining directions were distributed to a variety of telescopes (mostly wide-field, robotic, and optical). [63], such as TAROT[64], ZADKO[65], Pi in the sky, ROTSE, SkyMapper, the Palomar Transient Factory [61], and the Swift satellite [53].

3.4 Electromagnetic counterparts of gravitational wave sources

Electromagnetic counterparts of gravitational wave sources are electromagnetic signals that are emitted simultaneously with the gravitational waves produced by cosmic events, such as the merger of two black holes or the collision of two neutron stars. These signals can provide important information about the properties of the event that produced the gravitational waves, such as its location, distance, and energy.

The detection of electromagnetic counterparts to gravitational wave sources is an important area of research in modern astrophysics, as it allows scientists to study these events in more detail and to probe the nature of the universe on multiple fronts. Some of the most significant electromagnetic counterparts that have been detected so far include:

- Gamma-ray bursts: These are extremely energetic explosions that are thought to be produced by the merger of two neutron stars or the collapse of a massive star. They produce intense bursts of gamma-ray radiation, which can be detected by telescopes like Fermi and Swift.

- Optical transients: These are short-lived flashes of light that are produced by the merger of two neutron stars or the explosion of a supernova. They can be detected by optical telescopes like the Hubble Space Telescope or ground-based observatories like the Panoramic Survey Telescope and Rapid Response System (Pan-STARRS).

- Radio emissions: These are low-frequency radio waves that are produced by the acceleration of charged particles in extreme environments, such as the vicinity of a black hole or

neutron star. They can be detected by radio telescopes like the Very Large Array (VLA) or the Atacama Large Millimeter/submillimeter Array (ALMA).

The detection of electromagnetic counterparts to gravitational wave sources is a complex and challenging task, as these signals are often very faint and difficult to detect. However, advances in observational technology and data analysis techniques have made it possible to detect and study these signals in greater detail, providing important insights into the nature of the universe and the behavior of matter under extreme conditions.

3.4.1 Gamma ray bursts GRBs

Gamma-ray bursts (GRBs) are highly energetic bursts that have been observed in the Universe, they are the brightest and most energetic electromagnetic events in our universe, these bursts may last from ten milliseconds to some hours, After this gamma-ray flash, the "afterglow" is emitted for a relatively long time at lower energy and at longer wavelengths (X-rays, UV rays, optical, infrared IR, and radio)[66]

GRB can be classified according to its light curve into two main parts, short-duration GRBs (SGRBs) and long-duration GRBs (LGRBs), events with a $T_{90} < 2$ seconds are classified as short gamma-ray bursts (T_{90} is the time required for a gamma explosion to lose 90 percent of its energy), and events with a $T_{90} > 2$ seconds are classified as long-gamma ray bursts[67]

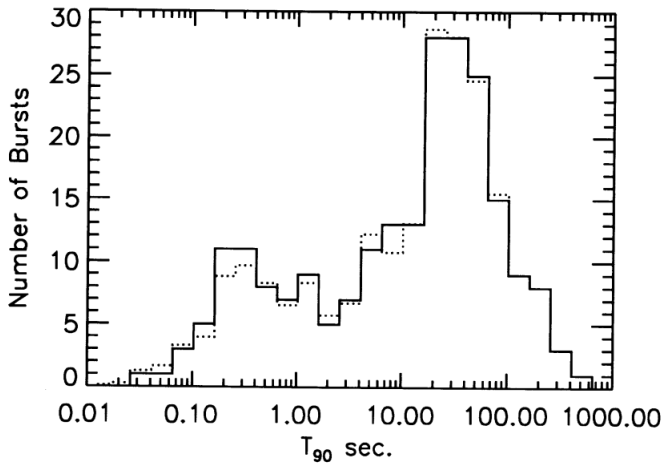

Figure 3.4.1: The two main classes of GRB, $T_{90} < 2$ (SGRB) and $T_{90} > 2$ (LGRB)

The SGRB is often caused by the collision of a binary neutron star (BNS) or neutron star-black hole binary(NS-BH), Eventually, a large part of the energy is emitted in the form

of gravitational waves[68]

3.4.2 "Fireball" and internal shocks

The so-called "fireball" model is not the only one proposed to explain the emission of gamma-ray bursts, but it is currently the most common. He associates the gamma-ray burst with the formation of a stellar black hole. The formation of the latter is associated with different phenomena depending on the duration of the prompt emission observed: hypernova for long bursts ($T_{90} > 2s$), a fusion of two compact objects for short bursts ($T_{90} < 2s$). The residual emissions of certain long bursts have made it possible to effectively link them to supernovae. During explosion or fusion, a black hole is formed in the center, while the rest of the matter, falling in rotation on the black hole, forms an accretion disc. The accretion of this material is accompanied by the formation of two relativistic plasma jets on either side of the plane of the disc, according to a mechanism that is still poorly understood.

The strong temporal variability of the prompt emission[69] of gamma-ray bursts suggests the variable activity of the central "engine" emitting the plasma jets[70]. This naturally leads to the hypothesis that the Lorentz factor of the ejected plasma varies during the duration of the burst. If one assimilates the plasma to solid layers of different Lorentz factors, a fast layer can catch up with a slow layer, to form "internal shock"[71]. The particles of the plasma are accelerated to the level of this shock by the Fermi process and emit radiation constituting the prompt emission of the burst. Each shock produces a gamma emission pulse so that the temporal variations of the Lorentz factor at the source are naturally linked to the temporal variability of the observed emission[72]. The remanent emission is more generally associated with the "front shock" between the end of the jet, which has already slowed down and which has widened, with the surrounding interstellar medium. The "Reverse Shock" between the material of the jet slowed down by the external environment and the material located upstream can also occur.

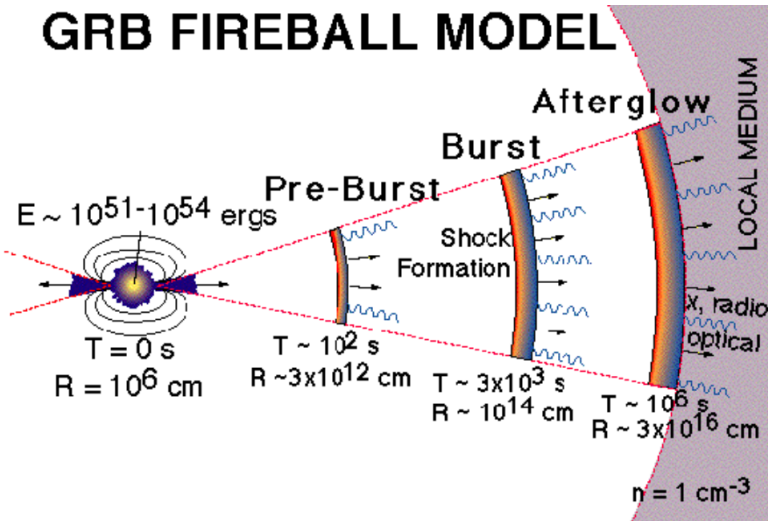

Figure 3.4.2: fireball model

3.5 Electromagnetic counterpart Observatory

There are numerous observatories around the world that are specifically designed to search for electromagnetic counterparts to gravitational wave sources. Some of the most significant observatories include:

- Swift: Swift is a NASA space telescope that is designed to detect gamma-ray bursts, which are thought to be produced by the merger of two neutron stars or the collapse of a massive star. It is capable of detecting and locating gamma-ray bursts within seconds of their occurrence, which makes it an important tool for follow-up observations of gravitational wave events.

- Hubble Space Telescope: The Hubble Space Telescope is a NASA observatory that is primarily designed to study the universe in visible, ultraviolet, and near-infrared light. It has been used to study a wide range of astronomical phenomena, including the optical transients produced by the merger of two neutron stars.

- Pan-STARRS: Pan-STARRS is a network of ground-based telescopes that is designed to survey the sky in visible and near-infrared light. It is capable of detecting and tracking optical transients, and has been used to study a wide range of astronomical phenomena, including the optical counterparts to gravitational wave events.

- VLA: The Very Large Array is a radio observatory located in New Mexico that is

capable of detecting and studying low-frequency radio waves produced by astrophysical phenomena, including the radio emissions produced by the acceleration of charged particles in the vicinity of black holes and neutron stars.

- ALMA: The Atacama Large Millimeter/submillimeter Array is a radio observatory located in Chile that is capable of detecting and studying high-frequency radio waves produced by astrophysical phenomena, including the emission of dust and gas in the vicinity of massive stars and black holes.

These observatories work together as a global network to detect and study the electromagnetic counterparts to gravitational wave events, providing important insights into the nature of the universe and the behavior of matter under extreme conditions.

3.5.1 Swift Observatory

Swift is a multispectral (hard and soft x-ray, ultraviolet, visible light) space telescope developed by NASA, with major contributions from Italy and the United Kingdom. Swift aims to identify, locate and observe gamma-ray bursts. And to complete this task it contains three Instruments, Burst Alert Telescope (BAT) detects GRB events and computes their coordinates in the sky. It covers a large fraction of the sky and X-ray Telescope (XRT) can take images and perform spectral analysis of the GRB afterglow. This provides a more precise location of the GRB, with a typical error circle of approximately 2 arcseconds radius and the third Ultraviolet/Optical Telescope (UVOT) monitors the afterglow in ultraviolet and visible light, its aperture is 30 cm and locates the source at an accuracy of one arcsecond.

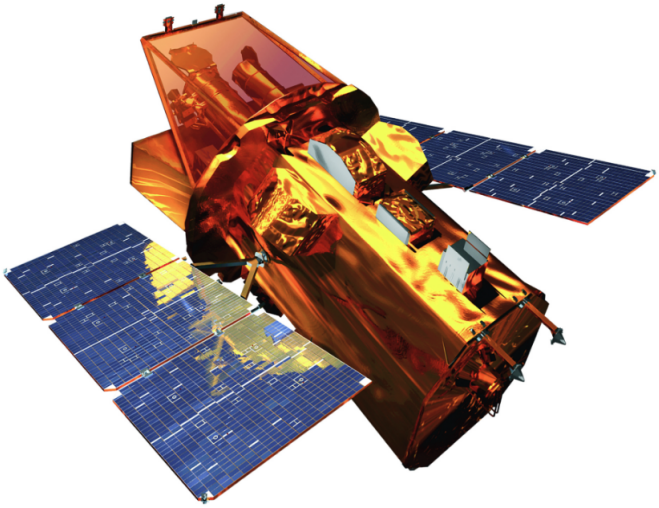

Figure 3.5.1: NASA's Swift Gamma Ray Burst Detecting Satellite

3.5.2 Fermi Gamma-ray Space Telescope

The Fermi Gamma-ray Space Telescope is a space telescope of the American space agency intended for the study of the gamma rays of high energy emitted by celestial objects. The main LAT(Large Area Telescope) instrument observes gamma rays from 20 MeV to 300 GeV. A second instrument, the GBM(Gamma Burst Monitor), is reserved for the study of gamma-ray bursts. The Fermi telescope aims to study the most violent phenomena observed in the universe such as relativistic blazars jets produced by supermassive black holes, and gamma-ray bursts and should contribute to a better understanding of phenomena such as pulsars, solar flares, and the origin of cosmic rays. This space mission is jointly funded by NASA.

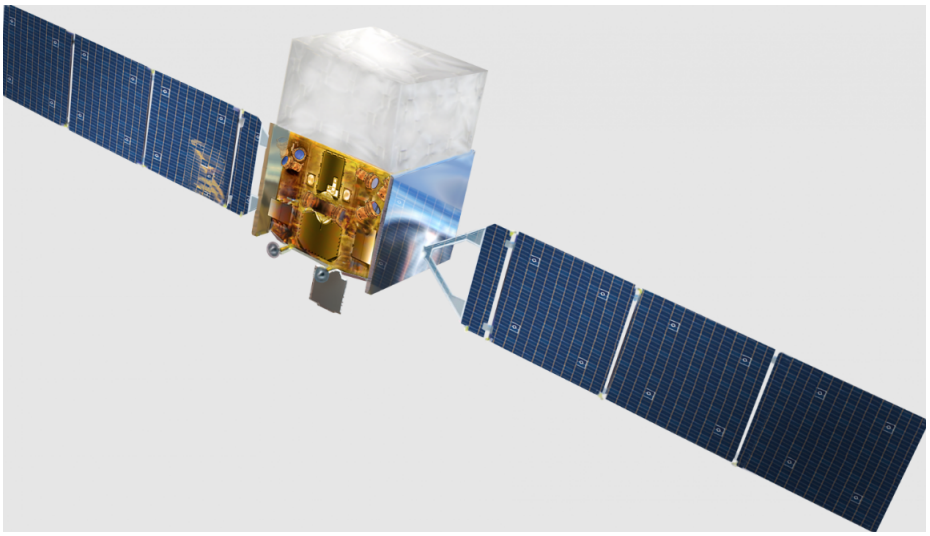

Figure 3.5.2: Fermi Gamma-ray Space Telescope

3.5.3 TAROT telescopes

TAROT(Télescope à action rapide pour les objets transitoires, "Rapid-action telescope for transient objects") is a network of automated telescopes located at three locations around the world that observe automatically without the need for human intervention[64]. The TAROT design was created in 1995 to track early GRB optical emissions. It's worth noting that no optical counterpart had been discovered at the time. Nobody has ever been able to calculate the optical brightness of a GRB's counterpart[73, 74].

Michel Boer, a CNRS researcher at the (Institut de Recherche en Astrophysique et Planétologie) (IRAP) at the time, has led the TAROT project since 1995. The IRAP director provided the initial funds and three engineers (mechanics, electronics, and software) were provided by the (Institut National des Sciences de l'Univers) direction technique (DT-INDU). DT-INDU engineers were replaced by Observatoire de Haute-Provence(OHP) engineers in 2005. The Centre National d'Etudes Spatiales (CNES) has provided recurrent funds since 2005, allowing the installation of two more telescopes in 2006 and 2016.

Because of their large field of view, TAROTs have been used to react to high-energy neutrino triggers provided by the Antares experiment since 2008. Routine scientific programs are carried out outside of GRB or neutrino events: 1175 new variable stars have been discovered[75], occultations of stars by minor planets[76], GAIA calibration quasars[77], Discoveries of supernovae[78], artificial-satellite tracking, and so on. TAROT was able to participate in the first prompt search for gravitational-wave transient electromagnetic

counterparts organized by the LIGO and Virgo teams in 2010 thanks to the knowledge gained from GRB observations[61]. This groundbreaking work served as a dress rehearsal for the GW interferometers' O1 run in 2015.

3.5.3.1 TAROT observations of GRBs

The Gama-ray Coordinate Network (GCN), which connects space satellites and ground telescopes, provides the internet transport protocol service for GRB alerts [79]. TAROT Calern (TCA) saw its first light in 1998, and the following year it was tested and prepared for GRB observations [80]). The CGRO-BATSE experiment provided GRB triggers, and the large error box forced TCA to cover the area with a mosaic of individual pointings. TCA recorded 21 GRBs between 1999 and 2000 [81], confirming the capability of TAROT in early GRB observations. With 20 seconds of exposures within R magnitude 15th, no detection of the early afterglow phase was possible. In the year 2000, the CGRO-BATSE experiment came to an end. HETE-II (NASA, 2020) and INTEGRAL (ESA, 2020) are two new experiments that have started to provide smaller GRB error boxes than TCA's FoV. Swift has provided more than 90% of the GRB triggers observed by TAROTs to date. TCA had 108 alerts, TAROT Chile (TCH) had 77 alerts, and TAROT Reunion (TRE) had three alerts in 2019.

GRB 050525A had a bright optical counterpart, allowing TCA to record its first GRB light curve. TAROT's initial goals were surpassed as a result of these findings. The TAROT light curve was useful because it was obtained during Swift's Earth occultation, avoiding the need to observe the experiment UVOT. The TAROT light curve [82] showing a re-brightening event explained an optical flux.

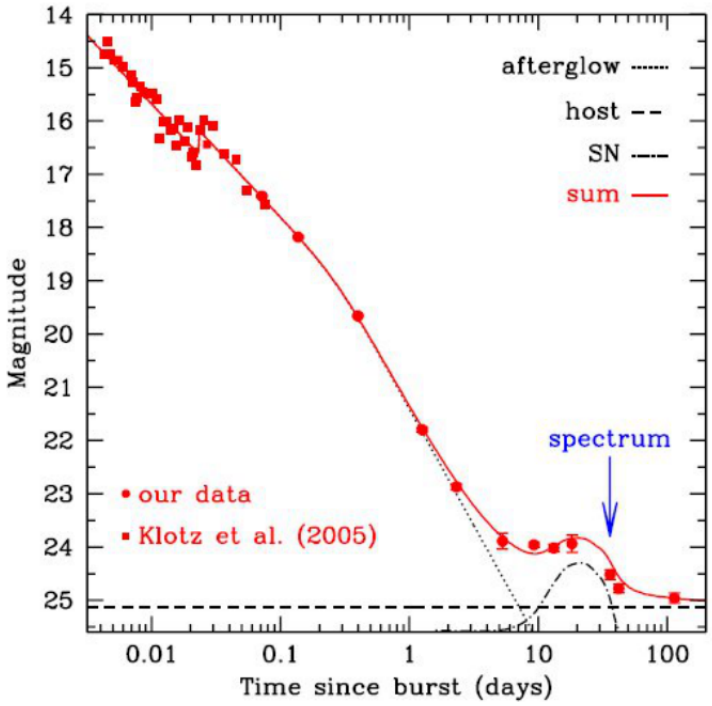

Figure 3.5.3: Light curve of GRB 050525A

Small telescopes are very important in the field of observing astronomical phenomena due to their high speed and are usually robotic, One of the most important robotic telescopes on the scene are the TAROT telescopes, the first of which was designed in 1995 to see the light for the first time a few years later, it has been specifically designed for observing the visible counterpart of cosmic gamma-ray bursts (GRBs)[64]. In the following table are some of the characteristics of the TAROT telescope, which is located at the TCA (TAROT Calern Observatory) [64].

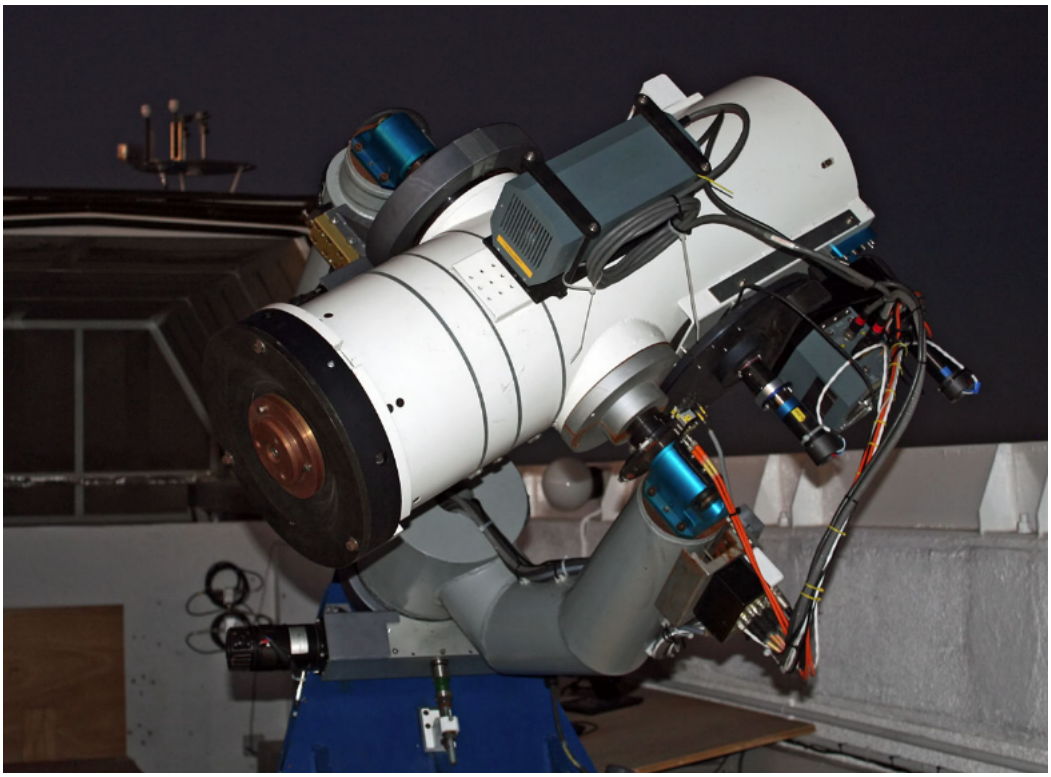

Figure 3.5.4: TAROT Calern (TCA) on La Silla

characteristic	TAROT telescope
Optical system	Newton hyperbolic
Aperture	0.25m
Focal ration	f/3.2
Mount type	Equatorial
Axes maximum speed	60°/s
Axes maximum acceleration	120°/s^2
Maximum pointing time	3s
Pointing precision	5arcmin
Camera manufacturer	ANDOR

Table 3.1: The main characteristics of the TAROT telescope

Chapter 4

National Aures Observatory optimal exploitation

This chapter, is divided into three sections. The first is for the definition of National Aures Observatory and a second for simplified explanation of the optimization method that we used in our research with some of the changes we made to fit the problem, we are about to solve. The third is to project the optimization method on our problem and the steps followed to simulate the RAMSES project and the mathematical structure used.

4.1 National Aures Observatory

Currently, Algeria does not have any astronomical observatories that can follow scientific developments, except for the Algiers Observatory, which is located in the center of the country's capital, whose site quality is no longer sufficient for scientific goals (large light pollution), Therefore, they decided to build a new observatory National Aures Observatory NAO is capable of following the successive scientific developments. This new observatory will be a qualitative leap in the field of scientific research in Algeria in the field of astrophysics due to the carefully chosen location of the observatory for more see [83], Which will be on the Aliness site in Khenchela Governorate in the Aures mountain range east of Algeria, This observatory will have two priorities: the first will be multi-messenger astronomy represented in the search for optical counterparts of gravitational waves (GW) and all transient astronomical phenomena such as GRB, the second priority is about early supernova search, variable stars, asteroids tracking, exoplanets, etc. For transient astronomical phenomena, there are constraints that must be met, one of them is that the error ellipse reaches $100^{\circ 2}$ degrees in the

sky and at the same time, the great speed with which the signal of astronomical phenomena fades. These constraints have been resolved after working with a network of telescopes of up to 12 or 16 TAROT-type telescopes of 400 or 500 millimeters, Each telescope has a wide field of view FoV of about $2.5^{\circ 2}$, and ultra-sensitive CCD or sCMOS cameras, The speed of telescope mounts is very large, up to 80 degrees per second, and acceleration up to 120 deg/s^2. Each telescope will be equipped with filters that enable it to see at different wavelengths. This group is equipped with a large telescope of about 1 meter with a spectrometer capable of tracking the target after its localization, with a system capable of processing images in less than 10 seconds. This is the RAMSES(Robotic Advanced Multimessenger and Space Environment Surveyor) the project, which we are about to simulate and exploit optimally by working to improve its scientific results.

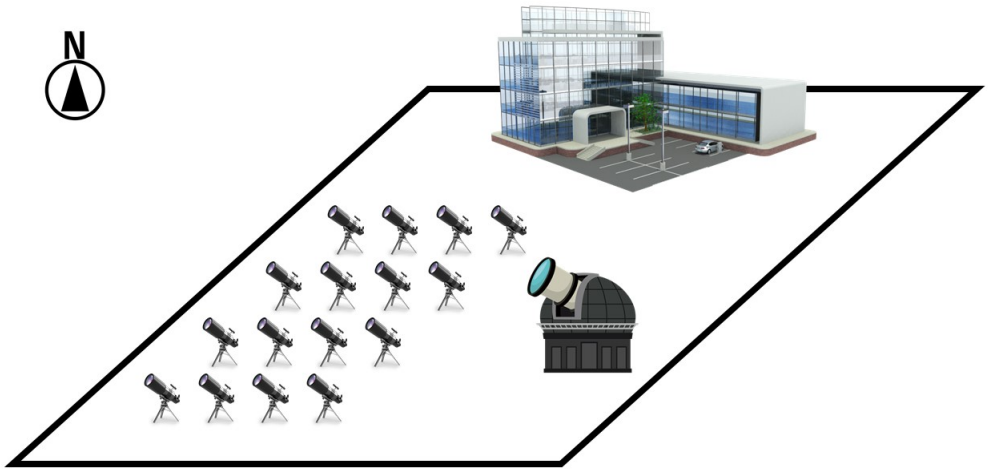

Figure 4.1.1: The RAMSES Project: A Metatelescope composed of 12 to 16 small fast telescopes with a 1m follow-up instrument. Design: Mourad Merzougui,

4.1.1 Scientific Goals of National Aures Observatory

Multi-messenger astronomy (MMA) is a rapidly growing field. Indeed, the detection of gravitational waves generated by the coalescence of binary black holes (BBH), GW 150914 [32], by the Advanced-LIGO experiment was the precursor to a revolution in the study of the Universe: up until now, information was primarily coming from a single particle messenger, the photon; however, the commissioning of gravitational interferometers now allows access to processes that directly involve mass dynamics in the Universe at all scales. More recently,

the detection of GW170817, which corresponds to the coalescence of a binary neutron star system (BNS) [43], was made even more significant because it was followed by the detection of a GRB associated with it (GRB170817) [84, 85], which was also observed in the visible band by terrestrial telescopes. Furthermore, neutrinos are known to be created during supernovae like SN 1987A [86] or in accelerated jets at near-light speeds as measured by IceCube [87] and ANTARES [88].

On the other hand, the electromagnetic spectrum has not yet fully unlocked all of its mysteries, particularly in light of the recent finding of Fast Radio Bursts (FRBs) [89], whose origin is still a mystery despite a number of theories being put forth [90]. Although the origins of these elusive messengers are not yet fully understood, they are either associated with star collapse for those with relatively low energies, or with the enormous acceleration and interaction of matter in shocks for those with higher energies, such as in the Active Galactic Nuclei, or in compact sources, such as for gamma-ray bursts. We are in fact at the beginning of a new era in astronomy known as multimessenger astronomy, in which the simultaneous detection of events in gravitational waves, electromagnetic waves, and neutrinos will provide us with a more complete and likely a very different understanding of the universe than we currently have. This necessitates the use of sensors in the visible and near-infrared spectrum that have extremely wide fields of vision, are rapid to respond, and can adapt to the unique shapes of the vast regions of the celestial sphere where the source is thought to be located. Due to all of these factors, multimessenger astronomy is currently one of the most fascinating areas of research, which is why it was selected as the primary research axis for the future Aures Observatory.

4.1.1.1 Detection and localization of Gamma-Ray Bursts

Although Gamma Ray Bursts were found in 1969, the finding wasn't made public until 1973 [91]. However, it wasn't until the 1990s that we were able to comprehend their physical causes and point of genesis. According to the size of the instrument, a Gamma Ray Burst is defined as a sudden explosion of photons at all energies lasting from a few milliseconds to a few minutes followed by a quick decay phase (t^{-1} or t^{-2}) of the emission that can be seen for a few hours to a few days Figure 4.1.2.

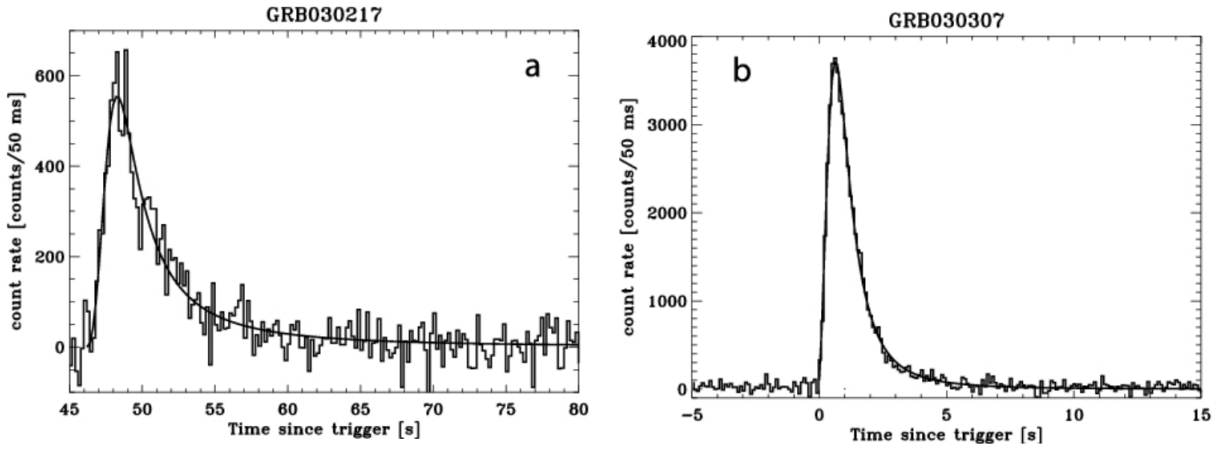

Figure 4.1.2: Examples of GRBs Light Curves

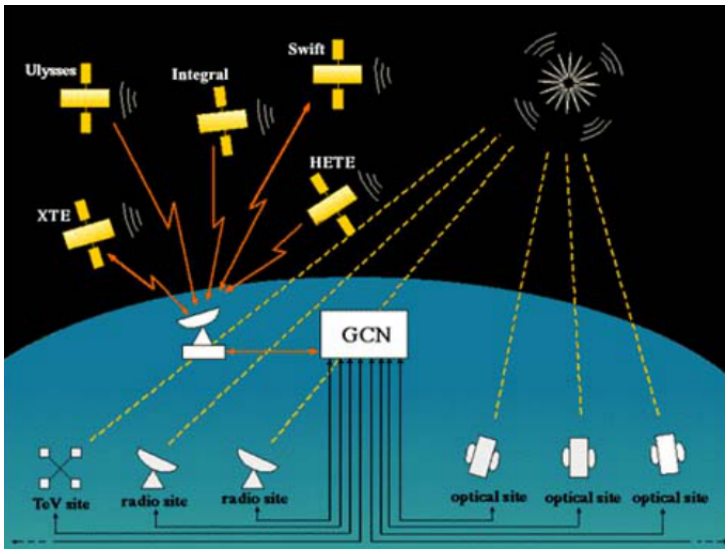

Figure 4.1.3: The physical GCN network

4.1.1.2 Localization of the gravitational waves sources

Localization of gravitational wave sources refers to the process of determining the sky position of a gravitational wave event based on the signals detected by multiple observatories. Since gravitational waves interact very weakly with matter, they can be detected by multiple observatories across the world, allowing scientists to triangulate the source location with increasing accuracy.

The process of localization typically involves comparing the signals detected by two or more gravitational wave observatories, and using the time delay between the signals to

determine the direction of the source in the sky. The accuracy of localization depends on the number and location of the observatories involved, as well as the properties of the gravitational wave signal itself.

The localization of gravitational wave sources is a critical step in follow-up observations, as it allows astronomers to direct other telescopes towards the source location in search of electromagnetic counterparts. The accuracy of localization has improved significantly since the first detection of gravitational waves in 2015, with the current generation of observatories able to pinpoint the location of a gravitational wave source to within a few square degrees of the sky.

Some of the most significant breakthroughs in gravitational wave localization have come from the development of new observatories and data analysis techniques, including the recent addition of the KAGRA detector in Japan and the use of machine learning algorithms to analyze gravitational wave signals.

Overall, the localization of gravitational wave sources is a rapidly evolving field, with new advances and techniques expected to improve our ability to pinpoint the location of these cosmic events in the years to come.

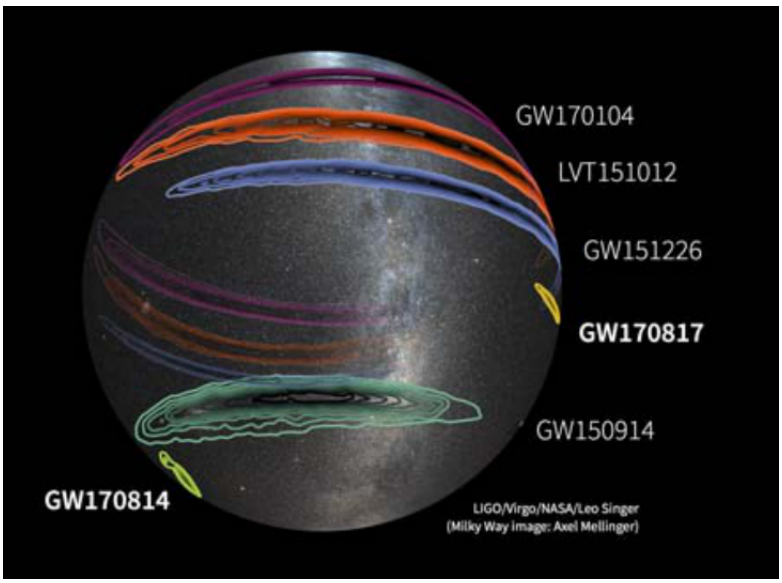

Figure 4.1.4: Skymap of gravitational wave detection patches. Credit: LIGO/Virgo/NASA/Leo Singer

4.1.1.3 Neutrino detection by optical telescopes

While neutrinos are typically detected using specialized detectors like those mentioned in my previous response, it is also possible to indirectly detect neutrinos using optical telescopes. This method is known as neutrino astronomy.

When a high-energy neutrino interacts with matter, it can produce other particles, such as muons, that travel through the surrounding material faster than the speed of light in that medium, producing a shockwave of blue light known as Cherenkov radiation. This Cherenkov radiation can be detected by optical telescopes, providing a way to indirectly detect neutrinos.

Several telescopes have been used in this way, including the IceCube Neutrino Observatory, which uses a combination of neutrino detectors and optical telescopes to study high-energy neutrinos. When a neutrino is detected by the IceCube detector, the telescope array is used to search for any associated Cherenkov radiation in the surrounding ice.

Other telescopes that have been used for neutrino astronomy include the ANTARES telescope located in the Mediterranean Sea, and the KM3NeT telescope, which is currently under construction in the Mediterranean.

While optical telescopes are not able to directly detect neutrinos, they provide an important tool for studying the properties and origins of these elusive particles. By combining information from neutrino detectors with optical observations, scientists are able to gain a more complete understanding of the astrophysical sources that produce neutrinos, and the extreme environments in which they are produced.

4.1.2 RAMSES project as a "hunter" and "follower" of transients events

In this section, we will estimate the number of transient events that RAMSES can observe, given the limiting magnitude of the network of telescopes, which is $m_{lim} = 18$. The limiting magnitude is the faintest magnitude that can be detected by the telescopes in the network. We will focus on GRBs, supernovae, and novae, which are among the most energetic and luminous transient events in the Universe.

It's important to note that the observation conditions are not taken into account in this analysis. In reality, the actual number of events observed by RAMSES will depend on a variety of factors, including the observing conditions, the sensitivity of the instruments, and the specific characteristics of the events themselves. However, this analysis will provide us with a rough estimate of the number of events that RAMSES may be able to detect under

ideal conditions.

4.1.2.1 GRBs rate estimation

The probability of detecting an optical GRB event by RAMSES can be estimated by using the following formula [92]:

$$P_{GRB} = P_{swift}(1 - P_{dark})P_{m<m_{lim}}$$

P_{swift} represents the probability of GRBs being observed by Swift for all GRBs observed in the same year, which is about [1] 90 %.

In our estimation, the "dark" GRB rate, denoted by the term P_{dark}, is taken to be the lower limit of 0.4 [92].

$P_{m<m_{lim}}$probability that the optical GRB is bright enough to be detected with a telescope having a limiting magnitude $m_{lim} = 18$. This probability, which is about 30%, is obtained using {SWIFT CATALOG} [2], by selecting all the events whose magnitude is less than 18 in the past five years. This means that 30 percent of the events observed in the last five years by Swift have a magnitude less than 18. Finally, knowing that about 100 GRBs are observed per year, we conclude that the RAMSES project can observe about 15 optical GRBs/year.

4.1.2.2 SNe rate estimation

To get a proper estimate, we need a simulation with the following input:

- The SN light curve and the SN rates for the different types (divided at least in Ia, Ib/c, II) as a function of redshift.
- The survey parameters: magnitude limit, the field of view, and cadence of the survey (how much area we cover in one day, how often we return in one field).

The output will be the number of SNe detected by the network.

However, since this is not the main purpose of our work, we can estimate very roughly this rate by considering that there are 10^{-3} SNe/square degree at $m_{lim} < 18$ at any given time in the sky.

Let us assume also that the fainter SNe, which largely dominates the magnitude limited search statistics remain at that magnitude for ten days.

[1] https://swift.gsfc.nasa.gov/archive/grb_table/stats/
[2] https://swift.gsfc.nasa.gov/archive/grb_table/

Therefore, if we observe the same field on two consecutive days, we find only a small fraction of new SNe (in our approximation 1/10). The number of SNe that we discover in a year are: $10^{-3} * 365/10 * (2.5 * 2.5) * N * 100 \sim 23 * N$ SN/yr.

where N is the number of telescopes and 100 is the number of fields per telescope per night [93]. With N=16, we find that the RAMSES Project will observe the total number of 370 SNe/yr which is not too distant from the actual discovery rate of the ASAS-SN survey [3].

4.1.2.3 Novae rate estimation

With small telescopes, we can discover novae in the galaxy and in a few very nearby galaxies. [94] report the discovery of about 10 novae per year at a limit magnitude $m_{lim} = 18$, see also [95, 96, 97, 98, 99, 100, 101, 102, 103, 104, 105].

4.1.3 National Aures Observatory Site selection and qualification

Selecting an optimal site is crucial for the success of any astronomical observatory. The location must have dark, clear night skies as frequently as possible. Other important factors include altitude, distance from cities, low humidity, stable weather conditions, and excellent atmospheric seeing.

Figure 4.1.5: Light Pollution. Panoramic picture from Djebel Chelia. Credit: Nassim Seghouani

For the National Aures Observatory, scientists surveyed mountainous areas across Algeria that could potentially host the observatory. Elevated sites were favored because they typically have less light pollution and better seeing conditions. After assessing different candidate

[3]https://www.astronomy.ohio-state.edu/asassn/index.shtml

locations, the Aliness plateau in the Aures mountain range was selected. At an altitude of around 1800 meters, the Aliness site provides sufficiently dark skies. It is distant from major cities, with minimal light pollution visible. To quantify the optical quality, satellite cloud cover data was analyzed. This found the site has approximately 72% clear nights per year - an excellent ratio.

A permanent testing station was established at Aliness to monitor key meteorological and atmospheric parameters. Sensors collect weather data like temperature, humidity, and wind profiles. A specialized seeing monitor called a DIMM continually measures atmospheric seeing conditions. Wide-field all-sky cameras also provide valuable data on cloud cover and night sky clarity.

Figure 4.1.6: Candidate Site for the Aures Observatory (surrounded in red) in the Aliness area. Source: Google Earth

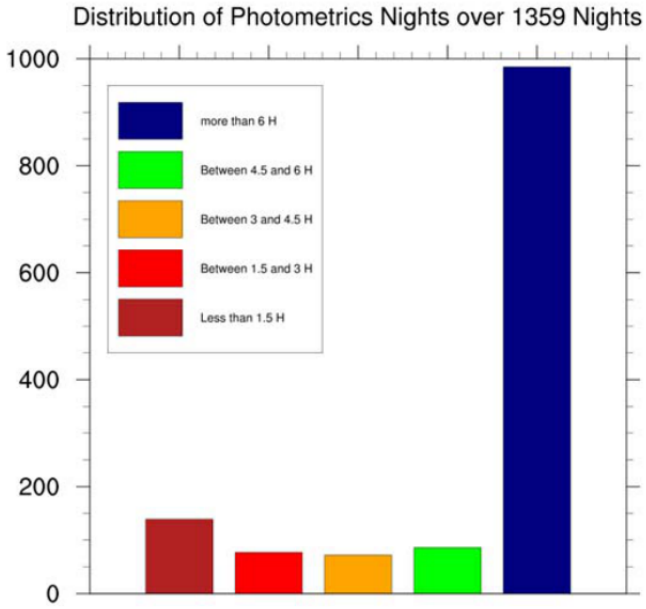

Figure 4.1.7: Statistical distribution of Photometric Nights.

This rigorous site testing regime provides crucial information to validate Aliness as a world-class astronomical observing location that can enable the science goals of the National Aures Observatory. Selecting and characterizing the best possible site is key for ensuring the observatory's future research productivity.

4.2 Assignment problem using branch and bound method (BB)

The assignment problem is a classic optimization problem in the field of computer science, specifically in the area of operations research. It involves finding the optimal assignment of a set of tasks to a set of agents or resources, subject to certain constraints.

In programming, the assignment problem can arise in a variety of contexts, such as task scheduling, resource allocation, and project management. For example, in a software development team, the assignment problem might involve finding the optimal allocation of tasks to team members, based on their skills, availability, and workload.

One common approach to solving the assignment problem is using the Hungarian algorithm or Branch and bound method, which is a well-known algorithm for finding the optimal assignment in a bipartite graph. The algorithm works by finding a set of alternating paths

in the graph that cover all the vertices and then augmenting these paths to improve the assignment.

4.2.1 Branch and bound method (BB)

The BB method is a generic method of solving combinatorial optimization problems. Combinatorial optimization consists in finding a point that minimizes a function, called cost, in a countable set. A naive method of solving this problem is to list all the solutions to the problem, calculate the cost for each, and then give the minimum. Sometimes it is possible to avoid listing solutions that we know, by analyzing the properties of the problem, that they are bad solutions, that is to say, solutions that cannot be the minimum.

The branch and bound method consist of enumerating these solutions intelligently in the sense that, by using certain properties of the problem in question. we represent the execution of the BB method through a tree structure, The root of this tree represents the set of all the solutions to the problem under consideration.

The method begins by considering the original problem with its set of solutions, called the root. Lower and upper-bound procedures are applied at the root. If these two bounds are equal, then an optimal solution is found, and we stop there. Otherwise, the set of solutions is divided into two or more sub-problems, thus becoming a sub-root. The method is then applied recursively to these sub-problems, thus generating a tree structure. If an optimal solution is found for a subproblem, it is feasible, but not necessarily optimal, for the starting problem. As it can be done, it can be used to eliminate all its descendants: if the lower bound of a node exceeds the value of an already known solution then one can affirm that the total optimal solution cannot be contained in the subset of the solution represented by this node. The search continues until all nodes are either explored or eliminated. For more details see[106].

4.2.2 Assignment problem

The assignment problem is how to best assign tasks to agents. Each agent can perform a single task for a given cost and each task must be performed by a single agent. The assignments (that is to say the agent-task pairs) all have a defined cost. The goal is to minimize the total cost of assignments to complete all tasks.

4.2.3 Formal definition

The problem can be stated as follows. Given a set of agents S and a set of tasks T. it is possible to model the problem by a bipartite graph $G = ((S, T),\mathrm{E})$ with a function of weight on the edges $c : E \to \mathbb{R}$. E is a set of edges. The assignment problem, therefore, consists in finding a perfect matching $F \subset E$ minimizing the sum $\sum_{e \epsilon F} c(e)$ of the weights of the edges of F [107].

4.2.4 adaptation with our problem

Description of the problem: We have a network of up to 12 telescopes, At a specific moment t_0, we receive an urgent alert of an astronomical event in a certain region of the sky. We divide this region into small sections. Each telescope scans a section, The condition here is that all telescopes must arrive in the shortest possible time.

From here it becomes clear that we must change the selection condition from **(the smallest total cost)** to **reduce** the **maximum INDIVIDUAL cost** as much as possible**,** Because the cost in our case is **time,** so we choose the case in which the time of arrival of the last telescope to its place is the least possible.

4.3 RAMSES Project simulation

The National Aures Observatory consists of a network of 12 to 16 telescopes, most of the time working on the second priority (tracking supernovas, variable stars, etc.), and at a certain moment t_0 the network receives an urgent alert of the existence of an astronomical event of the first priority (GW or GRB), telescopes abandon their current work and go to try to observe the transit astronomical phenomenon. At first, the telescopes are observing random locations in the sky, and after the urgent alert, they move to scan the error ellipse[4] that the event is supposed to be inside, The distances[5] may be very large, up to 180 degrees.

[4]Error ellipse is the region that contains 95% of all samples that can be drawn from the underlying Gaussian distribution. represents an iso-contour of the Gaussian distribution, and allows you to visualize a 2D confidence interval[108], Three parameters that determine the geometry of error ellipse are semi-major a semi-minor b and the angle θ between the major axis and y-axis

[5]meaning the distance here is the angle that the telescope must rotate to move from one observation position to another

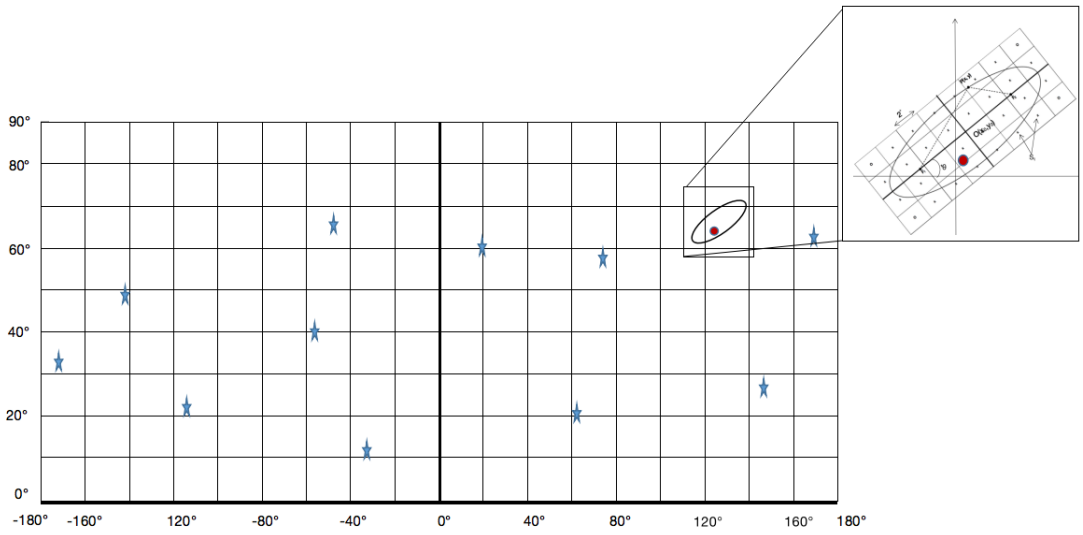

Figure 4.3.1: representation of the sky, the blue stars represent the random locations of the telescopes before the alert, and the red dot inside the ellipse represents the astronomical event that the network of telescopes must find.

The simulation begins with some random choices:

1. Choose a center point for the error ellipse (x_0, y_0) , $x_0 \epsilon\, [-180°, 180°]$ and $y_0 \epsilon\, [0°, 90°]$.
2. Choose the length a and b, to determine the area of the error ellipse, $S = \pi ab$.
3. Chose the rotation angle $\theta \epsilon\, [0, \pi]$.
4. Choosing a point inside the ellipse to represent the astronomical event to be detected (x_G, y_G).
5. Choose N points from the total sky area to represent the random locations of telescopes before the alert.

After selecting these parameters randomly, we have a simulation of the alert. Then we start working on this ellipse and divide it properly into small areas where each telescope is directed to its place using the BB method.

The work steps are summarized in the following steps:

- Divide the error region into squares suitable for TAROT's FoV.
- Find the coordinates of the two ellipse foci.
- Find the coordinates of the centers of the squares.

- Find the points inside the ellipse.
- Create a matrix whose components are the distance between the primary points of the telescopes and the points to be surveyed.
- Observation condition test (did the telescope watch the event).

After finding the final matrix and applying the BB optimization method, each telescope has its destination (coordinates it goes to), if the event is not observed in the new locations, the telescopes are redirected to the new locations. It is redirected until the signal from the astronomical phenomenon is observed.

Let us now explain the previous points in detail.

4.4 Division of the error ellipse

To simulate the RAMSES project, the first thing we do is work on the error ellipse that we receive in the form of an urgent alert from one of the observatories that track astronomical events continuously and that is collaborating with the National Aures Observatory. This alert comes with basic parameters about the astronomical event, through This information we can plot an error ellipse for that event, these parameters are the coordinates of the ellipse's center (x_0, y_0), the lengths $a$and b, the angle θ, it is enough to know the exact location to be scanned by telescopes.

The first thing we will do is divide this area into small parts of a size that fits the TAROT's FoV, in our case we divide it into squares of 2° (two degrees), This is done by drawing a rectangle surrounding the ellipse and dividing it into squares with a side length of 2° (the length and width of the rectangle must be a multiple of 2 so that the number of small squares is an integer) as shown in the figure(4.4.1).

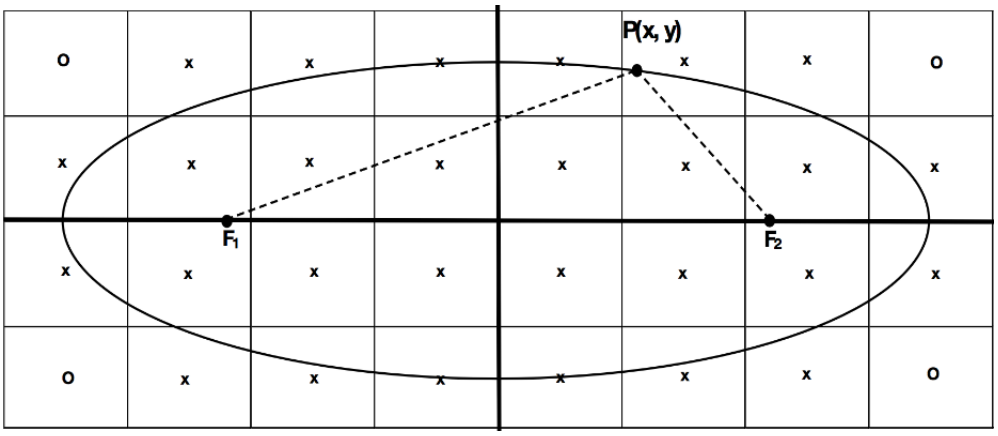

Figure 4.4.1: Method for dividing the rectangle surrounding the error ellipse, each small square has a side of 2 degrees, telescopes must scan all squares inside or intersect with the ellipse.

4.5 Find the coordinates of the two focal and rectangular dimensions

4.5.1 Find the coordinates of the two focal

The general equation of the ellipse (the parametric equation):

$$\begin{cases} x(t) = x_0 + a\cos\theta\cos t - b\sin\theta sint \\ y(t) = y_0 + a\sin\theta\cos t + b\cos\theta\sin t \end{cases} \tag{4.5.1}$$

Where$t$ is the parameter, $t\epsilon\,[0, 2\pi]$ radians, and $O(x_0, y_0)$ ellipse's center coordinates, a and b are the semi-major and semi-minor axes respectively $0 < b < a$, θ is the rotation angle.

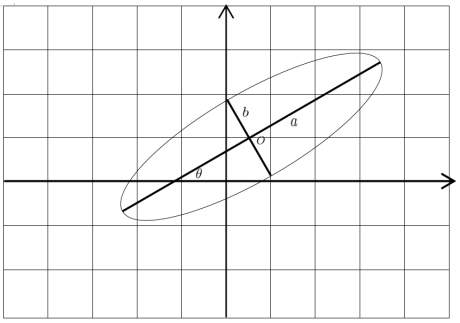

Figure 4.5.1: A representation of an ellipse in the general case, semi-major axis a and semi-minor axis b, and angle of rotation θ.

Now that the parameters a and b are known to us, finding c which is the distance of the two foci from the center of the ellipse is easy, and from it, we can deduce the coordinates of the two foci:

$$O(x_0, y_0)$$

$$F_1(x_0 - c, y_0)$$

$$F_2(x_0 + c, y_0)$$

We can find the general relationship between the coordinates of the two foci after rotation θ.

We apply rotation matrix $R = \begin{pmatrix} \cos\theta & -\sin\theta \\ \sin\theta & \cos\theta \end{pmatrix}$,

Then, the foci coordinates in the general case are:

$$F_1((x_0 - c)\cos\theta - y_0\sin\theta, (x_0 - c)\sin\theta + \cos\theta)$$

$$F_2((x_0 + c)\cos\theta - y_0\sin\theta, (x_0 + c)\sin\theta + y_0\cos\theta)$$

4.5.1.1 Length and width of the rectangle

As we divide the rectangle into squares of side 2, the length of the rectangle must be a multiple of 2 and greater than 2a,

then, $2 * 2\lceil a/2 \rceil$ is the Length and $2 * 2\lceil b/2 \rceil$ is the width. With $\lceil x \rceil$ the ceiling function maps x to the least integer greater than or equal to x.

4.5.1.2 Small squares center coordinates

After the above, we find the coordinates of the centers of the squares :

$$s_{ij}(x_0 - 2\lceil a/2 \rceil + 2j + 1\ , y_0 + 2\lceil b/2 \rceil - 2i - 1)$$

With the integer number i, j $i\epsilon[0, 2\lceil b/2 \rceil - 1]$ and $j\epsilon[0, 2\lceil a/2 \rceil - 1]$

To generalize s_{ij} we apply the rotation matrix R

$$R.s_{ij} = S_{ij} = \begin{pmatrix} (x_0 - 2\lceil a/2 \rceil + 2j + 1)\cos\theta - (y_0 + 2\lceil b/2 \rceil - 2i - 1)\sin\theta \\ (x_0 - 2\lceil a/2 \rceil + 2j + 1)\sin\theta + (y_0 + 2\lceil b/2 \rceil - 2i - 1)\cos\theta \end{pmatrix}$$

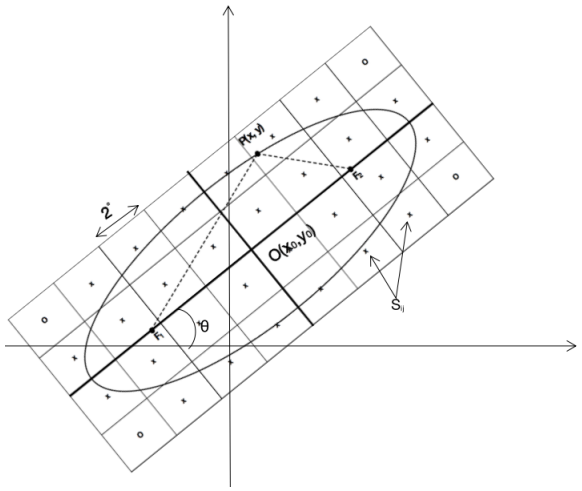

Figure 4.5.2: The general case of dividing an ellipse inside a rectangle into small squares, after the translation and rotation by an angle theta.

4.5.2 Finding points inside the ellipse

All points that telescopes have to scan must be inside the ellipse, all points S_{ij} inside the ellipse verify relation:

$$\|F_1S_{ij}\| + \|F_2S_{ij}\| \leq 2a$$

$\|AB\|$ distance between A and B, a is the semi-major axis.

4.5.3 The first and second scan priority

Telescopes should scan the space inside the ellipse, but since some small squares have a portion of it outside the ellipse, it would be a good idea to leave scanning it until after the squares inside the ellipse is finished.

So we have two scan priorities:

The first priority is all squares whose center is inside the ellipse, see figure (4.5.3a).

The second priority is all squares whose center is outside the ellipse and has a small contribution to the error ellipse, see figure(4.5.3b).

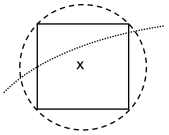

(a) The first scan priority.

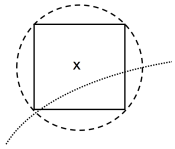

(b) The second scan priority.

Figure 4.5.3: (a) The first priority for scanning is given to every small square whose center is inside the ellipse, whether the square is entirely inside the ellipse or most of it is inside and part of it is outside. (b) The second priority of scanning is given to every small square whose center is outside the ellipse because most of it is outside the ellipse and the probability of the event occurring in the intersection is small.

4.5.4 The cost matrix for BB method

After we finished prioritizing surveys of telescopes and finding the coordinates of the positions of the small squares.

We suppose we have P positions, and we have N telescopes scanning in random positions in the sky, at moment the t_0 the urgent alert comes, the N telescope has to scan all the P positions, here we use the branch and bound method discussed in section 4.2.

In other words, we have a matrix M of dimensions $P \times N$, whose elements contain the time taken for the telescope T_i to reach the position P_j, we divide this matrix into several $N \times N$ small matrices M_i to apply the BB method to it.

$$M = \begin{pmatrix} M_1 \\ M_2 \\ . \\ . \\ . \\ M_i \end{pmatrix}$$

The BB method is applied to small matrices in order (because they are arranged in order of priority), each array simulating the process of pointing telescopes to scan a specific area

within the error ellipse. We apply the BB method to optimize the time required for all telescopes to reach their positions as quickly as possible.

Let's take a simple example to make it more clear.

$$M_1 = \begin{pmatrix} P_1 & P_2 & P_3 & \\ 1 & 7 & 1 & T_1 \\ 1 & 4 & 3 & T_2 \\ 2 & 2 & 1 & T_3 \end{pmatrix}$$

The process of applying the BB method begins with :

- The first stage (start): Choose the smallest cost from each line (even if forbidden values are chosen, such as choosing two values from the same column) and calculate the cost (the largest value in this series).

$$M_1 = \begin{pmatrix} P_1 & P_2 & P_3 & \\ \underline{1} & 7 & 1 & T_1 \\ \underline{1} & 4 & 3 & T_2 \\ 2 & 2 & \underline{1} & T_3 \end{pmatrix}$$

In our case, the underlined numbers were selected $\left\{T_1 \overset{1}{\longmapsto} P_1, T_2 \overset{1}{\longmapsto} P_1, T_3 \overset{1}{\longmapsto} P_3\right\}$, the cost = $max(1,1,1)$=1.

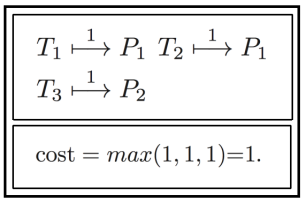

Figure 4.5.4: The first stage (start).

- The second stage: we study all possible states of the first telescope T1 (pointing at p1, p2, or p3), we choose from these possibilities the lowest possible cost,

so with this step, we have found the best orientation for T1.

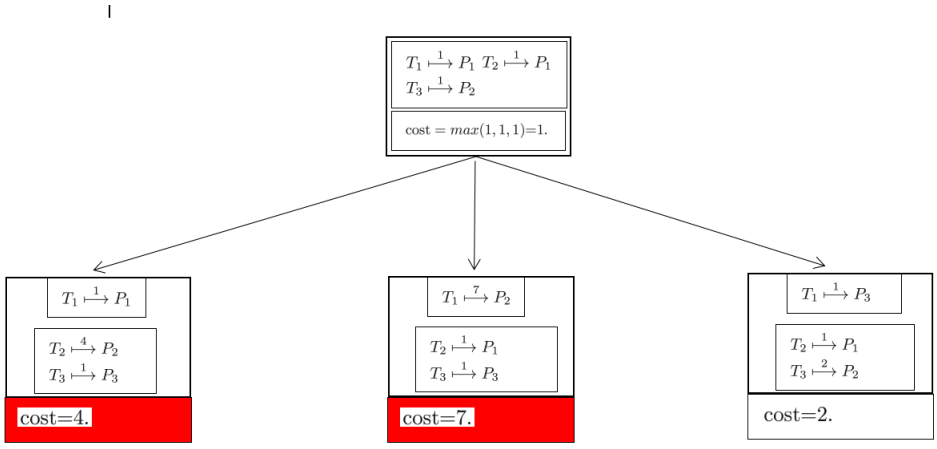

Figure 4.5.5: The second stage.

- The third stage: After we have found the best choice for T1, we study all possible cases of T2.

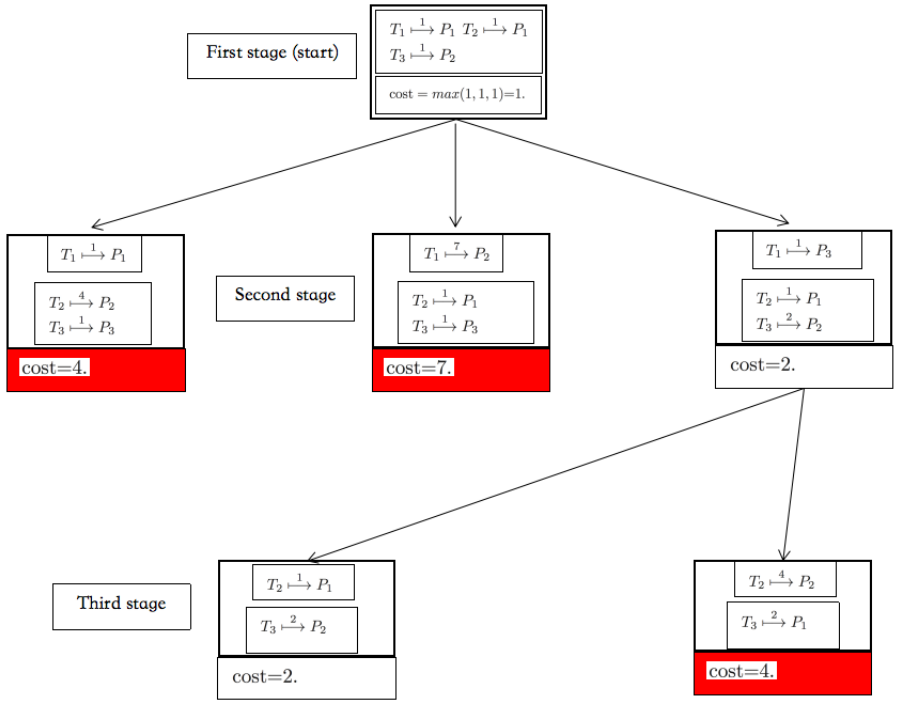

Figure 4.5.6: The third stage.

- In the last stage, after pointing T1 and T2, pointing T3 is automatic, Because it is the only possibility.

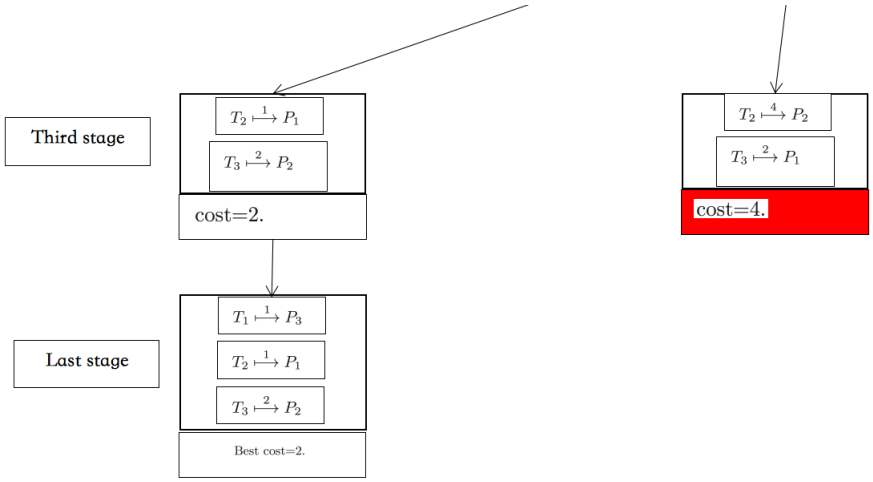

Figure 4.5.7: The last stage.

After the last stage, we get the best cost of all telescopes. So that each telescope can scan a specific area.

4.5.5 Observation condition test

After each telescope went to survey a specific area, the telescope is considered to have observed the astronomical event if the distance between the point representing the astronomical event (x_G, y_G). and the location to which was directed to take the telescope is less than or equal to $\sqrt{2}$ see Figure(4.5.8).

For real telescopes it takes time to process the image to verify the presence of the source or not, for National Aures Observatory the image processing time will be less than 10 seconds[83]. Which requires that we take it into account in the simulation.

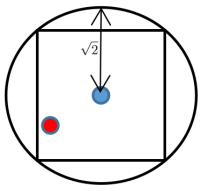

Figure 4.5.8: In the simulation process, to observe the event, the distance between the center of the square represented in blue and the point representing the event (x_G, y_G) represented in red must be less than $\sqrt{2}$. That is, within the circle of FoV.

If the event is not observed after the first pointing of the telescopes, the telescopes are re-pointed with a new array whose values are the time taken by the telescope T_i to reach the

new position P_j. This process is repeated until the astronomical event is observed and the observing telescope is known.

By knowing the distance D from the starting point to the endpoint of each telescope and by knowing the speed of rotation v and acceleration a see Table(4.1), we can calculate the time it takes for each telescope to move from one position to another, and by knowing the number of orientation O times we can know the total time t from starting to observing the event.

$$t = \sum_{i=1}^{O} \left\{ \left(\sqrt{\frac{D_i}{a}} \right) \Theta(2x_0\text{-D}) + \left(\sqrt{\frac{2x_0}{a}} + \frac{D_i - 2x_0}{\text{v}} \right) \Theta(\text{D-}2x_0) - \left(\sqrt{\frac{D_i}{a}} \right) \delta(2x_0\text{-}D_i) \right\} \tag{4.5.2}$$

Where x_0 is the distance traveled by the telescope before reaching its maximum speed, Θ is the Heaviside step function, and δ is Kronecker delta function[6].

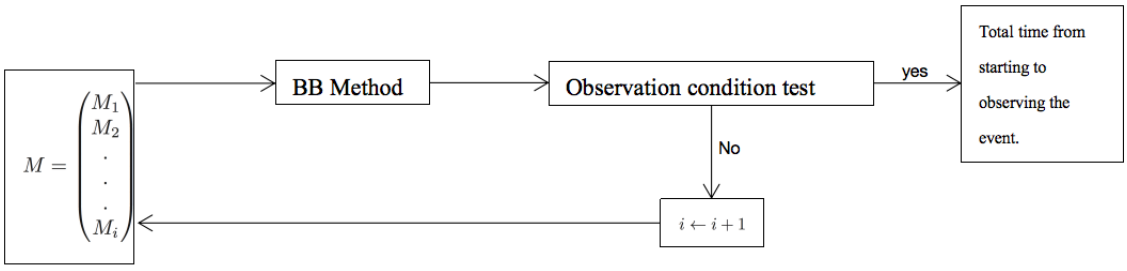

Figure 4.5.9: A diagram showing how the simulation works. From dividing the matrix M and then applying the BB method to the event detection and finding the total time from starting to observing the event.

After completing the method and finding the time required for the set of telescopes (N telescopes) to observe the event, we repeat this simulation process 10,000 times to make a comprehensive statistical study, where we change the number of telescopes used (N=6, N=7, N=8, N=9, N=10, N=11, N=12), in order to study the effect of the number of Telescopes in the time required for observation and change the area of the error ellipse to be scanned from 30 to 140 degrees for study the effect of the area to be surveyed on the number of telescopes needed. In the end, we get the results shown in the next section.

[6] $\delta(2x_0 - D_i) = \begin{cases} 1 & \text{if } 2x_0 = D_i \\ 0 & \text{if } 2x_0 \neq D_i \end{cases}$

Characteristic	Telescope array
Number of telescopes	6 to 12
Axes maximum speed	$80^\circ/s$
Axes maximum acceleration	$120^\circ/s^2$
Images processing time	10 seconds
Field of view	2.5°X2.5°

Table 4.1: The table shows the basic characteristics of the National Aures Observatory used in the simulation.

Chapter 5

Results and discussion

The branch and bound optimization method is a powerful technique that allows us to systematically explore the solution space of a problem by dividing it into smaller subspaces and evaluating each one to find the optimal solution. By applying this method to the RAMSES network of telescopes, we were able to identify the most efficient configuration of telescopes and minimize the time required to detect astronomical signals.

Moreover, the simulation program we developed allowed us to create a virtual environment that closely mimics the behavior of the real-world RAMSES network. This gave us the flexibility to test different scenarios and configurations without the need for costly and time-consuming experiments. By inputting the characteristics of the robotic network and the astrophysical phenomena it studies, we were able to accurately model the behavior of the network and obtain reliable results.

In addition, the study of the effect of the area to be surveyed on the number of telescopes needed is a critical aspect of the optimization of telescope networks. The size of the area to be surveyed can have a significant impact on the number of telescopes required to detect astronomical signals efficiently. By analyzing the relationship between the area to be surveyed and the optimal configuration of telescopes, we can design more effective telescope networks that maximize the detection of astronomical phenomena while minimizing the resources required.

Overall, the use of simulation and optimization methods is a powerful approach to improve the performance of robotic telescope networks. By combining these techniques with detailed knowledge of the characteristics of the network and the astrophysical phenomena it studies, we can design and optimize telescope networks that provide valuable insights into the universe and its workings.

This research, which is to find a way to simulate the future project RAMSES (Robotic Advanced Multimessenger Space Environment Surveyor), Which consists of a network of TAROT-type telescopes, and to ameliorate the Optimization of the time taken to survey an area of approximately 100 degrees square using the fewest number of telescopes, To be able to observe the transitional phenomena (gravitational waves, Gamma-Ray Bursts, astrophysical neutrinos, collapsing supernovae,..), which appear in relatively short periods (from several seconds to about one minute)[83]. In this research, we used the branch and bound optimization method to improve: **i)** The time required for the network of telescopes to find the source signal of the astronomical phenomenon, taking into account the number of telescopes used. And **ii)** the efficiency of telescopes every time they are redirected. And to study **iii)** The effect of the area to be surveyed on the number of telescopes needed.

We obtained the results after writing an integrated simulation program that simulates the RAMSES network, based on the characteristics we have about this robotic network (speed, acceleration, Field of view, image processing time,..) and the astrophysical phenomena it studies, taken from [83], Which indicates the following:

5.1 The effect of the number of telescopes used on the time required to observe.

For N=6: see Figure(5.1.1) We can pick up the source signal 63.33 seconds after the alert, using only 6 telescopes. This means that we can use half of the RAMSES network to get results in about a minute as presented as a challenge in [83] And that with 100% reliability (meaning that all of the 10,000 simulations all took 63.33 seconds or less to detect the signal).

But if we talk about the best 80% of cases**,** these six telescopes were able to pick up the signal 42.78 seconds after the alert. And 50% of the cases were able to pick up the signal in about half a minute 31.5 seconds and this indicates the great efficiency of the method of improving the time taken to pick up the signal by using half the number of telescopes.

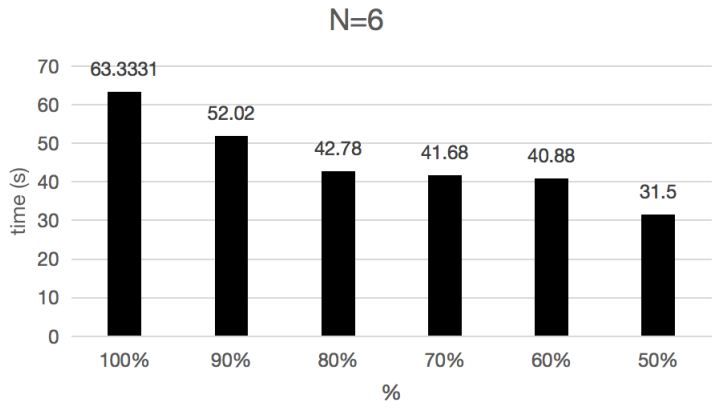

Figure 5.1.1: The histogram represents the time required for 6 telescopes to observe the event, each column represents the time required for the best cases to observe the event.

For N=8: see Figure(5.1.2)The time required to pick up the signal decreased to 42.99 seconds with 100% reliability, using only 8 telescopes. But if we talk about the best 80% of cases, the time required to pick up the signal was 32.3 seconds and 50% of the cases were able to pick up the signal in only 22.21 seconds.

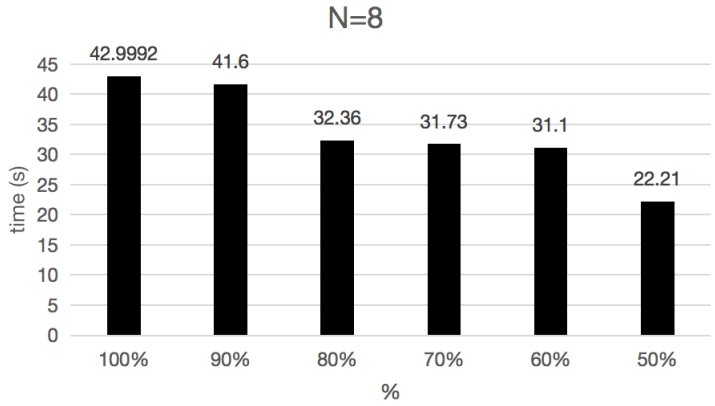

Figure 5.1.2: The histogram represents the time required for 8 telescopes to observe the event, each column represents the time required for the best cases to observe the event.

For N=12: see Figure(5.1.3)As for the maximum use of the network, all cases were able to survey all the areas and pick up the signal in a period not exceeding 31 seconds, As for the best 80% of cases, the signal was detected in only 21.96 seconds.

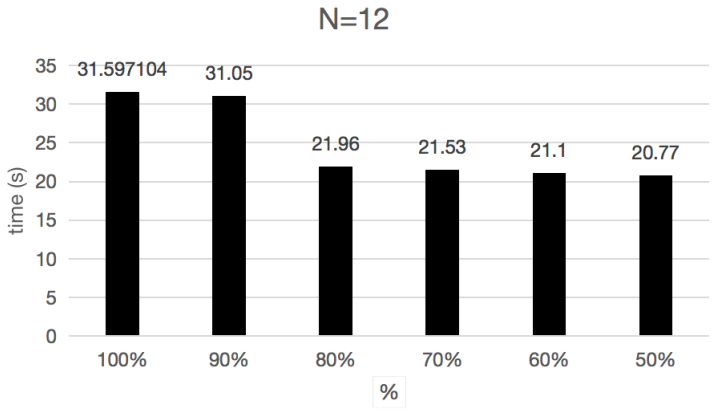

Figure 5.1.3: The histogram represents the time required for 12 telescopes to observe the event, each column represents the time required for the best cases to observe the event.

All the obtained data (for N=6 to 12) are shown in the histograms in **Appendix I**.

5.2 The efficiency of telescopes every time they are redirected.

Now from another point of view, which is the efficiency of telescopes every time they are redirected, we note that the number of orientations does not exceed 6 times even if only 6 telescopes are used.

First pointing: represented in blue in Figure(5.2.1) In first pointing telescopes from their random location into an error ellipse to track the event, 42.04% of the cases were able to catch the signal when we used 12 telescopes, while when using 11 telescopes 39.43% of the cases were able to detect the event immediately after positioning. As for 10 telescopes, 30.76% of the cases were able to complete the monitoring task in the first step. It is expected that this percentage will decrease as the number of telescopes decreases until it reaches 16.82% when using only 6 telescopes.

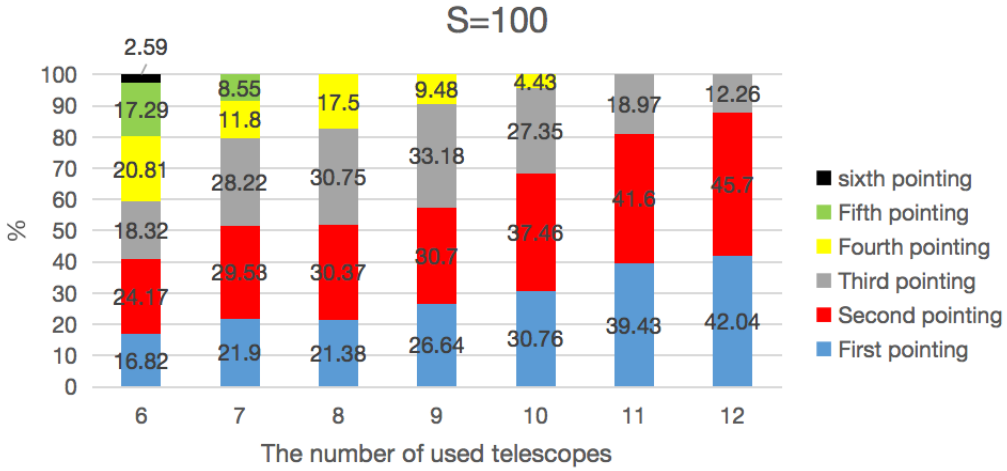

Figure 5.2.1: The efficiency of telescopes every time they are redirected for scanning an error ellipse of $100^{\circ 2}$

Second pointing: represented in red in Figure(5.2.1) After redirecting telescopes in cases that failed to observe the first time, the percentage of cases that captured the signal using 12 telescopes increased by 45.7%, While the percentage increased by 41.6 in the case of 11 telescopes, and 37.46 in the case of 10 telescopes. It is also expected that this percentage will decrease as the number of telescopes in use decreases So that the percentage of observing the signal in the second pointing is increased by (24.17%) using 6 telescopes.

Third pointing: represented in gray in Figure(5.2.1) After the third pointing, the event was observed in all cases that we used 11 and 12 telescopes, and only 4% of the cases were unable to detect the signal when using 10 telescopes, as for 9 telescopes, the probability of observing the event increased by 27,35% after the third pointing. while the probability increased by 18.32 when using 6 telescopes.

Fourth pointing: represented in yellow in Figure(5.2.1) After the fourth pointing, the event was observed in all cases that we used 8, 9, and 10 telescopes, and the percentage of cases that did not see the source signal was 8.55% when using 7 telescopes after the fourth pointing.

Fifth pointing: represented in green in Figure(5.2.1) After the fifth pointing, the event is monitored in all cases of 7 telescopes, as for 6 telescopes, 2.59% of the cases were unable to detect the signal, that is, practically observed the event in all cases. That is, after the sixth pointing of the group of six telescopes, the event will be observed in all cases.

5.3 The effect of the area to be surveyed on the number of telescopes needed.

We studied the small areas that usually come from urgent alerts from gamma-ray tracking satellites such as "swift " (the area of error decreases to about 30 square degrees)[109]. And relatively large areas, come from gravitational wave observatories (error area within 100 degrees and more).

To study the effect of the area to be surveyed on the number of telescopes needed we change the area S to be scanned from $30^{\circ 2}$ to $140^{\circ 2}$ And every time we study the effectiveness of telescopes from N=6 to N=12. The results were as follows:

For S=30: In the case of studying small areas, a group of telescopes may be enough to cover the entire area, so the event will be observed immediately after directing the telescopes see Figure (5.3.1). In the case of an area of 30 square degrees, 9 telescopes are enough to observe directly after the orientation, as for 8 telescopes, they are enough to observe the event, with a rate of 89.4% in their first pointing. While 6 telescopes can observe the event in their first pointing with a percentage of 61.8%, and they need a second pointing to be monitored in all cases.

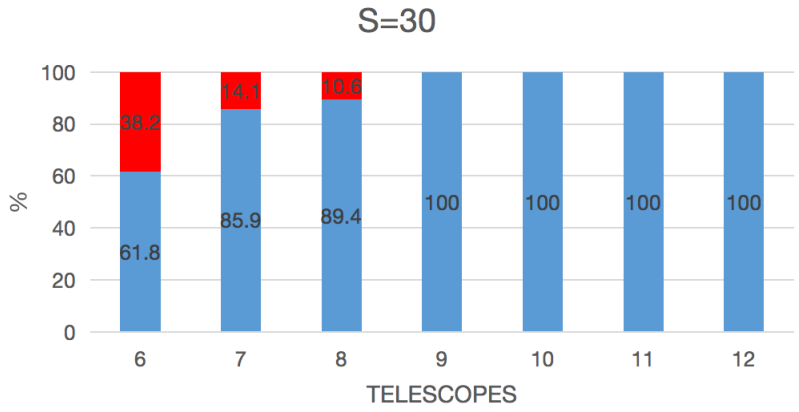

Figure 5.3.1: The histogram represents the effect of the number of telescopes used on the number of re-pointing needed to observe the event in an error ellipse of $30^{\circ 2}$. The blue color represents the first direction to the error area, and the red color represents the second direction.

For S=40: The area is still small as a network of 11 telescopes can observe directly after positioning see Figure(5.3.2). While a network of 8, 9, or 10 needs a second pointing to monitor the event in all cases, as for a network of 6 telescopes, the effectiveness will decrease

and it needs a third direction to be monitored in all cases.

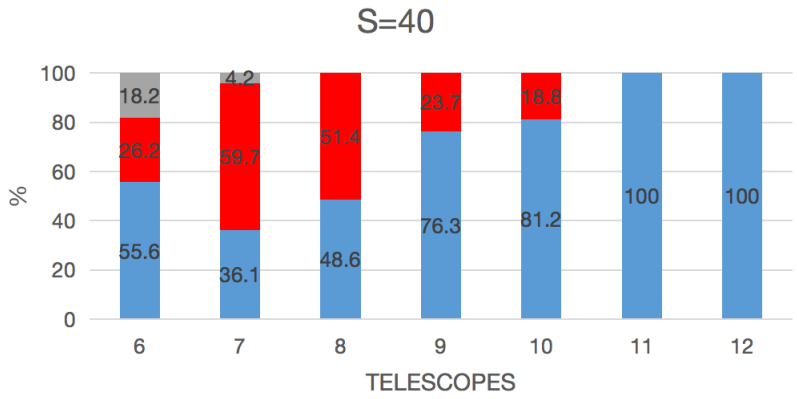

Figure 5.3.2: The histogram represents the effect of the number of telescopes used on the number of re-pointing needed to observe the event in an error ellipse of $40^{\circ 2}$. The blue color represents the first direction to the error area and the red color represents the second direction..etc.

For S=70: A network of 9, 10, and 11 telescopes would need a second pointing to complete the mission. see Figure(5.3.3), In the first pointing, the event was monitored by 64.87%, and after the second guidance, the remaining 35.13% was completed. And a network of six telescopes would need four orienting times to detect the event in all cases. In the first pointing, the event was detected in 22.65% of cases.

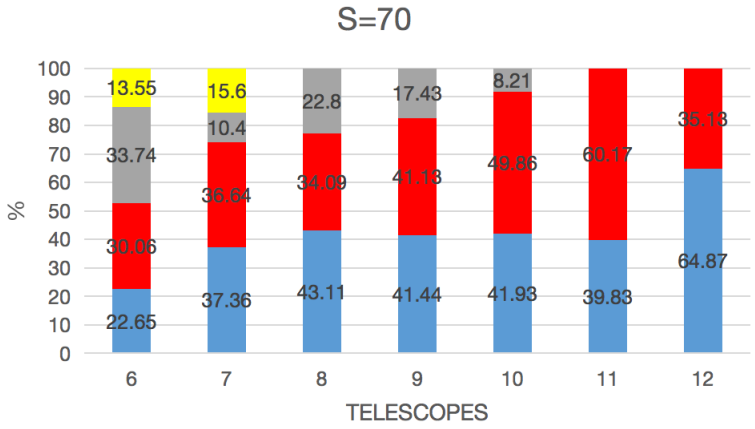

Figure 5.3.3: The histogram represents the effect of the number of telescopes used on the number of re-pointing needed to observe the event in an error ellipse of $70^{\circ 2}$.

For S=110: The area of error ellipse that comes from GW observatories such as LIGO and Virgo is large compared to the error ellipses from satellites that monitor the optical part

associated with gravitational waves such as Swift, In the case of S=110, see Figure (5.3.4), a network of 12 telescopes can observe the event in all cases in three steps, The first pointing was detected in 40.3% of cases, while the second pointing was detected in 35.5% of cases. while a network of 10 telescopes needed 4 times of orientation, As expected, fewer telescopes in the network, the greater the number of orientations needed, as a network of 6 telescopes needs 6 times orientation to complete the observation in all cases.

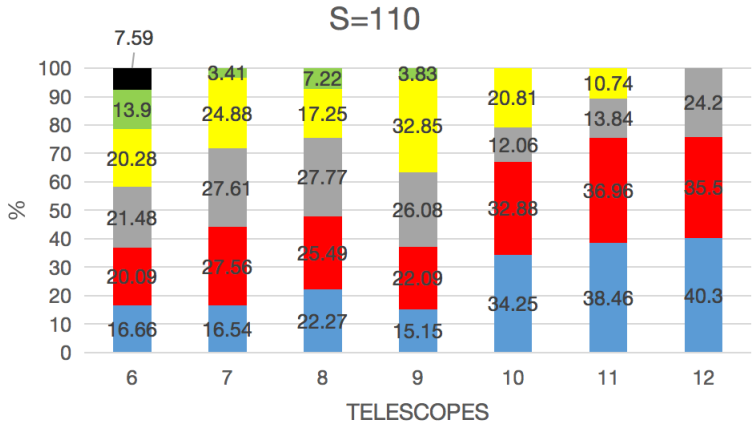

Figure 5.3.4: The histogram represents the effect of the number of telescopes used on the number of re-pointing needed to observe the event in an error ellipse of $110^{\circ 2}$.

For S=140: To survey an area of 140 square degrees, see Figure(5.3.5), using 12 telescopes, we need four times orientation, while using only 6 telescopes we need 8 times of orientation to observe the event in all cases.

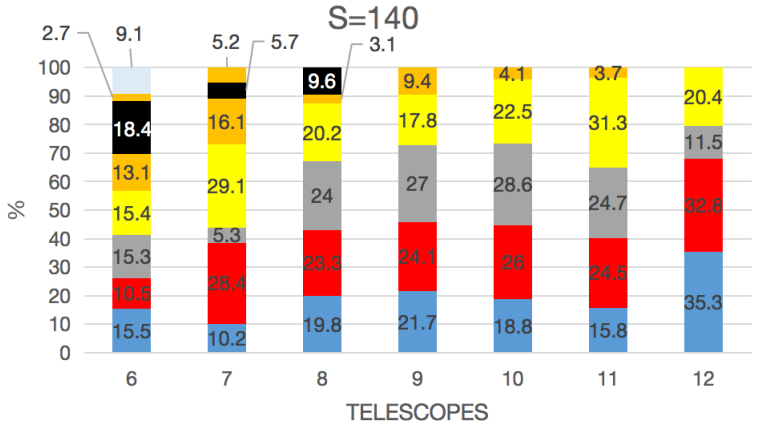

Figure 5.3.5: The histogram represents the effect of the number of telescopes used on the number of re-pointing needed to observe the event in an error ellipse of $140^{\circ 2}$

5.4 Building a strategy to know the number of telescopes needed for observation after knowing the area to be surveyed.

Through the results we obtained, which are shown in **appendix II**, and based on the fact that most of the GRB remains in the prompt[1] phase for about 40 seconds for the TAROT telescope[73], we will choose the number of telescopes needed for each area so that the observation time is about 40 seconds or less.

The results were as shown in the table.

Areas S to be scanned, in square degrees	The number of telescopes needed
less than or equal to 70	6
$70 < S \leq 90$	7
$90 < S \leq 100$	8
$100 < S \leq 120$	9
$120 < S \leq 130$	11
$130 < S \leq 140$	12

Table 5.1: The number of telescopes needed to scan the error ellipse and monitor the event in a period not exceeding 40 seconds with a 100% chance of detection.

Areas S to be scanned, in square degrees	The number of telescopes needed
less than or equal to 110	6
$110 < S \leq 130$	7
$130 < S \leq 140$	8

Table 5.2: The number of telescopes needed to scan the error ellipse and monitor the event in a period not exceeding 40 seconds with an 80% chance of detection.

The importance of this study is that it simulates a network of telescopes under construction, through which we can exploit it optimally, by finding ways to improve the time taken to observe an astronomical event (the least possible), and reduce the number of used telescopes sufficient to monitor the astronomical event in the shortest possible time after the alert.

We can apply the same methodology to other telescopes with known properties. By analyzing the speed, acceleration, and field of view of these telescopes, we can determine

[1]The prompt phase here means the photons observed when the GRB is active

how they can be effectively networked together to improve our ability to observe and study various phenomena in space.

Furthermore, we can also consider the potential impact of new technologies and advancements in telescope design on our ability to network telescopes in the future. As we continue to develop more advanced instruments, we may be able to create even more powerful networks of telescopes that can help us unlock new insights into the universe around us.

Chapter 6

General conclusion and perspectives

In conclusion, the field of gravitational waves and multi-messenger astrophysics has seen tremendous progress in recent years. With the advent of advanced gravitational wave detectors, we have now entered a new era of astrophysics where we can directly observe the universe in a completely new way. The detections of gravitational waves from the mergers of binary black holes, binary neutron stars, and other sources have opened up new avenues of research and have provided us with a wealth of new information about the universe.

Moreover, the combination of gravitational wave observations with other messengers such as electromagnetic radiation and neutrinos has given us a more complete picture of the astrophysical events that give rise to gravitational waves. The ability to detect and follow up on these events with telescopes and observatories across the electromagnetic spectrum has opened up new avenues for discovery and has enabled us to study some of the most extreme objects in the universe.

The National Aures Observatory, with its unique location and capabilities, is well-positioned to contribute to this exciting field of research. The RAMSES project, with its focus on the detection and follow-up of transient events, will play a key role in the search for gravitational wave sources and their electromagnetic counterparts. By optimizing the use of telescopes and other resources, the RAMSES project can help to maximize the scientific output of the National Aures Observatory.

In this thesis, we have developed a branch and bound method for the assignment problem of telescopes for the RAMSES project. This method has allowed us to find an optimal solution for the assignment of telescopes that minimizes the time required for observations while taking into account various constraints such as the size of the error ellipse and the observation conditions.

We have also shown that the number of telescopes required for a given observation area depends on various factors such as the size of the error ellipse and the efficiency of the telescopes. By developing a strategy for estimating the number of telescopes required for a given observation area, we have shown that it is possible to optimize the use of resources and reduce the time required for observations.

Overall, the results of this thesis provide valuable insights into the optimal use of telescopes for the RAMSES project at the National Aures Observatory. With further research and development, these methods could be applied to other observatories and could help to advance our understanding of the universe and the sources of gravitational waves.

perspectives

Further optimization of the RAMSES project: While our thesis has focused on the assignment problem using the branch and bound method and the RAMSES project simulation, there may be additional ways to optimize the project's efficiency and accuracy. For example, we could explore alternative algorithms for the assignment problem or investigate how changes to the telescope configuration could impact the project's performance, We hope to develop more effective methods for estimating parameters and improve the exploitation of this observatory, especially in terms of the time required for monitoring, and in this regard, we will work to introduce methods based on artificial intelligence, such as the PSO method, which is supposed to increase the efficiency of the observatory by a large percentage. because it depends on more variables and needs less time.

Looking ahead, there are several areas of research that could build upon the findings of this thesis. One potential avenue is to further explore the capabilities of the RAMSES project as a tool for detecting and localizing transient events. This could involve investigating additional sources beyond gamma-ray bursts, supernovae, and novae and evaluating the effectiveness of the BB method for assigning telescopes to observation areas in these contexts.

Exploration of new astrophysical phenomena: As our ability to detect and study gravitational waves electromagnetic counterparts and other astrophysical events continues to improve, we may discover entirely new phenomena that were previously unknown. Future research could focus on identifying and characterizing these phenomena, potentially leading to new insights into the nature of the universe.

Another area for future research is to continue improving the assignment problem algorithm used in this thesis. While the BB method showed promising results, there may be other

algorithms or modifications that could yield even better outcomes. Additionally, there may be ways to optimize the algorithm parameters for specific observational conditions or types of transient events.

Finally, there is the potential for future work in the field of multi-messenger astrophysics, particularly with regard to combining gravitational wave observations with other types of messengers such as neutrinos and electromagnetic radiation. As new observatories and instruments come online, there will be more opportunities for identifying and characterizing these events. It will be important to continue developing strategies for coordinating observations across different messengers and to explore the ways in which each messenger can inform and enhance the analysis of the others.

Bibliography

[1] H. A. Lorentz, "Considerations on gravitation," *Koninklijke Nederlandse Akademie van Wetenschappen Proceedings Series B Physical Sciences*, vol. 2, pp. 559–574, 1899. 17

[2] H. Poincaré, "La dynamique de l'électron par henri poincaré (thé dynamics of the electron by henri poincaré)." 17

[3] A. Einstein *et al.*, "On the electrodynamics of moving bodies," *Annalen der physik*, vol. 17, no. 10, pp. 891–921, 1905. 17

[4] F. A. Pirani, "On the physical significance of the riemann tensor," *Acta Physica Polonica*, vol. 15, pp. 389–405, 1956. 17

[5] J. Aasi, B. Abbott, R. Abbott, T. Abbott, M. Abernathy, K. Ackley, C. Adams, T. Adams, P. Addesso, R. Adhikari *et al.*, "Advanced ligo," *Classical and quantum gravity*, vol. 32, no. 7, p. 074001, 2015. 17, 29

[6] V. Frey, "Recherche de signaux d'ondes gravitationnelles transitoires de longue durée avec les données des détecteurs advanced virgo et advanced ligo," Ph.D. dissertation, Université Paris-Saclay, 2018. 20

[7] K. Schwarzschild, "On the gravitational field of a mass point according to einstein's theory," *arXiv preprint physics/9905030*, 1999. 21

[8] R. P. Kerr, "Gravitational field of a spinning mass as an example of algebraically special metrics," *Physical review letters*, vol. 11, no. 5, p. 237, 1963. 21

[9] L. Bildsten, "Gravitational radiation and rotation of accreting neutron stars," *The Astrophysical Journal Letters*, vol. 501, no. 1, p. L89, 1998. 21

[10] C. Cutler, "Gravitational waves from neutron stars with large toroidal b fields," *Physical Review D*, vol. 66, no. 8, p. 084025, 2002. 21

[11] N. Andersson, "A new class of unstable modes of rotating relativistic stars," *The Astrophysical Journal*, vol. 502, no. 2, p. 708, 1998. 21

[12] J. L. Friedman and B. F. Schutz, "Secular instability of rotating newtonian stars," *The Astrophysical Journal*, vol. 222, pp. 281–296, 1978. 21

[13] K. Glampedakis and L. Gualtieri, "Gravitational waves from single neutron stars: an advanced detector era survey," *The Physics and Astrophysics of Neutron Stars*, pp. 673–736, 2018. 22

[14] R. A. Hulse and J. H. Taylor, "Discovery of a pulsar in a binary system," *The Astrophysical Journal*, vol. 195, pp. L51–L53, 1975. 23

[15] A. L. Piro, B. Giacomazzo, and R. Perna, "The fate of neutron star binary mergers," *The Astrophysical Journal Letters*, vol. 844, no. 2, p. L19, 2017. 24

[16] R. L. Forward, "Multidirectional, multipolarization antennas for scalar and tensor gravitational radiation," *General Relativity and Gravitation*, vol. 2, no. 2, pp. 149–159, 1971. 25

[17] R. Weiss and D. Muehlner, "Electronically coupled broadband gravitational antenna," *Research Laboratory of Electronics (MIT),(105)*, vol. 54, 1972. 25

[18] R. Vogt, F. Raab, R. Drever, K. Thorne, and R. Weiss, "Proposal to the nsf for the initial ligo," 1993. 25, 29

[19] R. Vogt, "Proposal for the construction of a large interferometric detector of gravitational waves," *Proposal to the National Science Foundation, California Institute of Technology, Pasadena, California, USA*, 1989. 26

[20] D. Buskulic, "Ondes gravitationnelles, aspects théoriques et expérimentaux." 26

[21] T. Accadia, F. Acernese, M. Alshourbagy, P. Amico, F. Antonucci, S. Aoudia, N. Arnaud, C. Arnault, K. Arun, P. Astone *et al.*, "Virgo: a laser interferometer to detect gravitational waves," *Journal of Instrumentation*, vol. 7, no. 03, p. P03012, 2012. 27

[22] F. a. Acernese, M. Agathos, K. Agatsuma, D. Aisa, N. Allemandou, A. Allocca, J. Amarni, P. Astone, G. Balestri, G. Ballardin *et al.*, "Advanced virgo: a

second-generation interferometric gravitational wave detector," *Classical and Quantum Gravity*, vol. 32, no. 2, p. 024001, 2014. 28

[23] R. Gouaty, "Analyse de la sensibilité du détecteur d'ondes gravitationnelles virgo," Ph.D. dissertation, Université de Savoie, 2006. 28

[24] H. Lück, G. Team *et al.*, "The geo600 project," *Classical and quantum gravity*, vol. 14, no. 6, p. 1471, 1997. 29

[25] C. Affeldt, K. Danzmann, K. Dooley, H. Grote, M. Hewitson, S. Hild, J. Hough, J. Leong, H. Lück, M. Prijatelj *et al.*, "Advanced techniques in geo 600," *Classical and quantum gravity*, vol. 31, no. 22, p. 224002, 2014. 29

[26] Y. Aso, Y. Michimura, K. Somiya, M. Ando, O. Miyakawa, T. Sekiguchi, D. Tatsumi, H. Yamamoto, K. Collaboration *et al.*, "Interferometer design of the kagra gravitational wave detector," *Physical Review D*, vol. 88, no. 4, p. 043007, 2013. 29

[27] B. Iyer, T. Souradeep, C. Unnikrishnan, S. Dhurandhar, S. Raja, A. Kumar, and A. Sengupta, "Proposal of the consortium for indian initiative in gravitational-wave observations (indigo)," *LIGO-India Tech. Rep. No. LIGO-M1100296*, 2011. 30

[28] J. Aasi, J. Abadie, B. Abbott, R. Abbott, T. Abbott, M. Abernathy, T. Accadia, F. Acernese, C. Adams, T. Adams *et al.*, "The characterization of virgo data and its impact on gravitational-wave searches," *Classical and Quantum Gravity*, vol. 29, no. 15, p. 155002, 2012. 30

[29] (2021). [Online]. Available: https://www.lisamission.org/?q=articles/lisa-mission/lisa-mission-gravitational-universe 31

[30] B. P. Abbott, R. Abbott, T. Abbott, S. Abraham, F. Acernese, K. Ackley, C. Adams, V. Adya, C. Affeldt, M. Agathos *et al.*, "Prospects for observing and localizing gravitational-wave transients with advanced ligo, advanced virgo and kagra," *Living reviews in relativity*, vol. 23, no. 1, pp. 1–69, 2020. 33

[31] (2019, 05). [Online]. Available: https://www.ligo.caltech.edu/news/ligo20190502 33

[32] B. P. Abbott, R. Abbott, T. Abbott, M. Abernathy, F. Acernese, K. Ackley, C. Adams, T. Adams, P. Addesso, R. Adhikari *et al.*, "Observation of gravitational waves from a binary black hole merger," *Physical review letters*, vol. 116, no. 6, p. 061102, 2016. 33, 34, 52

[33] B. P. Abbott, R. Abbott, T. Abbott, F. Acernese, K. Ackley, C. Adams, T. Adams, P. Addesso, R. X. Adhikari, V. Adya *et al.*, "Gw170814: a three-detector observation of gravitational waves from a binary black hole coalescence," *Physical review letters*, vol. 119, no. 14, p. 141101, 2017. 35

[34] M. Soares-Santos, D. Holz, J. Annis, R. Chornock, K. Herner, E. Berger, D. Brout, H.-Y. Chen, R. Kessler, M. Sako *et al.*, "The electromagnetic counterpart of the binary neutron star merger ligo/virgo gw170817. i. discovery of the optical counterpart using the dark energy camera," *The Astrophysical Journal Letters*, vol. 848, no. 2, p. L16, 2017. 36

[35] P. Cowperthwaite, E. Berger, V. Villar, B. Metzger, M. Nicholl, R. Chornock, P. Blanchard, W. f. Fong, R. Margutti, M. Soares-Santos *et al.*, "The electromagnetic counterpart of the binary neutron star merger ligo/virgo gw170817. ii. uv, optical, and near-infrared light curves and comparison to kilonova models," *The Astrophysical Journal Letters*, vol. 848, no. 2, p. L17, 2017. 36

[36] M. Nicholl, E. Berger, D. Kasen, B. Metzger, J. Elias, C. Briceño, K. Alexander, P. Blanchard, R. Chornock, P. Cowperthwaite *et al.*, "The electromagnetic counterpart of the binary neutron star merger ligo/virgo gw170817. iii. optical and uv spectra of a blue kilonova from fast polar ejecta," *The Astrophysical Journal Letters*, vol. 848, no. 2, p. L18, 2017. 36

[37] R. Chornock, E. Berger, D. Kasen, P. Cowperthwaite, M. Nicholl, V. Villar, K. Alexander, P. Blanchard, T. Eftekhari, W. Fong *et al.*, "The electromagnetic counterpart of the binary neutron star merger ligo/virgo gw170817. iv. detection of near-infrared signatures of r-process nucleosynthesis with gemini-south," *The Astrophysical Journal Letters*, vol. 848, no. 2, p. L19, 2017. 36

[38] R. Margutti, E. Berger, W.-f. Fong, C. Guidorzi, K. Alexander, B. Metzger, P. Blanchard, P. Cowperthwaite, R. Chornock, T. Eftekhari *et al.*, "The electromagnetic counterpart of the binary neutron star merger ligo/virgo gw170817. v. rising x-ray emission from an off-axis jet," *The Astrophysical Journal Letters*, vol. 848, no. 2, p. L20, 2017. 36

[39] K. Alexander, E. Berger, W. Fong, P. Williams, C. Guidorzi, R. Margutti, B. Metzger, J. Annis, P. Blanchard, D. Brout *et al.*, "The electromagnetic counterpart of the binary

neutron star merger ligo/virgo gw170817. vi. radio constraints on a relativistic jet and predictions for late-time emission from the kilonova ejecta," *The Astrophysical Journal Letters*, vol. 848, no. 2, p. L21, 2017. 36

[40] P. Blanchard, E. Berger, W. Fong, M. Nicholl, J. Leja, C. Conroy, K. Alexander, R. Margutti, P. Williams, Z. Doctor *et al.*, "The electromagnetic counterpart of the binary neutron star merger ligo/virgo gw170817. vii. properties of the host galaxy and constraints on the merger timescale," *The Astrophysical Journal Letters*, vol. 848, no. 2, p. L22, 2017. 36

[41] W.-f. Fong, E. Berger, P. Blanchard, R. Margutti, P. Cowperthwaite, R. Chornock, K. Alexander, B. Metzger, V. Villar, M. Nicholl *et al.*, "The electromagnetic counterpart of the binary neutron star merger ligo/virgo gw170817. viii. a comparison to cosmological short-duration gamma-ray bursts," *The Astrophysical Journal Letters*, vol. 848, no. 2, p. L23, 2017. 36

[42] B. P. Abbott, R. Abbott, T. Abbott, F. Acernese, K. Ackley, C. Adams, T. Adams, P. Addesso, R. Adhikari, V. Adya *et al.*, "Estimating the contribution of dynamical ejecta in the kilonova associated with gw170817," *The Astrophysical Journal Letters*, vol. 850, no. 2, p. L39, 2017. 36

[43] ——, "Gw170817: observation of gravitational waves from a binary neutron star inspiral," *Physical review letters*, vol. 119, no. 16, p. 161101, 2017. 36, 53

[44] J. G. Rollins, *Multimessenger astronomy with low-latency searches for transient gravitational waves*. Columbia University, 2011. 38

[45] M. Branchesi, "Multi-messenger astronomy: gravitational waves, neutrinos, photons, and cosmic rays," in *Journal of Physics: Conference Series*, vol. 718, no. 2. IOP Publishing, 2016, p. 022004. 38

[46] J. E. Beckman, "Multimessenger astronomy," *Multimessenger Astronomy. ISBN: 978-3-030-68372-6. Cham: Springer International Publishing*, 2021. 38

[47] D. Coulter, R. Foley, C. Kilpatrick, M. Drout, A. Piro, B. Shappee, M. Siebert, J. Simon, N. Ulloa, D. Kasen *et al.*, "Swope supernova survey 2017a (sss17a), the optical counterpart to a gravitational wave source," *Science*, vol. 358, no. 6370, pp. 1556–1558, 2017. 38

[48] I. Bartos, "Gravitation and multimessenger astrophysics," Ph.D. dissertation, Columbia University, 2012. 38, 39, 40

[49] J. Abadie, B. Abbott, R. Abbott, T. Accadia, F. Acernese, R. Adhikari, P. Ajith, B. Allen, G. Allen, E. A. Ceron *et al.*, "All-sky search for gravitational-wave bursts in the first joint ligo-geo-virgo run," *Physical Review D*, vol. 81, no. 10, p. 102001, 2010. 38

[50] J. Abadie, B. Abbott, R. Abbott, T. Accadia, F. Acernese, R. Adhikari, P. Ajith, B. Allen, G. Allen, and E. A. Ceron, "Search for gravitational-wave inspiral signals associated with short gamma-ray bursts during ligo's fifth and virgo's first science run," *The Astrophysical Journal*, vol. 715, no. 2, p. 1453, 2010. 38

[51] B. Abbott, R. Abbott, F. Acernese, R. Adhikari, P. Ajith, B. Allen, G. Allen, M. Alshourbagy, R. Amin, S. Anderson *et al.*, "Search for gravitational-wave bursts associated with gamma-ray bursts using data from ligo science run 5 and virgo science run 1," *The Astrophysical Journal*, vol. 715, no. 2, p. 1438, 2010. 38

[52] B. Baret, I. Bartos, B. Bouhou, A. Corsi, I. Di Palma, C. Donzaud, V. Van Elewyck, C. Finley, G. Jones, A. Kouchner *et al.*, "Bounding the time delay between high-energy neutrinos and gravitational-wave transients from gamma-ray bursts," *Astroparticle Physics*, vol. 35, no. 1, pp. 1–7, 2011. 39

[53] V. Van Elewyck, S. Ando, Y. Aso, B. Baret, M. Barsuglia, I. Bartos, E. Chassande-Mottin, I. Di Palma, J. Dwyer, C. Finley *et al.*, "Joint searches between gravitational-wave interferometers and high-energy neutrino telescopes: science reach and analysis strategies," *International Journal of Modern Physics D*, vol. 18, no. 10, pp. 1655–1659, 2009. 39, 41

[54] J. Piscionere, S. Marka, P. Shawhan, J. Kanner, T. Huard, and D. Murphy, "Looc up: locating and observing optical counterparts to unmodeled pulses in gravitational waves," in *American Astronomical Society Meeting Abstracts*, vol. 211, 2007, pp. 99–03. 39

[55] P. S. Shawhan, L. S. Collaboration, V. Collaboration *et al.*, "Looc-up: seeking optical counterparts to gravitational-wave signal candidates," in *American Astronomical Society Meeting Abstracts# 215*, vol. 215, 2010, pp. 406–06. 39

[56] W.-X. Chen and A. M. Beloborodov, "Neutrino-cooled accretion disks around spinning black holes," *The Astrophysical Journal*, vol. 657, no. 1, p. 383, 2007. 39

[57] L. Dessart, C. Ott, A. Burrows, S. Rosswog, and E. Livne, "Neutrino signatures and the neutrino-driven wind in binary neutron star mergers," *The Astrophysical Journal*, vol. 690, no. 2, p. 1681, 2008. 39

[58] E. Waxman and J. Bahcall, "High energy neutrinos from cosmological gamma-ray burst fireballs," *Physical Review Letters*, vol. 78, no. 12, p. 2292, 1997. 39

[59] K. Hirata, T. Kajita, M. Koshiba, M. Nakahata, Y. Oyama, N. Sato, A. Suzuki, M. Takita, Y. Totsuka, T. Kifune *et al.*, "Observation of a neutrino burst from the supernova sn1987a," *Physical Review Letters*, vol. 58, no. 14, p. 1490, 1987. 39

[60] B. Baret, I. Bartos, B. Bouhou, E. Chassande-Mottin, A. Corsi, I. Di Palma, C. Donzaud, M. Drago, C. Finley, G. Jones *et al.*, "Multimessenger science reach and analysis method for common sources of gravitational waves and high-energy neutrinos," *Physical Review D*, vol. 85, no. 10, p. 103004, 2012. 39

[61] J. Abadie, B. Abbott, R. Abbott, T. Abbott, M. Abernathy, T. Accadia, F. Acernese, C. Adams, R. Adhikari, C. Affeldt *et al.*, "Implementation and testing of the first prompt search for gravitational wave transients with electromagnetic counterparts," *Astronomy & Astrophysics*, vol. 539, p. A124, 2012. 41, 48

[62] D. J. White, E. Daw, and V. Dhillon, "A list of galaxies for gravitational wave searches," *Classical and Quantum Gravity*, vol. 28, no. 8, p. 085016, 2011. 41

[63] V. G. Kornilov, V. M. Lipunov, E. S. Gorbovskoy, A. A. Belinski, D. A. Kuvshinov, N. V. Tyurina, N. I. Shatsky, A. V. Sankovich, A. V. Krylov, P. V. Balanutsa *et al.*, "Robotic optical telescopes global network master ii. equipment, structure, algorithms," *Experimental Astronomy*, vol. 33, no. 1, pp. 173–196, 2012. 41

[64] M. Boër, A. Klotz, R. Laugier, P. Richard, J. C. D. Pérez, L. Lapasset, A. Verzeni, S. Théron, D. Coward, and J. Kennewell, "Tarot: a network for space surveillance and tracking operations," in *7th European Conference on Space Debris ESA/ESOC, Darmstadt/Germany*, 2017. 41, 47, 49

[65] D. M. Coward, M. Todd, T. P. Vaalsta, M. Laas-Bourez, A. Klotz, A. Imerito, L. Yan, P. Luckas, A. B. Fletcher, M. Zadnik *et al.*, "The zadko telescope: a southern

hemisphere telescope for optical transient searches, multi-messenger astronomy and education," *Publications of the Astronomical Society of Australia*, vol. 27, no. 3, pp. 331–339, 2010. 41

[66] P. Meszaros, "Gamma-ray bursts," *Reports on Progress in Physics*, vol. 69, no. 8, p. 2259, 2006. 42

[67] C. Kouveliotou, C. A. Meegan, G. J. Fishman, N. P. Bhat, M. S. Briggs, T. M. Koshut, W. S. Paciesas, and G. N. Pendleton, "Identification of two classes of gamma-ray bursts," *The Astrophysical Journal*, vol. 413, pp. L101–L104, 1993. 42

[68] E. Berger, "Short-duration gamma-ray bursts," *Annual review of Astronomy and Astrophysics*, vol. 52, pp. 43–105, 2014. 43

[69] A. Pe'Er, "Physics of gamma-ray bursts prompt emission," *Advances in Astronomy*, vol. 2015, 2015. 43

[70] P. Kumar and B. Zhang, "The physics of gamma-ray bursts & relativistic jets," *Physics Reports*, vol. 561, pp. 1–109, 2015. 43

[71] M. J. Rees and P. Mészáros, "Unsteady outflow models for cosmological gamma-ray bursts," *arXiv preprint astro-ph/9404038*, 1994. 43

[72] F. Daigne and R. Mochkovitch, "Gamma-ray bursts from internal shocks in a relativistic wind: temporal and spectral properties," *Monthly Notices of the Royal Astronomical Society*, vol. 296, no. 2, pp. 275–286, 1998. 43

[73] A. Klotz, M. Boër, J. Atteia, and B. Gendre, "Early optical observations of gamma-ray bursts by the tarot telescopes: Period 2001-2008," *The Astronomical Journal*, vol. 137, no. 5, p. 4100, 2009. 47, 82

[74] M. Boër, A. Klotz, J.-L. Atteia, G. Buchholtz, F. Daigne, J. Eysseric, P. Goldoni, P. Jean, A. Lecavelier Des Etangs, M. Lopez *et al.*, "The gamma-ray burst hunt at la silla the tarot-s very fast moving telescope," *The Messenger*, vol. 113, pp. 45–48, 2003. 47

[75] Y. Damerdji, A. Klotz, and M. Boër, "The tarot suspected variable star catalog," *The Astronomical Journal*, vol. 133, no. 4, p. 1470, 2007. 47

[76] F. Braga-Ribas, B. Sicardy, J. Ortiz, E. Lellouch, G. Tancredi, J. Lecacheux, R. Vieira-Martins, J. Camargo, M. Assafin, R. Behrend *et al.*, "The size, shape, albedo, density, and atmospheric limit of transneptunian object (50000) quaoar from multi-chord stellar occultations," *The Astrophysical Journal*, vol. 773, no. 1, p. 26, 2013. 47

[77] F. Taris, G. Damljanovic, A. Andrei, J. Souchay, A. Klotz, and F. Vachier, "Variability of extragalactic sources: its contribution to the link between icrf and the future gaia celestial reference frame," *Astronomy & Astrophysics*, vol. 611, p. A52, 2018. 47

[78] C. Contreras, M. Phillips, C. R. Burns, A. L. Piro, B. Shappee, M. D. Stritzinger, C. Baltay, P. J. Brown, E. Conseil, A. Klotz *et al.*, "Sn 2012fr: ultraviolet, optical, and near-infrared light curves of a type ia supernova observed within a day of explosion," *The Astrophysical Journal*, vol. 859, no. 1, p. 24, 2018. 47

[79] S. Barthelmy, P. Butterworth, T. Cline, N. Gehrels, G. Fishman, C. Kouveliotou, and C. Meegan, "Bacodine, the real-time batse gamma-ray burst coordinates distribution network," *Astrophysics and Space Science*, vol. 231, no. 1, pp. 235–238, 1995. 48

[80] M. Boër, M. Bringer, A. Klotz, A. Moly, D. Toublanc, G. Calvet, J. Eysseric, A. Leroy, M. Meissonnier, R. Malina *et al.*, "Tarot: Observing gamma-ray bursts" in progress"," *Astronomy and Astrophysics Supplement Series*, vol. 138, no. 3, pp. 579–580, 1999. 48

[81] M. Boër, J. Atteia, M. Bringer, B. Gendre, A. Klotz, R. Malina, and H. Pedersen, "Limits on the early afterglow phase of gamma-ray burst sources from tarot-1," *Astronomy & Astrophysics*, vol. 378, no. 1, pp. 76–81, 2001. 48

[82] A. Klotz, M. Boër, J. Atteia, G. Stratta, R. Behrend, F. Malacrino, and Y. Damerdji, "Early re-brightening of the afterglow of grb 050525a," *Astronomy & Astrophysics*, vol. 439, no. 3, pp. L35–L38, 2005. 48

[83] N. Seghouani, M. Boer, and J. Mimouni, "National aures observatory: A new multimessenger facility," in *Journal of Physics: Conference Series*, vol. 1269, no. 1. IOP Publishing, 2019, p. 012001. 51, 71, 75

[84] A. Goldstein, P. Veres, E. Burns, M. Briggs, R. Hamburg, D. Kocevski, C. Wilson-Hodge, R. Preece, S. Poolakkil, O. Roberts *et al.*, "An ordinary short gamma-ray burst with extraordinary implications: Fermi-gbm detection of grb 170817a," *The Astrophysical Journal Letters*, vol. 848, no. 2, p. L14, 2017. 53

[85] I. Andreoni, K. Ackley, J. Cooke, A. Acharyya, J. Allison, G. Anderson, M. Ashley, D. Baade, M. Bailes, K. Bannister *et al.*, "Follow up of gw170817 and its electromagnetic counterpart by australian-led observing programmes," *Publications of the Astronomical Society of Australia*, vol. 34, 2017. 53

[86] W. D. Arnett, J. N. Bahcall, R. P. Kirshner, and S. E. Woosley, "Supernova 1987a," *Annual review of Astronomy and Astrophysics*, vol. 27, pp. 629–700, 1989. 53

[87] I. Collaboration *et al.*, "South pole glacial climate reconstruction from multi-borehole laser particulate stratigraphy," *Journal of Glaciology*, vol. 59, no. 218, pp. 1117–1128, 2013. 53

[88] S. Adrián-Martínez, A. Albert, M. André, M. Anghinolfi, G. Anton, M. Ardid, J.-J. Aubert, B. Baret, J. Barrios-Martí, S. Basa *et al.*, "Searches for point-like and extended neutrino sources close to the galactic center using the antares neutrino telescope," *The Astrophysical journal letters*, vol. 786, no. 1, p. L5, 2014. 53

[89] D. e. a. Thornton, B. Stappers, M. Bailes, B. Barsdell, S. Bates, N. Bhat, M. Burgay, S. Burke-Spolaor, D. Champion, P. Coster *et al.*, "A population of fast radio bursts at cosmological distances," *Science*, vol. 341, no. 6141, pp. 53–56, 2013. 53

[90] B. D. Metzger, B. Margalit, and L. Sironi, "Fast radio bursts as synchrotron maser emission from decelerating relativistic blast waves," *Monthly Notices of the Royal Astronomical Society*, vol. 485, no. 3, pp. 4091–4106, 2019. 53

[91] R. W. Klebesadel, I. B. Strong, and R. A. Olson, "Observations of gamma-ray bursts of cosmic origin," *The Astrophysical Journal*, vol. 182, p. L85, 1973. 53

[92] J. Greiner, T. Krühler, S. Klose, P. Afonso, C. Clemens, R. Filgas, D. H. Hartmann, A. K. Yoldaş, M. Nardini, A. Rau *et al.*, "The nature of â€śdarkâ€ť gamma-ray bursts," *Astronomy & Astrophysics*, vol. 526, p. A30, 2011. 57

[93] U. Feindt, J. Nordin, M. Rigault, V. Brinnel, S. Dhawan, A. Goobar, and M. Kowalski, "simsurvey: estimating transient discovery rates for the zwicky transient facility," *Journal of Cosmology and Astroparticle Physics*, vol. 2019, no. 10, p. 005, 2019. 58

[94] M. Della Valle and L. Izzo, "Observations of galactic and extragalactic novae," *The Astronomy and Astrophysics Review*, vol. 28, no. 1, p. 3, 2020. 58

[95] C. Allen, "Whole-sky statistics of celestial objects," *Monthly Notices of the Royal Astronomical Society*, vol. 114, no. 4, pp. 387–405, 1954. 58

[96] I. Kopylov, "Comparison of morphological properties and spatial distribution of novae and supernovae," *Proceedings of the Crimean Astrophysical Observatory*, vol. 15, pp. 140–146, 1955. 58

[97] A. Sharov, "Estimate for the frequency of novae in the andromeda nebula and our galaxy." *Soviet Astronomy*, vol. 16, p. 41, 1972. 58

[98] W. Liller and B. Mayer, "The rate of nova production in the galaxy." *Publications of the Astronomical Society of the Pacific*, vol. 99, no. 617, p. 606, 1987. 58

[99] R. Ciardullo, H. C. Ford, R. Williams, P. Tamblyn, and G. H. Jacoby, "The nova rate in the elliptical component of ngc 5128," *Astronomical Journal (ISSN 0004-6256), vol. 99, April 1990, p. 1079-1087, 1339.*, vol. 99, pp. 1079–1087, 1990. 58

[100] S. Van Den Bergh, "Supernova rates: A progress report," *Physics reports*, vol. 204, no. 6, pp. 385–400, 1991. 58

[101] M. della Valle, A. Bianchini, M. Livio, and M. Orio, "On the possible existence of two classes of progenitors for classical novae," *Astronomy and Astrophysics*, vol. 266, pp. 232–236, 1992. 58

[102] M. Della Valle and M. Livio, "On the nova rate in the galaxy," 1994. 58

[103] A. Shafter, "On the nova rate in the galaxy," *The Astrophysical Journal*, vol. 487, no. 1, p. 226, 1997. 58

[104] K. Hatano, D. Branch, A. Fisher, and S. Starrfield, "On the spatial distribution and occurrence rate of galactic classical novae," *Monthly Notices of the Royal Astronomical Society*, vol. 290, no. 1, pp. 113–118, 1997. 58

[105] A. Shafter, R. Ciardullo, and C. Pritchet, "Novae in external galaxies: M51, m87, and m101," *The Astrophysical Journal*, vol. 530, no. 1, p. 193, 2000. 58

[106] A. Levitin, "Introduction to the design and analysis of algorithms addison-wesley," *Boston, MA*, 2003. 61

[107] M. Azmoodeh, *Abstract data types and algorithms.* Springer, 1990. 62

[108] L. Wen and Y. Chen, "Geometrical expression for the angular resolution of a network of gravitational-wave detectors," *Physical Review D*, vol. 81, no. 8, p. 082001, 2010. 62

[109] B. P. Abbott, R. Abbott, T. Abbott, F. Acernese, C. Adams, T. Adams, P. Addesso, R. Adhikari, V. Adya, C. Affeldt *et al.*, "Multi-messenger observations of a binary neutron star merger," *Astrophys. J. Lett.*, vol. 848, no. 2, p. L12, 2017. 79

[110] J. M. Hartman, D. K. Galloway, and D. Chakrabarty, "A double outburst from igr j00291+ 5934: implications for accretion disk instability theory," *The Astrophysical Journal*, vol. 726, no. 1, p. 26, 2010.

[111] M. Wang, S. Chen, and J. Jing, "Effect of gravitational wave on shadow of a schwarzschild black hole," *The European Physical Journal C*, vol. 81, no. 6, pp. 1–13, 2021.

[112] C. L. Fryer, D. E. Holz, and S. A. Hughes, "Gravitational wave emission from core collapse of massive stars," *The Astrophysical Journal*, vol. 565, no. 1, p. 430, 2002.

[113] F. Ryde, L. Borgonovo, S. Larsson, N. Lund, A. von Kienlin, and G. Lichti, "Gamma-ray bursts observed by the integral-spi anticoincidence shield: A study of individual pulses and temporal variability," *Astronomy & Astrophysics*, vol. 411, no. 1, pp. L331–L342, 2003.

[114] J. Camp, S. Barthelmy, L. Blackburn, K. Carpenter, N. Gehrels, J. Kanner, F. E. Marshall, J. L. Racusin, and T. Sakamoto, "Using iss telescopes for electromagnetic follow-up of gravitational wave detections of ns-ns and ns-bh mergers," *Experimental Astronomy*, vol. 36, no. 3, pp. 505–522, 2013.

[115] N. Seghouani, "Un observatoire dans la région des aurès," *African Skies*, vol. 14, p. 44, 2010.

Appendices

Appendix I

In our study, we aimed to investigate how the number of telescopes used affects the time required to observe an astronomical event. We conducted the experiment by varying the number of telescopes used from N=6 to N=12 and measured the time required for the best cases to observe the event for each configuration.

Our study is important because it sheds light on the efficiency of using multiple telescopes in observing astronomical events. Astronomical events are often rare and occur over short timeframes, so maximizing the efficiency of telescope usage is critical to obtaining valuable data.

We used histograms to represent the distribution of the time required for the best cases to observe the event for each configuration. Each column in the histograms represents a different number of telescopes used, ranging from N=6 to N=12. By analyzing the histograms, we can draw conclusions about how the number of telescopes used affects the time required to observe the event.

Our results show that as the number of telescopes used increases from N=6 to N=12, the time required to observe the event decreases. This suggests that using more telescopes can significantly increase the efficiency of observing astronomical events.

However, it is important to note that our study has limitations. We only examined the effect of the number of telescopes used on the time required to observe the event and did not investigate other factors such as the quality of the telescopes or the expertise of the observers. Additionally, the results of our study may not be generalizable to all astronomical events, as different events may have different requirements for observing them.

Overall, our study provides valuable insights into the efficiency of using multiple telescopes to observe astronomical events and highlights the potential benefits of increasing the number of telescopes used in such observations.

Here we show our results about the effect of the number of telescopes used (N=6 to N=12) on the time required to observe the event. Each column in the histograms represents the

time required for the best cases to observe the event.

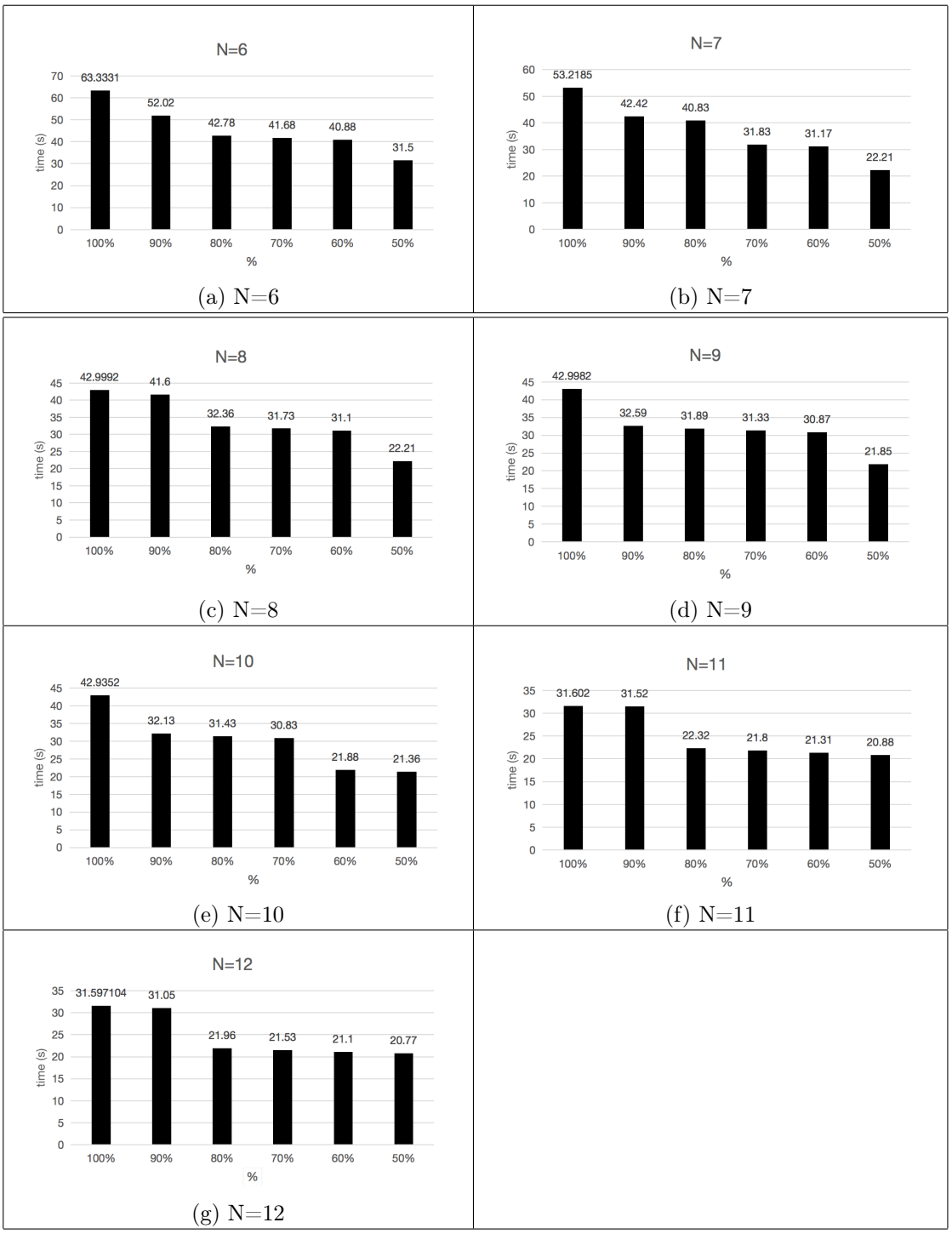

Table 6.1: All the data we obtained after the simulations (N=6 to N=12). each column in the histograms represents the time required for the best cases that observed the event.

Appendix II

In our study, we aimed to investigate the relationship between the number of telescopes used and the area to be surveyed in order to detect an astronomical event. We varied the area to be scanned by the telescopes from 30 to 140 and repeated the simulation 10,000 times for each number of telescopes used, ranging from 6 to 12. To measure the effectiveness of the different configurations, we used probabilities to represent the likelihood of detecting the event after a certain number of pointings. For example, the blue color in our results represents the probability of detecting the event immediately after the first pointing, while the red color represents the probability of detecting the event after the second pointing, and so on. Our study is important because it provides insight into the optimal number of telescopes needed to detect an astronomical event based on the size of the area to be surveyed. This information can be useful in optimizing the use of telescopes and increasing the efficiency of detecting rare and time-sensitive astronomical events.

Our results show that the probability of detecting the event increases as the number of telescopes used increases. However, the rate of increase in probability decreases as the number of telescopes used becomes higher. This suggests that using more telescopes can significantly increase the chances of detecting the event, but the marginal gains decrease as the number of telescopes used becomes higher. Additionally, our results show that the optimal number of telescopes needed to detect the event varies depending on the size of the area to be surveyed. For smaller areas, a smaller number of telescopes may be sufficient, while for larger areas, a higher number of telescopes may be needed.

It is important to note that our study has limitations. We only examined the relationship between the number of telescopes used and the area to be surveyed, and did not investigate other factors such as the quality of the telescopes or the expertise of the observers. Additionally, the results of our study may not be generalizable to all astronomical events, as different events may have different requirements for detecting them.

Overall, our study provides valuable insights into the optimal number of telescopes needed

to detect an astronomical event based on the size of the area to be surveyed. These findings can be useful in optimizing the use of telescopes and increasing the efficiency of detecting rare and time-sensitive astronomical events.

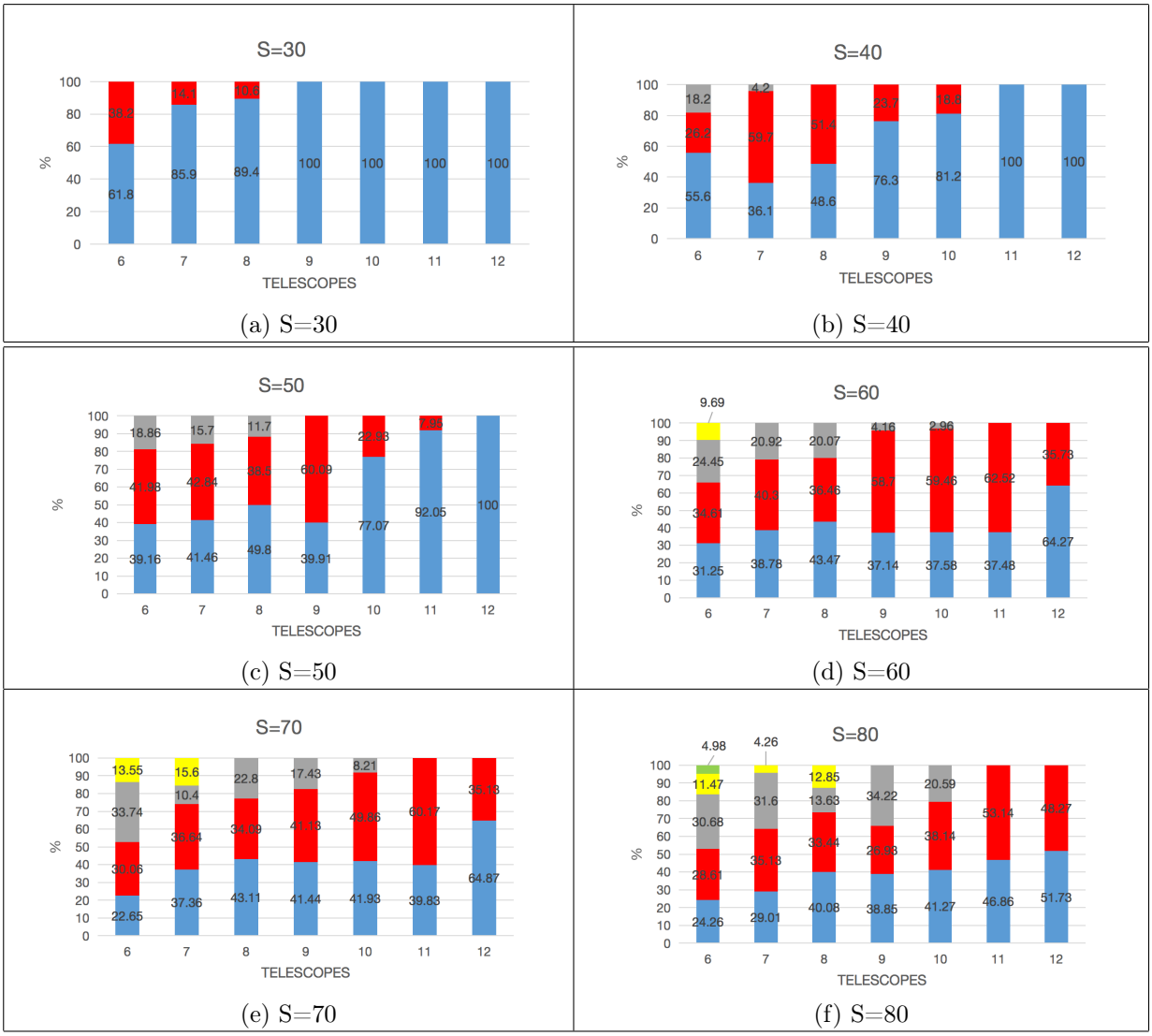

(a) S=30 (b) S=40

(c) S=50 (d) S=60

(e) S=70 (f) S=80

Table 6.2: All the data we have obtained, the area to be scanned by the telescopes is changed from 30 to 80, every time we change the number of used telescopes (from 6 to 12) we repeat the simulation 10,000 times. Each color represents the probability of detecting the event, for example, the blue color represents the probability of detecting the event immediately after the first pointing, the red color represents the second direction, the gray represents the third direction...etc.

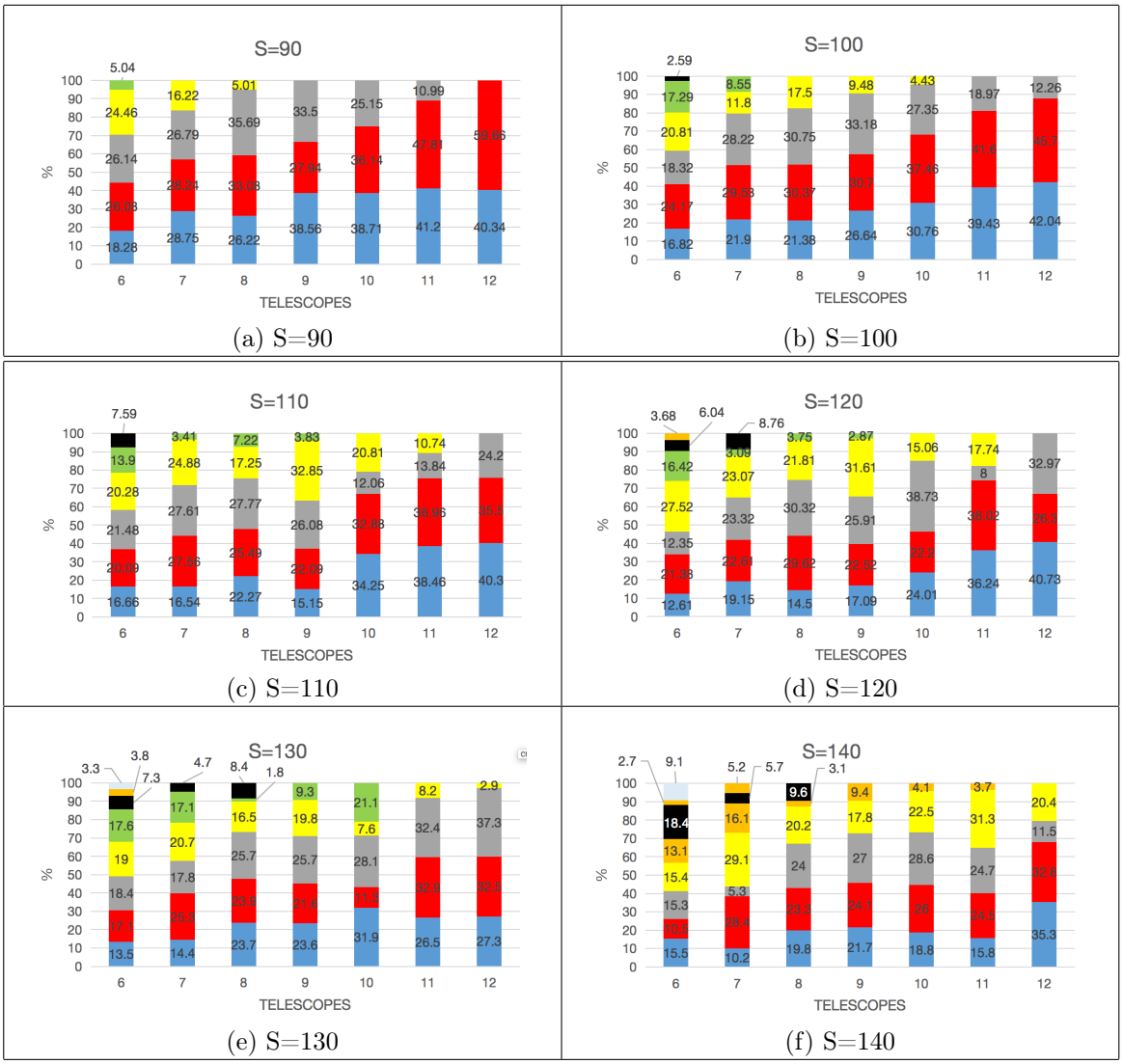

(a) S=90 (b) S=100

(c) S=110 (d) S=120

(e) S=130 (f) S=140

Table 6.3: All the data we have obtained, the area to be scanned by the telescopes is changed from 90 to 140, every time we change the number of used telescopes (from 6 to 12) we repeat the simulation 10,000 times. Each color represents the probability of detecting the event, for example the blue color represents the probability of detecting the event immediately after the first pointing, the red color represents the second direction, the gray represents the third direction...etc.

.

Astronomical and Astrophysical Transactions (*AApTr*), 2023, Vol. 33, Issue 4, pp. 411–436,
ISSN 1055-6796, Photocopying permitted by license only, ©Cambridge Scientific Publishers

A simulation of the RAMSES project and a study of the effect of the number of used telescopes on the time required for the observation of transient astrophysical event

A. Gueboudji, S. Aoudia*

Laboratoire de Physique Théorique, Faculté des Sciences Exactes, Université de Bejaia, Bejaia, 06000 Algeria

Received 15 February, 2022; in revised form 30 July 2022

National Aures Observatory is an observatory under construction, which consists of a network of 12 to 16 small robotic telescopes associated with a large telescope (of 1 or 2 m) equipped with a spectrometer. Its first interests will be multi-messenger astronomy and tracking of the optical counterpart of gravitational waves. In this work, we optimized the use of this network by using the branch and bound optimization method. In addition we also studied the effect of the number of used telescopes on the time required for an observation. This was done by analyzing how the number of used telescopes affects the probability of observing, each time the telescopes are re-pointed. Thus, we could build a strategy allowing us to know the number of telescopes needed for an observation knowing the size of the area to be surveyed. Accordingly we were able to reduce the time required to observe an astronomical event in a sky position error area of about 100°^2} with the use of a network of 6 telescopes to only about a minute. Moreover, we found that by using the whole network of 12 telescopes, 42.04% of the simulation runs were able to observe the event in the first pointing to the error area.

Keywords: Multi-messenger, gravitational waves, gamma ray bursts, RAMSES Project, National Aures Observatory, branch and bound method, TAROT telescope

1 Introduction

Gravitational waves (GW) were first detected by the two detectors of LIGO (Hanford, WA, and Livingston, LA) simultaneously on September 14, 2015 (Aasi et al. 2015; Abbott et al. 2016) which represents an experimental verification of what the theory of general relativity came up with a century ago. About two years later, on August 17, 2017, a gravitational wave signal was detected by Virgo and LIGO (Abbott et

*Email: sofiane.aoudia@univ-bejaia.dz

al. 2017), and a few seconds later, a gamma ray burst (GRB) signal was detected from the same source (Abbott et al. 2017), heralding a new era in astrophysics, meaning multi-messenger astrophysics (MMA). The use of the MMA will enable us to solve major problems in the field of GW astronomy. More precisely, it will allow a much better localization of the GW sources (estimated to 100°^2}, at best, with a GW detection alone (Camp et al. 2013)).

Small telescopes, like TAROT (Télescope à action rapide pour les objets transitoires, "Rapid-action telescope for transient objects") (Klotz et al. 2009), play a very important role in following up and localizing these transient phenomena because they are usually very fast and robotic, which makes them quick to respond and highly effective. In this regard, the implementation of the Robotic Advanced Multimessenger and Space Environment Surveyor (RAMSES) project was chosen by a team of specialists (Seghouani and Boër et al) (Seghouani et al. 2019) at the National Aures Observatory (NAO), which is an association of a network of telescopes of up to 16 very fast robotic telescopes of the TAROT type and a large telescope equipped with a spectrometer, whose main objectives will be multi-messenger astronomy and the observation of optical counterparts of GWs and GRBs, as well as some secondary objectives such as the early supernovae search and tracking of asteroids, variable stars, and exoplanets.

In this research paper, which represents a simulation of this observatory (where some of its main features are given in detail in Section 4), we will see how to exploit it optimally and achieve its primary and secondary objectives completely and consistently, by studying the effect of the number of telescopes on the time needed to observe the astronomical phenomenon and the effectiveness of telescopes in finding the source every time they are redirected.

This simulation programming is based on an optimization method, called branch and bound (BB) technique, which solves the assignment problem that simulates the process of pointing each telescope to a given place to be scanned. The simulation steps are detailed in Section 5. We get interesting results that we will show and discuss in Section 6.

2 Gravitational waves

The notion of GW appears in scientific literature as early as 1900 with Lorentz who imagined a gravitational field to propagate (Lorentz 1899). In 1905, Poincaré introduced the concept of a "gravity wave" (Poincaré 1905). Although, he defined waves that do not carry energy and his concept already conveys the idea that these waves travel at the speed of light.

It was not until 1916 that Einstein theoretically predicted the existence of GWs by presenting them as solutions of his equations (Einstein et al. 1905). To reach this conclusion, Einstein considered a perturbation of flat space-time, thus linearizing his equations.

The nature of GWs was first determined in the early 1950s. Pirani showed the relationship between the Riemann tensor and the strain of the metric (Pirani 1956). Considerations on the perturbation of a flat space-time become a special case of GW theory. Unlike other aspects of general relativity, the experimental validation of

Einstein's predictions about the existence of GWs took many years. the binary pulsar PSR1913+16 provided indirect evidence for the existence of gravitational radiation. But it wasn't until 100 years after Einstein's work that the first direct detection of GWs was made in LIGO detector data in 2015, putting an end to all controversies over their existence for good. (Aasi et al. 2015) Then, on August 17, 2017, Virgo and LIGO detected a gravitational wave (GW170817), and two seconds later, a gamma-ray burst GRB170817A was detected, resulting from the merger of two neutron stars by Fermi-GBM in the same region. This was a scientific achievement with far-reaching prospects in improving the estimation of the GW source parameters. One of the most important problems in this field is, in fact, to improve the estimation of the source localization of the astrophysical phenomenon, which using the initial operating phase of the GW network observatories alone, reaches 100 square degrees (Camp et al. 2013), which is very large. The solution to this problem lies in the combination of GW and electromagnetic (EM) data, in the so-called multi-messenger astronomy.

Multi-messenger astronomy MMA is astronomy that relies on the recording and interpretation of various signals from the same region of the space (Rollins 2011). The four messenger signals are gravitational waves, electromagnetic radiation, cosmic radiation, and particles, including neutrinos, as well as electrons, protons, etc, which are generated by various astrophysical processes (Branchesi 2016), and allow us to obtain various information about the sources in which they occur. The most famous event that is a gateway to multi-messenger astronomy is the GW170817, a source with over 4000 Messengers (Beckman 2021). The GRB 170817A gamma-ray burst was observed by the Fermi Gamma-ray Space Telescope and INTEGRALE, and its optical counterpart SSS17a was detected 11 hours later in the host galaxy NGC4993 at the Las Campanas Observatory (Coulter et al. 2017). This observation was supplemented by other observations in optics by the Hubble Space Telescope and the Dark Energy Survey, in ultraviolet rays by the Swift Gamma-Ray Burst Mission, in X-rays by the Chandra X-ray Observatory and in radio waves by the Karl G. Jansky very large array (VLA) (Beckman 2021).

Gravitational wave sources The most compact known stars are neutron stars and black holes. Cataclysmic phenomena including these compact objects can be of several types, and they can be classified into three families (Frey 2018):

1. Transient sources lasting from a few milliseconds to a few seconds, such as the collapse of a star's core at the end of its life or the fusion of black holes.
2. Continuous and stable sources over the observation time scale. For example, the stochastic background is the accumulation of all emissions since the beginning of the Universe or pulsars.
3. Long-term transient sources range from a few tens of seconds to several minutes.

In this paper, we are particularly interested in long-term transient sources because the RAMSES project telescopes have a slewing time of about 1.5 seconds, and the alert (eg: from Swift-GCN) takes about 20 seconds. Only long-term transient sources can be studied with this network of telescopes during the prompt phase.

Long-term transient sources For most long-term transient sources, the mechanisms involved are associated with complex dynamics and hydrodynamic instabilities for which there is no analytical description. However, there are many models that more or less realistically describe the emitted gravitational waves. Among the most important are Accretion disk instability (ADI) (Wang et al. 2021; Hartman et al. 2010) and Fallback accretion (FA), that can predict the emission of gravitational waves for the duration of the phenomenon, which usually lasts between 20 seconds and 2000 seconds (Fryer et al. 2002). There is also the magnetars, which produce a black hole or a supermassive neutron star that will rapidly collapse into either a black hole or a stable neutron star (Piro et al. 2017). In this case, the amplification of the magnetic field during the fusion phase leads to the appearance of a magnetar inducing a quadrupole moment, which emits gravitational waves.

3 Gamma ray bursts

Gamma-ray bursts (GRBs) are the brightest and most energetic electromagnetic events in our universe. These bursts may last from ten milliseconds to some hours. After this gamma-ray flash, the "afterglow" is emitted for a relatively long time at lower energy and longer wavelengths (X-rays, UV rays, optical, infrared IR, and radio) (Meszaros 2006).

GRBs classification GRB can be classified according to its light curve into two main parts, i) short-duration GRBs (SGRBs) and ii) long-duration GRBs (LGRBs). Events with a $T_{90} < 2$ seconds are classified as short gamma-ray bursts (T_{90} is the time required for a gamma explosion to lose 90 percent of its energy, i.e. from 5% to 95% of the accumulated photon fluence), and events with a $T_{90} > 2$ seconds are classified as long-gamma ray bursts (Kouveliotou et al. 1993).

The SGRB is often caused by the collision of a neutron star binary (NS–NS) or neutron star-black hole binary (NS-BH). Eventually, a large part of the energy is emitted in the form of GW (Berger 2014). On the other hand, most of the phenomena that produce a LGRB are the collapse of a very massive star, which eventually leads to the formation of a black hole or magnetar.

Prompt phase The defining characteristic of a gamma-ray burst is the instantaneous emission (prompt) of gamma rays, The model most often used to explain the phenomenon of gamma-ray bursts is called the fireball model. In this model, a progenitor will expel matter at ultra-relativistic speeds. Even if the fireball is not something homogeneous, this matter is composed almost entirely of electrons. Besides the fact that it must have a geometry (we are talking about jets of particles focused in our direction), the "fireball" is made up of successive layers, which travel at different speeds corresponding to Lorentz factors between 50 and 500, that is to say very close to the speed of light. When two layers come together (the fastest catching up to the other), this forms a semi-relativistic shock called internal shock and this radiation is the Prompt emission (Daigne and Mochkovitch 2002; Kumar and Zhang 2015), During the interaction between the fireball and the environment surrounding, the fireball is braked in the middle, and will begin to radiate energy at all wavelengths,

this radiation is the afterglow emission. The prompt emission takes a relatively short time, from milliseconds to minutes before the afterglow starts (Pe'Er 2015; Ryde et al. 2003; Boër et al. 2003).

Afterglow phase The afterglow is thought to arise from the external shock generated when the projectile collides with the material in the surrounding interstellar medium and is swept away by it (Meszaros 2006). When electrons are accelerated in the presence of a magnetic field, rays of different wavelengths (X-ray, optical, radio) are emitted, and this is called synchrotron emission. All GRBs are observed to have X-ray afterglows, but only about 50% of them have afterglows at optical and radio wavelengths. A GRB is called a dark burst if no afterglow is detected at optical wavelengths (Kumar and Zhang 2015).

4 National Aures Observatory

Currently, Algeria does not have any astronomical observatory that can follow scientific developments, except for the Algiers Observatory, which is located in the center of the country's capital, whose site quality is no longer sufficient for scientific goals (large light pollution), Therefore, a team of specialists (Seghouani and Boër et al.) (Seghouani et al. 2019) decided to build a new observatory, namely the National Aures Observatory NAO, capable of following the successive scientific developments. This new observatory will be a qualitative leap in the field of scientific research in Algeria, especially in that of astrophysics due to the carefully chosen location of the observatory (Seghouani et al. 2019), which will be in the Aliness site in Khenchela Governorate in the Aures mountain range east of Algeria (Seghouani 2010). This observatory will have two priorities: the first will be multi-messenger astronomy represented in the search for optical counterparts of gravitational waves (GW) and all transient astronomical phenomena such as GRB, the second priority is about early supernova search, variable stars, asteroids tracking, exoplanets, etc. For transient astronomical phenomena, some constraints must be met. One of them is that the error ellipse reaches 100°^2} degrees in the sky localization of the GW source and at the same time, the great speed with which the signal of the astronomical phenomena fades. To resolve these constraints, the RAMSES project team proposes working with a network of up to 12 or 16 robotic telescopes of 400 or 500 millimeters. Each telescope has a wide field of view FoV[1] of about 2.5°^2}, and ultra-sensitive CCD or sCMOS cameras. The speed of telescope mounts is very large, up to 80 degrees per second, and its acceleration is up to 120 deg/s^2. Each telescope will be equipped with filters that enable it to see at different wavelengths and connected to a processing system capable of analyzing images in less than 10 seconds. This group is associated with a large telescope of about 1 meter, equipped with a spectrometer and capable of tracking the target after its localization. This is the RAMSES (Robotic Advanced Multimessenger and Space Environment Surveyor) project (Figure 1), which we are

[1]The field of view is the extent of the observable world that is seen at any given moment. In the case of optical instruments or sensors, it is a solid angle through which a detector is sensitive to electromagnetic radiation.

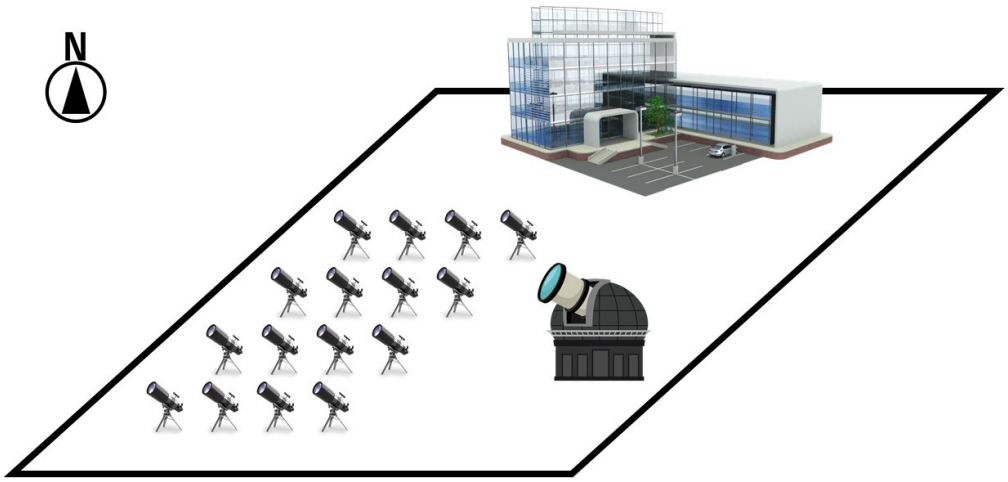

Figure 1 A simple design of The RAMSES Project. An array of 16 small telescopes associated with a large telescope equipped with a spectrometer.

Table 1 The main characteristics of the National Aures Observatory TAROT-type telescopes.

Characteristic	Telescope array
Number of telescopes	12 to 16
Optical system	Newton hyperbolic
Aperture	400 to 500 mm
Focal ration	f/3.2
Mount type	Equatorial
Axes maximum speed	$80^\circ/s$
Axes maximum acceleration	$120^\circ/s^2$
Maximum pointing time	1–1.5 s
Pointing precision	arcsec
Camera manufacturer	CCD or sCMOS
Images processing time	less than 10 seconds
Field of view	$2.5^\circ \times 2.5^\circ$
Limiting magnitude in 10 s	18

about to simulate and exploit optimally by working to improve its scientific results (Seghouani et al. 2019).

TAROT Small telescopes are very important in the field of observing astronomical phenomena due to their high speed and are usually robotic. One of the most important robotic telescopes currently on the scene is the TAROT telescopes (Télescope à Action Rapide pour les Objets Transitoires, "Rapid-action telescope for transient objects"). The first TAROT-type telescope was designed in 1995 (Klotz et al. 2009), and it has been specifically designed for observing the visible counterpart of cosmic gamma-ray bursts (GRBs) (Boër et al. 2017). Table 1 gives some of the main characteristics of the TAROT-type telescopes that we will simulate in this work (Seghouani et al. 2019; Klotz et al. 2009; Boër et al. 2003; Boër et al. 2017).

4.1 RAMSES project as a "hunter" and "follower" of transients events

In this section we will estimate the number of transient events that RAMSES can observe, given that the limiting magnitude of the network of telescopes is $m_{lim} = 18$. The transient events that we consider are GRBs, Supernovae and Novae. The observation conditions are not taken into account.

GRBs rate estimation The probability of detecting an optical GRB event by RAMSES can be estimated by using the following formula (Greiner et al. 2011):

$$P_{GRB} = P_{swift}(1 - P_{dark})P_{m<m_{lim}}$$

P_{swift} represents the probability of GRBs being observed by Swift for all GRBs observed in the same year, which is about[2] 90%.

In our estimation, the "dark" GRB rate, denoted by the term P_{dark}, is taken to be the lower limit of 0.4 (Greiner et al. 2011).

$P_{m<m_{lim}}$ probability that the optical GRB is bright enough to be detected with a telescope having a limiting magnitude $m_{lim} = 18$. This probability, which is about 30%, is obtained using SWIFT CATALOG[3], by selecting all the events whose magnitude is less than 18 in the past five years. This means that 30 percent of the events observed in the last five years by Swift have a magnitude less than 18. Finally, knowing that about 100 GRBs are observed per year, we conclude that the RAMSES project can observe about 15 optical GRBs/year.

SNe rate estimation To get a proper estimate, we need a simulation with the following input:

a) the SN light curve and the SN rates for the different types (divided at least in Ia, Ib/c, II) as function of redshift; (b) the survey parameters: magnitude limit, field of view and cadence of the survey (how much area we cover in one day, how often we return in one field).

The output will be the number of SNe detected by the network.

However, since this is not the main purpose of our work, we can estimate very roughly this rate by considering that there are 10^{-3} SNe/square degree at $m_{lim} < 18$ at any given time in the sky. Let us assume also that the fainter SNe, which largely dominates the magnitude limited search statistics, remains at that magnitude for ten days. Therefore, if we observe the same field in two consecutive days, we find only a small fraction of new SNe (in our approximation 1/10). The number of SNe that we discover in a year are: $10^{-3} \times 365/10 \times (2.5 \times 2.5) \times N \times 100 \sim 23 \times N$ SN/year, where N is the number of telescopes and 100 is the number of field per telescope per night (Feindt et al. 2019). With $N = 16$, we find that the RAMSES Project will observe the total number of 370 SNe/yr which is not too distant from the actual discovery rate of the ASAS-SN survey[4].

Novae rate estimation With a small telescopes we can discover novae in the galaxy and in few very nearby galaxies. (Della Valle et al. 2020) report the discovery

[2]https://swift.gsfc.nasa.gov/archive/grb_table/stats/
[3]https://swift.gsfc.nasa.gov/archive/grb_table/
[4]https://www.astronomy.ohio-state.edu/asassn/index.shtml

of about 10 novae per year at a limit magnitude $m_{lim} = 18$, see also (Allen. 1954; Kopylov 1955; Sharov. 1972; Liller et al. 1987; Ciardullo et al. 1990; Van Den Bergh. 1991; Della Valle et al. 1992; Della Valle et al. 1994; Shafter. 1997; Hatano et al. 1997; Shafter et al. 2000).

5 Simulation and work method

This section is divided into two subsections. The first is a simplified explanation of the optimization method that we used in our research with some of the changes we made to fit the problem we are about to solve. The second is to project the optimization method on our problem and the steps followed to simulate the RAMSES project and the mathematical structure used.

5.1 Assignment problem using branch and bound method

5.1.1 Branch and bound method

The BB method is a generic method of solving combinatorial optimization problems. Combinatorial optimization consists in finding a point that minimizes a function, called cost, in a countable set. A naive method of solving this problem is to list all the solutions to the problem, calculate the cost for each, and then give the minimum. Sometimes it is possible to avoid listing solutions which we know, by analyzing the properties of the problem, that they are bad solutions, that is to say, solutions that cannot be the minimum.

The branch and bound method consists of enumerating these solutions intelligently by using certain properties of the problem in question. We represent the execution of the BB method through a tree structure. The root of this tree represents the set of all the solutions of the problem under consideration.

The method begins by considering the original problem with its set of solutions, called the root. Lower and upper bound procedures are applied at the root. If these two bounds are equal, then an optimal solution is found, and we stop there. Otherwise, the set of solutions is divided into two or more sub-problems, thus becoming a sub-root. The method is then applied recursively to these sub-problems, thus generating a tree structure. If an optimal solution is found for a subproblem, it is feasible, but not necessarily optimal, for the starting problem. As it can be done, it can be used to eliminate all its descendants if the lower bound of a node exceeds the value of an already known solution. Thus, one can affirm that the total optimal solution cannot be contained in the subset of the solution represented by this node. The search continues until all nodes are either explored or eliminated. For more details see (Levitin 2003).

5.1.2 Assignment problem

The assignment problem is how to best assign tasks to agents. Each agent can perform a single task for a given cost and each task must be performed by a single agent. The assignments (that is to say the agent-task pairs) all have a defined cost. The goal is to minimize the total cost of assignments to complete all tasks.

Formal definition The problem can be stated as follows. Given a set of agents S and a set of tasks T, it is possible to model the problem by a bipartite graph $G = ((S, T),\mathrm{E})$ with a function of weight on the edges $c : E \to \mathbb{R}$. E is a set of edges. The assignment problem, therefore, consists in finding a perfect matching $F \subset E$ minimizing the sum $\sum_{e \epsilon F} c(e)$ of the weights of the edges of F (Azmoodeh 1990).

Adaptation with our problem In our case, we have a network of up to 12 telescopes. At a specific moment t_0, we receive an urgent alert of an astronomical event in a certain region of the sky. We divide this region into small sections. Each telescope scans a section and the condition here is that all telescopes must arrive to their target in the shortest possible time.

From here it becomes clear that we must change the selection condition from **(the smallest total cost)** to **reduce** the **maximum individual cost** as much as possible**.** Because the cost in our case is **time,** so we choose the case in which the time of arrival of the last telescope to its place is the least possible.

5.2 RAMSES Project simulation

The National Aures Observatory consists of a network of $N \epsilon [6, 12]$ telescopes, most of the time working on the second priority (tracking supernovas, variable stars, etc.) (Figure 2), and at a certain moment t_0 the network receives an urgent alert of the existence of an astronomical event of the first priority (GW or GRB). Telescopes abandon their current work and go to try to observe the transit astronomical phenomenon. At first, the telescopes are observing random locations in the sky, and after the urgent alert, they move to scan the error ellipse[5] that the event is supposed to be inside. The three parameters that determine the geometry of an error ellipse are the semi-major axis a, the semi-minor axis b and the angle θ between the major axis and the y-axis. Note here that the distances[6] between the initial positions of the telescopes and their targets maybe very large, up to 180 degrees.

After fixing the number N of telescopes, the simulation begins with some random choices:

1. Choose a center point for error ellipse (x_0, y_0), $x_0 \epsilon [-180°, 180°]$ and $y_0 \epsilon [0°, 90°]$.
2. Choose the length a and b, to determine the area of the error ellipse, $S = \pi ab$.
3. Choose the rotation angle $\theta \epsilon [0, \pi]$.
4. Choosing a point inside the ellipse to represent the astronomical event to be detected (x_G, y_G).
5. Choose N points from the total sky area to represent the random locations of telescopes before the alert.

After selecting these parameters randomly, which is equivalent to a simulation of the initial conditions preceding the alert, we start working on this ellipse and divide it

[5]Error ellipse is the region that contains 95% of all samples that can be drawn from the underlying Gaussian distribution. It represents an iso-contour of the Gaussian distribution, and allows you to visualize a 2D confidence interval (Wen and Chen 2010).

[6]Distance means here the angle that the telescope must rotate to move from one observation position to another.

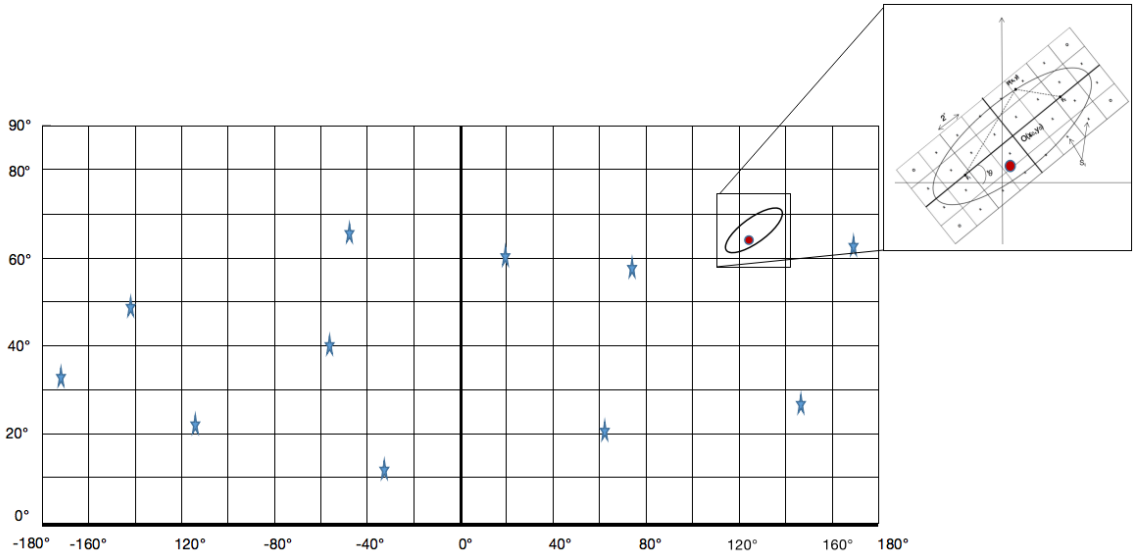

Figure 2 Representation of the sky. The blue stars represent the random locations of the telescopes before the alert, and the red dot inside the ellipse represents the astronomical event that the network of telescopes must find.

properly into small areas to be scanned by the network, and where each telescope is directed to a specific area using the BB method.

The work steps are summarized in the following:

- Divide the error region into squares suitable for TAROT's FoV.
- Find the coordinates of the two ellipse foci.
- Find the coordinates of the centers of the squares.
- Find the points inside the ellipse.
- Create a matrix whose components are the distance between the initial points of the telescopes and the points to be surveyed.
- Observation condition test (did the telescope detect the event).

After finding the final matrix and applying the BB optimization method, each telescope has its destination (coordinates where it goes to). If the event is not observed in these locations, the telescopes are redirected to new locations. Thus, they are redirected until the signal from the astronomical phenomenon is observed.

Let us now explain the previous points in detail.

5.2.1 Division of the error ellipse

To simulate the RAMSES project, the first thing we do is to work on the sky position error ellipse that we receive in the form of an urgent alert from one of the observatories that track astronomical events continuously and that are collaborating with the National Aures Observatory. This alert comes with basic parameters about the astronomical event, through which, we can plot an error ellipse to be scanned by telescopes. These parameters are the coordinates of the ellipse's center (x_0, y_0), the lengths a and b, the angle θ.

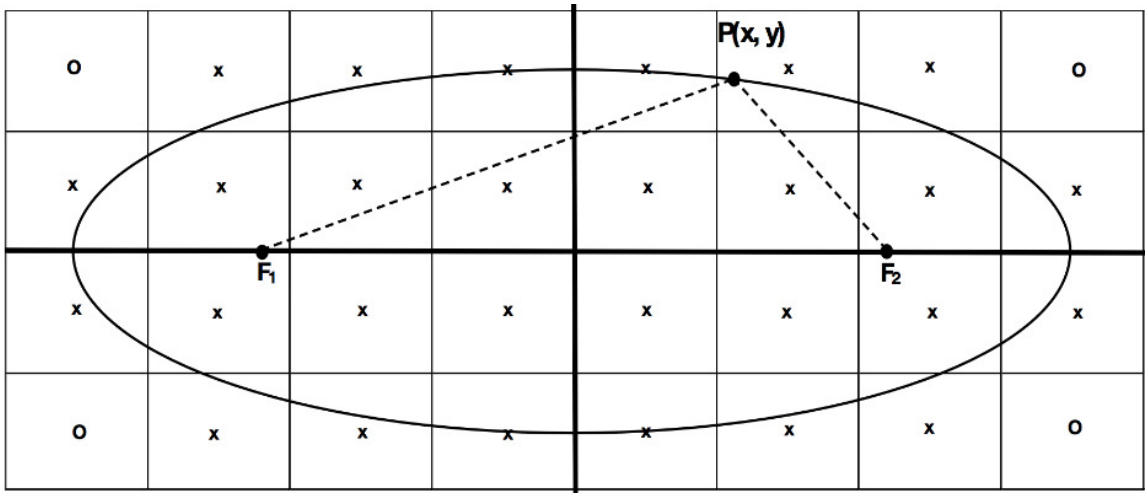

Figure 3 Method for dividing the rectangle surrounding the error ellipse. Each small square has a side length of 2 degrees. Telescopes must scan all squares inside or intersect with the ellipse.

Then we will divide this area into P small parts of a size that fits the TAROT's FoV. In our case we divide it into squares of 2° (two degrees) side length. This is done by drawing a rectangle surrounding the ellipse and dividing it into squares with a side length of 2° as shown in Figure 3. Note that the length and width of the rectangle must be a multiple of 2 so that the number of small squares is an integer.

5.2.2 Find the coordinates of the two foci and rectangular dimensions

Find the coordinates of the two foci The general equation of the ellipse (the parametric equation):

$$\begin{cases} x(t) = x_0 + a\cos\theta\cos t - b\sin\theta\sin t \\ y(t) = y_0 + a\sin\theta\cos t + b\cos\theta\sin t \end{cases} \tag{1}$$

where t is the parameter, $t\epsilon\,[0, 2\pi]$ radians, $O(x_0, y_0)$ is the ellipse's center coordinates, a and b are the semi-major and semi-minor axes respectively $(0 < b < a)$ and θ is the rotation angle, see Figure 4.

Now that the parameters a and b are known to us, finding c, which is the distance of the two foci from the center of the ellipse, is easy $(c^2 = a^2 - b^2)$, and from it, we can deduce the coordinates of the two foci F_1 and F_2:

$$F_1(x_0 - c, y_0)$$

$$F_2(x_0 + c, y_0)$$

We can, then, deduce the general relationship of the coordinates of the two foci after a rotation with an angle θ, by applying the rotation matrix $R = \begin{pmatrix} \cos\theta & -\sin\theta \\ \sin\theta & \cos\theta \end{pmatrix}$,

Thus, the foci coordinates in the general case are:

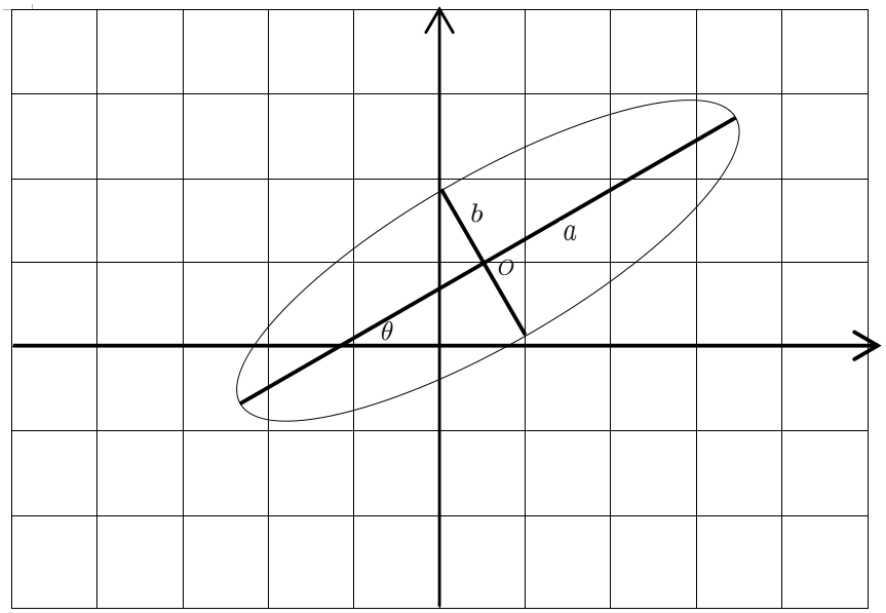

Figure 4 A representation of an ellipse in the general case, semi-major axis a and semi-minor axis b, and angle of rotation θ are shown.

$$F_1((x_0 - c)\cos\theta - y_0 \sin\theta, (x_0 - c)\sin\theta + \cos\theta)$$

$$F_2((x_0 + c)\cos\theta - y_0 \sin\theta, (x_0 + c)\sin\theta + y_0 \cos\theta)$$

Length and width of the rectangle As we divide the rectangle surrounding the error ellipse into P squares of side lengths 2°, both length and width of the rectangle must be multiple of 2 and greater than $2a$ and $2b$, respectively.

This means that the length of the rectangle is $2{*}2\lceil a/2\rceil$ and its width is $2{*}2\lceil b/2\rceil$. Here $\lceil x\rceil$ is the ceiling function that maps x to the least integer greater than or equal to x.

5.2.3 Small squares center coordinates

After the above, we find the coordinates of the centers of the squares (see Figure 5):

$$s_{ij}(x_0 - 2\lceil a/2\rceil + 2j + 1\ , y_0 + 2\lceil b/2\rceil - 2i - 1)$$

i and j are integer numbers, with $i\epsilon[0, 2\lceil b/2\rceil - 1]$ and $j\epsilon[0, 2\lceil a/2\rceil - 1]$.

To generalize s_{ij} coordinates, we apply the rotation matrix R

$$R.s_{ij} = S_{ij} = \begin{pmatrix}(x_0 - 2\lceil a/2\rceil + 2j + 1)\cos\theta - (y_0 + 2\lceil b/2\rceil - 2i - 1)\sin\theta \\ (x_0 - 2\lceil a/2\rceil + 2j + 1)\sin\theta + (y_0 + 2\lceil b/2\rceil - 2i - 1)\cos\theta\end{pmatrix}$$

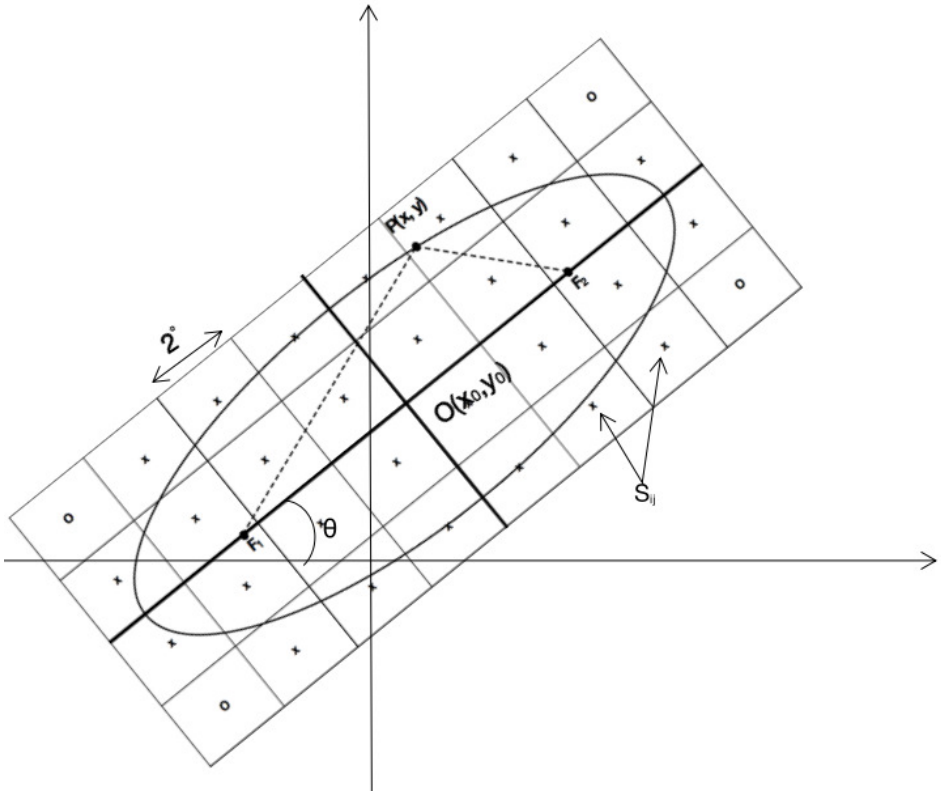

Figure 5 The general case of dividing an ellipse inside a rectangle into small squares, after a translation and a rotation by an angle θ.

5.2.4 Finding points inside the ellipse

All the area that telescopes have to scan must be inside the ellipse. This means that all points P_{ij} inside the ellipse verify the relation:

$$\|F_1P_{ij}\| + \|F_2P_{ij}\| \leq 2a$$

where $\|AB\|$ represents the distance between A and B, a is the semi-major axis.

The first and second scan priority Telescopes should scan the space inside the ellipse, but since some small squares have a portion of them outside the ellipse, it would be a good idea to leave scanning them until after the squares inside the ellipse are examined.

So we have two scan priorities:

- The first priority is all squares whose center is inside the ellipse, see Figure 6a.
- The second priority is all squares whose center is outside the ellipse and has a small contribution to the error ellipse, see Figure 6b.

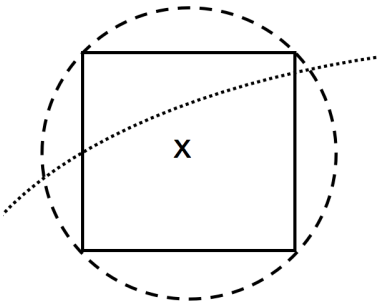

(a) The first scan priority.

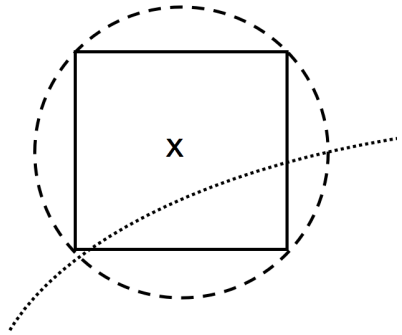

(b) The second scan priority.

Figure 6 (a) The first priority for scanning is given to every small square whose center is inside the ellipse, whether the square is entirely inside the ellipse or most of it is inside and part of it is outside. (b) The second priority of scanning is given to every small square whose center is outside the ellipse because most of it is outside the ellipse and the probability of the event occurring in the intersection is small.

5.2.5 The cost matrix for branch and bound method

After we finished prioritizing surveys of telescopes and finding the coordinates of the small squares positions delimiting the error ellipse, we use the branch and bound method discussed in Section 5.1 to minimize the time needed to scan all these positions.

For that, we define a matrix $M$of dimensions $P \times N$, whose elements contain the time taken for each telescope T_i to reach its target position P_j. Then, we divide this matrix into several $N \times N$ small matrices M_i to apply the BB method to it.

$$M = \begin{pmatrix} M_1 \\ M_2 \\ . \\ . \\ . \\ M_i \end{pmatrix}$$

The BB method is applied to small matrices in order (because they are arranged in order of priority), each array simulating the process of pointing telescopes to scan

specific small areas within the error ellipse. We should emphasize here that we are applying the BB method to optimize the time required for all telescopes to reach their positions as quickly as possible.

5.2.6 Observation condition test

After assigning each telescope to survey a specific area, the telescope is considered to have observed the astronomical event if the distance between the point representing the astronomical event (x_G, y_G) and the location to which the telescope was directed to is less than or equal to $\sqrt{2}$, see Figure 7.

For real telescopes, it takes time to process the image to verify the presence of the source or not. For the National Aures Observatory the image processing time will be less than 10 seconds (Seghouani et al. 2019), and we should take it into account in our simulation.

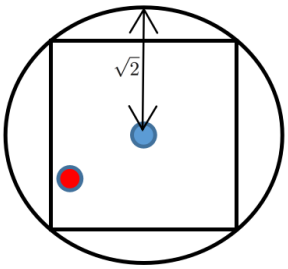

Figure 7 In the simulation process, to observe the event, the distance between the center of the square (represented in blue) and the point representing the event (x_G, y_G) (represented in red) must be less than $\sqrt{2}$. That is, the event position should be within the circle of FoV.

If the event is not observed after the first pointing of the telescopes, the telescopes are re-pointed with a new matrix whose values are the time taken by the telescope T_i to reach the new position P_j. This process is repeated until the astronomical event is observed and the observing telescope is known (Figure 8).

By knowing the distance D from the starting point to the target point of each telescope and by knowing the speed of rotation v and acceleration a of the telescopes, see Table 2, we can calculate the time it takes for each telescope to move from one position to another. By knowing also the number of orientation times O needed, we can estimate the total time t from starting the survey to observing the event.

$$t = \sum_{i=1}^{O} \left\{ \left(\sqrt{\frac{D_i}{a}} \right) \Theta(2x_0\text{-D}) + \left(\sqrt{\frac{2x_0}{a}} + \frac{D_i - 2x_0}{\text{v}} \right) \Theta(\text{D-}2x_0) - \left(\sqrt{\frac{D_i}{a}} \right) \delta(2x_0\text{-}D_i) \right\} \tag{2}$$

where x_0 is the distance traveled by the telescope before reaching its maximum speed, Θ is the Heaviside step function, and δ is Kronecker delta function[7].

[7] $\delta(2x_0 - D_i) = \begin{cases} 1 & \text{if } 2x_0 = D_i \\ 0 & \text{if } 2x_0 \neq D_i \end{cases}$

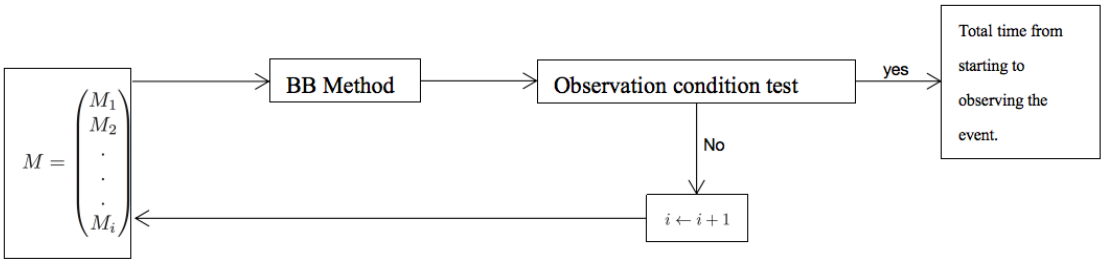

Figure 8 A diagram showing how the simulation works. From dividing the matrix M, then applying the BB method and finally finding the total time from starting the search to observing the event.

Table 2 The table shows the main characteristics of the National Aures Observatory used in the simulation.

Characteristic	Telescope array
Number of telescopes	6 to 12
Axes maximum speed	$80^\circ/s$
Axes maximum acceleration	$120^\circ/s^2$
Images processing time	10 seconds
Field of view	$2.5^\circ \times 2.5^\circ$

After completing the method and finding the time required for the set of N telescopes to observe the event, we repeat this simulation process 10,000 times to make a comprehensive statistical study.

Note that for this work we change the number of telescopes used ($N = 6$, $N = 7$, $N = 8$, $N = 9$, $N = 10$, $N = 11$, $N = 12$), in order to study the effect of the number of telescopes on the time required for observation and change the area of the error ellipse to be scanned from 30 to 140°^2} for studying the effect of the area to be surveyed on the number of telescopes needed. Our results are shown in the next section.

6 Results and discussion

In this research, which is a simulation of the future RAMSES project (Seghouani et al. 2019), we used the branch and bound optimization method to: i) improve the time required for the network of telescopes to find the source signal of the astronomical phenomenon, taking into account the number of telescopes used, ii) study the efficiency of telescopes every time they are redirected, and iii) study the effect of the area to be surveyed on the number of telescopes needed.

We obtained the results after writing an integrated simulation program based on the characteristics we have about this robotic network (speed, acceleration, field of view, image processing time,...) and the astrophysical phenomena it studies, taken from (Seghouani et al. 2019). These results indicate the following:

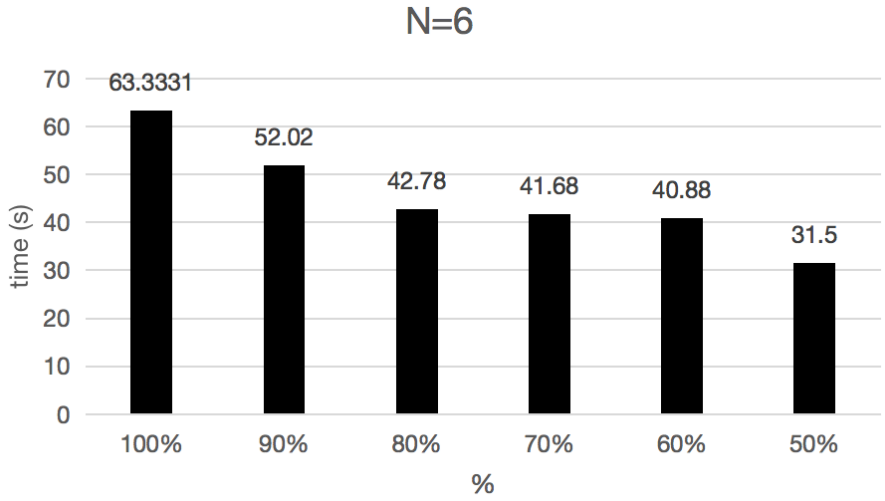

Figure 9 The histogram represents the time required for 6 telescopes to observe the event. Each column represents the time required for the best cases to observe the event.

i) The effect of the number of telescopes used on the time required to observe the event. For $N = 6$, see Figure 9, results show that we can observe the signal source 63.33 seconds after the alert, using only 6 telescopes. This means that we can use half of the RAMSES network to get results in about a minute, which is presented as a challenge in (Seghouani et al. 2019), and that with 100% reliability (meaning that all of the 10,000 simulations took 63.33 seconds or less to detect the signal).

But if we talk about the best 80% of cases**,** these six telescopes were able to pick up the signal 42.78 seconds after the alert. And 50% of the cases were able to pick up the signal in about half a minute, 31.5 seconds. This indicates the great efficiency of the method of improving the time taken to pick up the signal, even if we use only half the number of available telescopes.

All of the obtained data (from $N = 6$ to $N = 12$) are shown in the histograms of Appendix A1.

ii) The efficiency of telescopes every time they are redirected. Now from another point of view, which is the efficiency of telescopes every time they are redirected, we note that the number of orientations does not exceed 6 times even if only 6 telescopes are used.

First pointing: represented in blue in Figure 10. For the first pointing, where telescopes from their random location are directed into a small target area within the error ellipse to track the event, 42.04% of the cases were able to catch the signal when we used 12 telescopes, while when using 11 telescopes 39.43% of the cases were able to detect the event immediately after this first positioning. For the use of 10 telescopes, 30.76% of the cases were able to complete successfully the monitoring task in the first step. Finally, as expected, this percentage will decrease as the number of telescopes decreases until it reaches 16.82% when using only 6 telescopes.

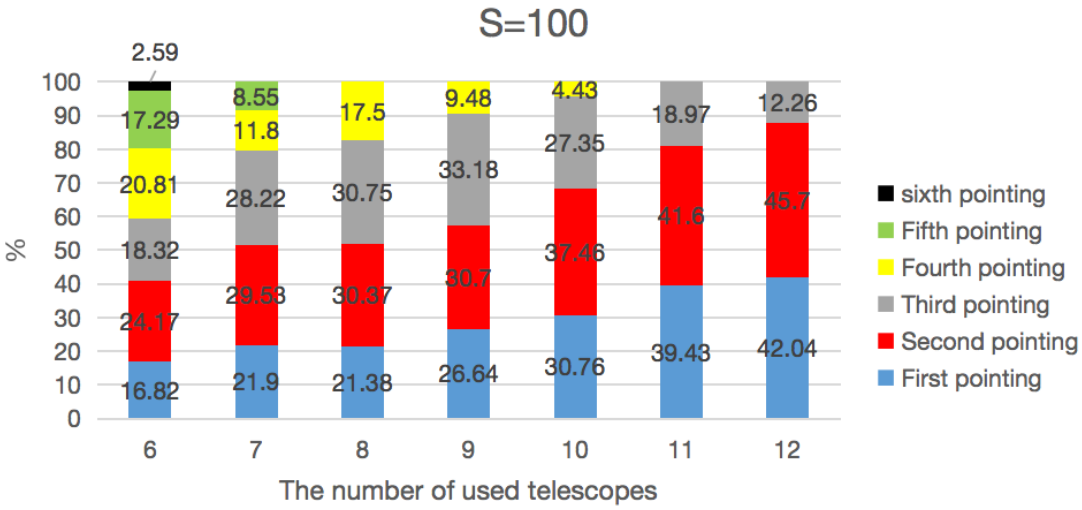

Figure 10 The efficiency of telescopes every time they are redirected for scanning an error ellipse of 100°^2}, each color represents a transition from one position to the next.

iii) The effect of the area to be surveyed on the number of telescopes needed The areas to be surveyed by the RAMSES project could be relatively small ones as those that usually come from urgent alerts sent by gamma-ray tracking satellites such as "Swift" (the area of error could be about 30 square degrees) (Abbott et al. 2017). or relatively large areas, as those sent by gravitational wave observatories (error area within 100 square degrees and more).

To study the effect of the area to be surveyed on the number of telescopes needed, we change the area S to be scanned from 30 to 140°^2}, and, for each fixed value of S, we study the effectiveness of telescopes from $N = 6$ to $N = 12$. The results are as follows:

For S=30: In the case of studying small areas, a group of telescopes may be enough to cover the entire area, so the event will be observed immediately after directing the telescopes, see Figure 11. In the case of an area of 30 square degrees, 9 telescopes are enough to observe the event directly after the first orientation. In the same conditions, 8 telescopes are enough to observe the event, with a rate of 89.4%. While 6 telescopes can observe the event in their first pointing with a percentage of 61.8%, and they need a second pointing to achieve their task in all cases.

For S=110: As seen previously, the area of error ellipse that comes from GW observatories such as LIGO and Virgo is large compared to the error ellipses sent by satellites that monitor the optical part associated with gravitational waves such as Swift, In the case of $S = 110^{\circ^2}$, see Figure 12, a network of 12 telescopes can observe the event in all cases after three steps. The event was detected after a first pointing in 40.3% of cases, while the second pointing allows a detection in 35.5% of cases. A network of 10 telescopes needs 4 successive orientations of the telescopes, whereas a network of 6 telescopes needs 6 successive orientations to complete successfully the observation in all cases.

All of the obtained data (from S=30 to S=140) are shown in the histograms of Appendix A2.

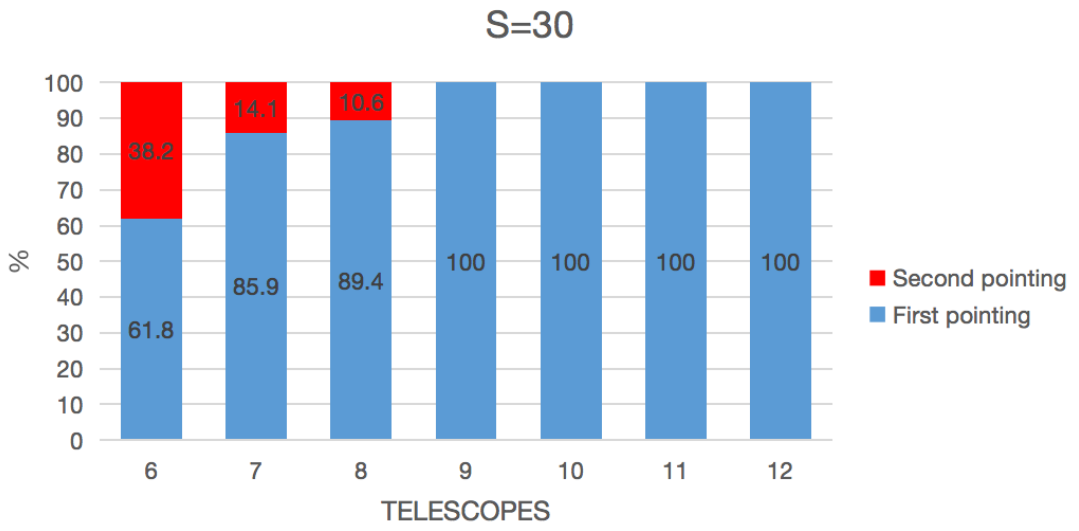

Figure 11 The histogram represents the effect of the number of telescopes used on the number of re-pointing needed to observe the event in an error ellipse of 30°^2}. The blue color represents the first direction to the error area, the red color represents the second direction.

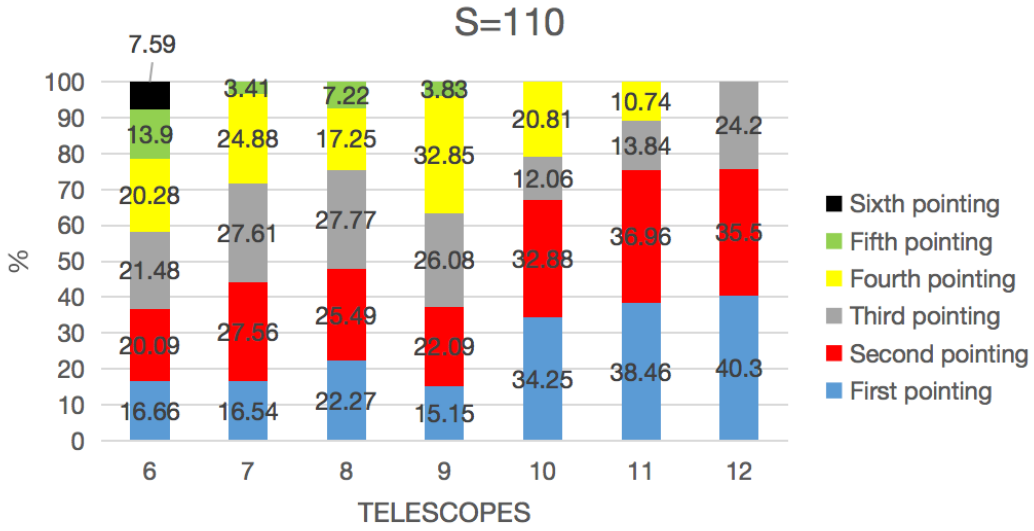

Figure 12 The histogram represents the effect of the number of telescopes used on the number of re-pointing needed to observe the event in an error ellipse of 110°^2}.

Number of telescopes needed for an observation after knowing the area to be surveyed Through the results we obtained, which are shown in Appendix A2, we will set the number of telescopes needed for each area to be successfully scanned in less than 40 seconds. The results about 100% chance of detection are shown in Table 3, and for 80% chance of detection, they are shown in Table 4.

Table 3 The number of telescopes needed to scan the error ellipse and monitor successfully the event in a period not exceeding 40 seconds with a 100% chance of detection.

Areas S to be scanned, in square degrees	Number of telescopes needed
Less than or equal to 70	6
$70 < S \leq 90$	7
$90 < S \leq 100$	8
$100 < S \leq 120$	9
$120 < S \leq 130$	11
$130 < S \leq 140$	12

Table 4 The number of telescopes needed to scan the error ellipse and monitor successfully the event in a period not exceeding 40 seconds with an 80% chance of detection.

Areas S to be scanned, in square degrees	Number of telescopes needed
Less than or equal to 110	6
$110 < S \leq 130$	7
$130 < S \leq 140$	8

7 Conclusion

In conclusion, this study revolves around the use of optimization methods to reduce the time required to scan sky position error ellipses of astronomical events that will be sent by multi-messenger surveyors, like gamma-ray tracking satellites or gravitational wave observatories, by a TAROT-type telescopes network.

The importance of this study is that it simulates a network of telescopes under construction, through which we can exploit it optimally, by finding ways to improve the time taken to observe an astronomical event (the least possible), and reduce the number of used telescopes sufficient to monitor the astronomical event in the shortest possible time after the alert.

Additionally we studied the effect of the number of telescopes on the speed of observation, and the effectiveness of telescopes in finding the source, every time they are redirected, is analysed. Moreover we saw that by using half of the National Aures Observatory network, we can monitor successfully the astronomical event in one minute, while the time required for 12 telescopes to discover the source does not exceed half a minute. Furthermore, a network of 12 telescopes can pick up the source signal from the first positioning step in 42% of cases.

By investigating the effect of the area to be surveyed on the number of telescopes needed, we were able to propose a statistical method through which we can know the number of telescopes to be dedicated in order to monitor successfully the event in a specific area, which guarantees an optimal use of the observatory.

Moreover, the fastest reaction to an alert coming from a Swift is in the range of 140 s, while the typical time for nighttime bursts is in the range of 200–300 s (Greiner et al. 2011), while we were able to reduce this time to just 40 seconds using this network of telescopes.

Therefore, these are important findings, especially for studying the prompt emission and early afterglow of gamma-ray bursts associated with gravitational waves, and we can easily generalize this study to include any other network of telescopes whose main features are known such as speed, acceleration and field of view.

References

Aasi, J.; Abbott, B.P.; Abbott, R.; et al. (2015). Advanced ligo. CQGra, 32(7): 074001.

Abbott, B.P.; Abbott, R.; Abbott, T.D.; et al. (2016). Observation of gravitational waves from a binary black hole merger. PhRvL, 116(6):061102.

Abbott, B.P.; Abbott, R.; Abbott, T.D.; et al. (2017). Multi-messenger observations of a binary neutron star merger. ApJ, 848(2):L12.

Allen, C. W. (1954). Whole-sky statistics of celestial objects. MNRAS, 114(4), 387-405.

Azmoodeh, M. (1990). Abstract data types and algorithms. Springer.

Beckman, J.E. (2021). Multimessenger astronomy. ISBN: 978-3-030-68372-6. Cham: Springer International Publishing.

Berger, E. (2014). Short-duration gamma-ray bursts. ARA&A, 52:43–105.

Boër, M.; Klotz, A.; Atteia, J.L. ; et al. (2003). The gamma-ray burst hunt at la silla the tarot-s very fast moving telescope. Msngr, 113:45–48.

Boër, M.; Klotz, A.; Laugier, R.; et al. (2017). Tarot: a network for space surveillance and tracking operations. In 7th European Conference on Space Debris ESA/ESOC, Darmstadt/Germany.

Branchesi, M. (2016). Multi-messenger astronomy: gravitational waves, neutrinos, photons, and cosmic rays. In Journal of Physics: Conference Series, volume 718, page 022004. IOP Publishing.

Camp, J.; Barthelmy, S.; Blackburn, L.; et al. (2013). Using iss telescopes for electromagnetic follow-up of gravitational wave detections of ns-ns and ns-bh mergers. ExA, 36(3):505–522.

Ciardullo, R.; Ford, H. C.; Williams, R. E.; et al. (1990). The nova rate in the elliptical component of NGC 5128. AJ, 99, 1079-1087.

Coulter, D.A.; Foley, R.J.; Kilpatrick, C.D.; et al. (2017). Swope supernova survey 2017a (sss17a), the optical counterpart to a gravitational wave source. Sci, 358(6370):1556–1558.

Daigne, F.; Mochkovitch, R. (2002). The expected thermal precursors of gamma-ray bursts in the internal shock model. MNRAS, 336(4):1271–1280.

Della Valle, M.; Bianchini, A.; Livio, M.;et al. (1992). On the possible existence of two classes of progenitors for classical novae. A&A, 266, 232-236.

Della Valle; M.; Livio, M. (1994). On the nova rate in the Galaxy. A&A, 286, 786-788.

Della Valle, M.; Izzo, L. (2020). Observations of galactic and extragalactic novae. A&ARV, 28(1), 1-118.

Einstein, A.; et al. (1905). On the electrodynamics of moving bodies. AnP, 17(10): 891–921.

Feindt, U.; Nordin, J.; Rigault, M.; et al. (2019). simsurvey: estimating transient discovery rates for the Zwicky transient facility. JCAP, 2019(10), 005.

Frey, V. (2018). Recherche de signaux d'ondes gravitationnelles transitoires de longue durée avec les données des détecteurs advanced Virgo et advanced LIGO. PhD thesis, Université Paris-Saclay.

Fryer, C.L.; Holz, D.E.; Hughes, S.A. (2002). Gravitational wave emission from core collapse of massive stars. ApJ, 565(1):430.

Greiner, J.; Krühler, T.; Klose, S.; et al. (2011). The nature of "dark" gamma-ray bursts. A&A, 526, A30.

Hartman, J.M.; Galloway, D.K.; Chakrabarty, D. (2010). A double outburst from igrj00291+ 5934: implications for accretion disk instability theory. ApJ, 726(1):26.

Hatano, K.; Branch, D.; Fisher, A.; et al. (1997). On the spatial distribution and occurrence rate of Galactic classical novae. MNRAS, 290(1), 113-118.

Klotz, A.; Boër, M.; Atteia, J. L.; et al. (2009). Early optical observations of gamma-ray bursts by the tarot telescopes: Period 2001-2008. ApJ, 137(5):4100.

Kopylov, I. M. (1955). Comparison of morphological properties and spatial distribution of novae and supernovae. BCrAO, 15, 140-146.

Kouveliotou, C.; Meegan, C.A.; Fishman, G.J.; et al. (1993). Identification of two classes of gamma-ray bursts. ApJ, 413:L101–L104.

Kumar, P.; Zhang, B. (2015). The physics of gamma-ray bursts & relativistic jets. PhR, 561:1–109.

Levitin, A. (2003). Introduction to the design and analysis of algorithms addison-wesley. Boston, MA.

Lorentz, H. A. (1899). Considerations on gravitation. KNAB, 2:559–574.

Meszaros, P. (2006). Gamma-ray bursts. RPPh, 69(8):2259.

Pe'er, A. (2015). Physics of gamma-ray bursts prompt emission. AdAst, 2015.

Liller, W.; Mayer, B. (1987). The rate of nova production in the galaxy. PASP, 99(617), 606.

Pirani, F.A.E. (1956). On the physical significance of the riemann tensor. AcPP, 15:389–405.

Piro, A.L.; Giacomazzo, B.; Perna, R. (2017). The fate of neutron star binary mergers. ApJ, 844(2):L19.

Poincaré, H. (1905). La dynamique de l'électron par Henri Poincaré (The dynamics of the electron by Henri Poincaré).

Rollins, J. G. (2011). Multimessenger astronomy with low-latency searches for transient gravitational waves. Columbia University.

Ryde, F.; Borgonovo, L.; Larsson, S.; et al. (2003). Gamma-ray bursts observed by the integral-spi anticoincidence shield: A study of individual pulses and temporal variability. A&A, 411(1):L331–L342.

Seghouani, N. (2010). Un Observatoire dans la région des Aurès. AfrSK, 14:44.

Seghouani, N.; Boër, M.; Mimouni, J. (2019). National aures observatory: A new multimessenger facility. JPhCo, 1269(012001). IOP Publishing.

Shafter, A. W. (1997). On the nova rate in the galaxy. ApJ, 487(1), 226.

Shafter, A. W.; Ciardullo, R.; Pritchet, C. J. (2000). Novae in external galaxies: M51, M87, and M101. ApJ, 530(1), 193.

Sharov, A. S. (1972). Estimate for the Frequency of Novae in the Andromeda Nebula and our Galaxy. SvA, 16, 41.

Van Den Bergh, S. (1991). Supernova rates: A progress report. PhR, 204(6), 385-400.

Wang, M.; Chen, S.; Jing, J. (2021). Effect of gravitational wave on shadow of a schwarzschild black hole. EPJC, 81(6):1–13.
Wen, L.; Chen, Y. (2010). Geometrical expression for the angular resolution of a network of gravitational-wave detectors. PhRvD, 81(8):082001.

Appendix A1

Here we show our results about the effect of the number of telescopes used ($N = 6$ to $N = 12$) on the time required to observe the event. Each column in the histograms represents the time required for the best cases to observe the event.

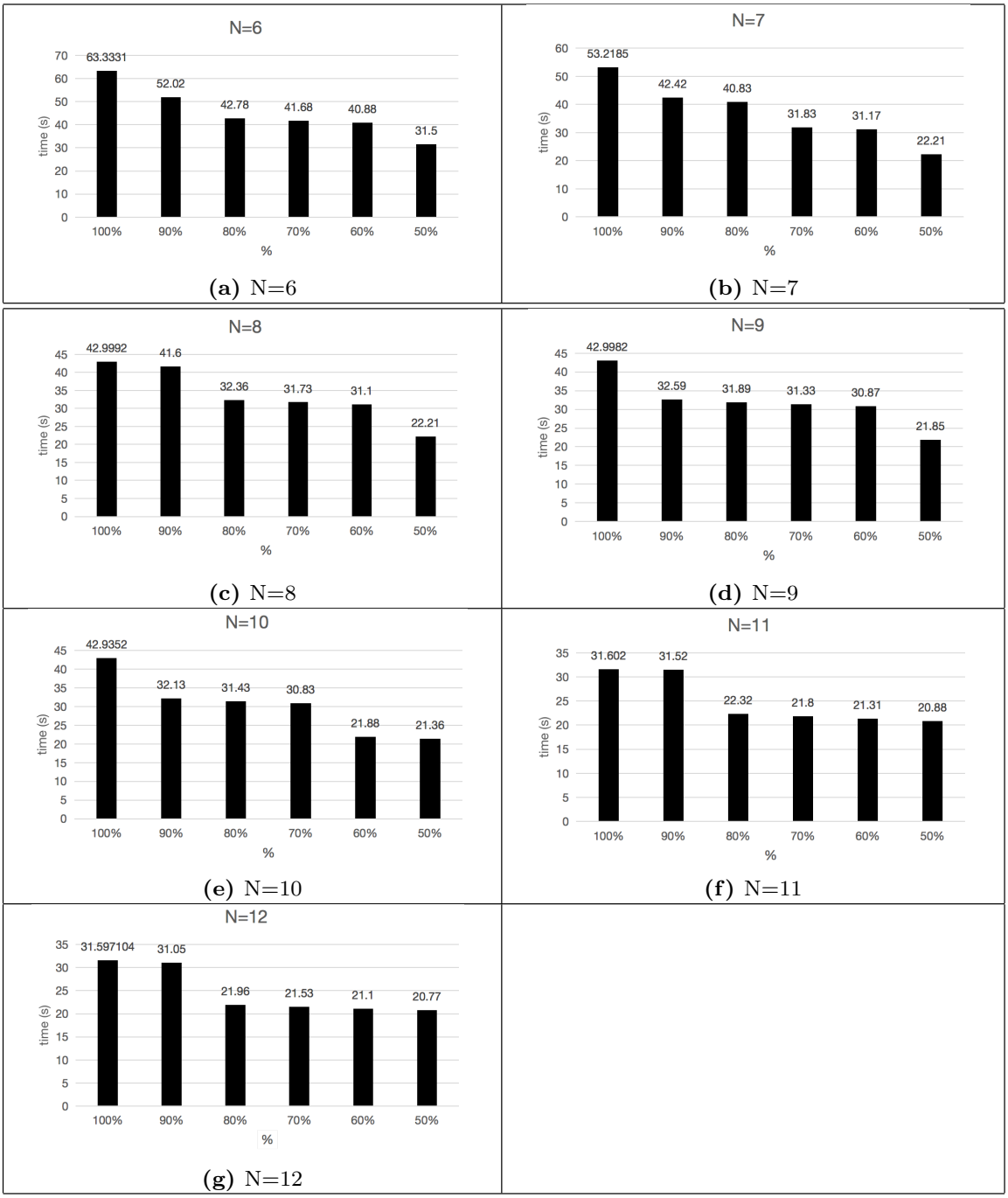

(a) N=6 **(b)** N=7 **(c)** N=8 **(d)** N=9 **(e)** N=10 **(f)** N=11 **(g)** N=12

Appendix A2

Here we show our results about the study of the number of telescopes needed for an observation after knowing the area to be surveyed. The area to be scanned by the telescopes is varying from 30 to 140. Every time we change the number of used telescopes (from 6 to 12), we repeat the simulation 10,000 times. Each color represents the probability of detecting the event, for example, the blue color represents the probability of detecting the event immediately after the first pointing, the red color represents the same probability after the second pointing, ... etc.

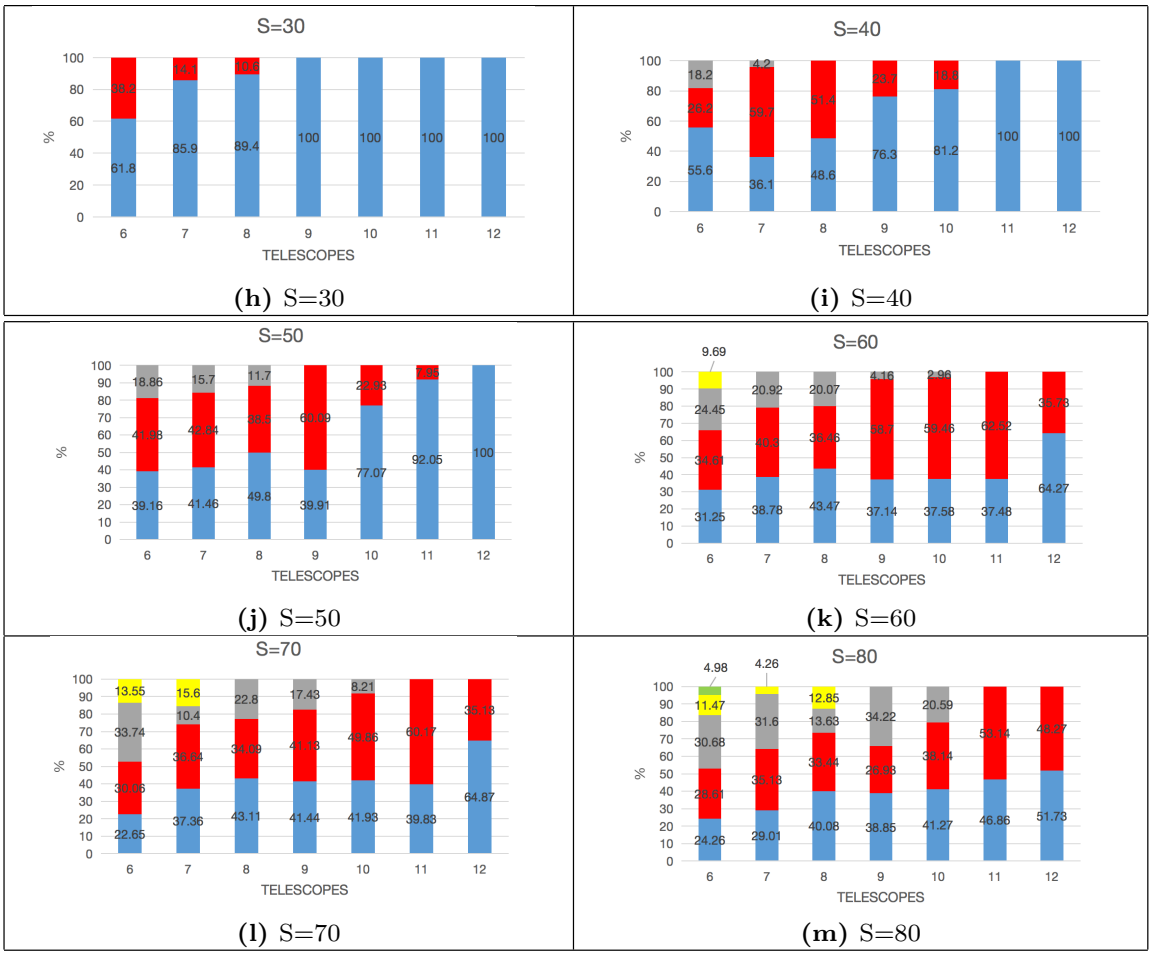

(h) S=30 **(i)** S=40

(j) S=50 **(k)** S=60

(l) S=70 **(m)** S=80

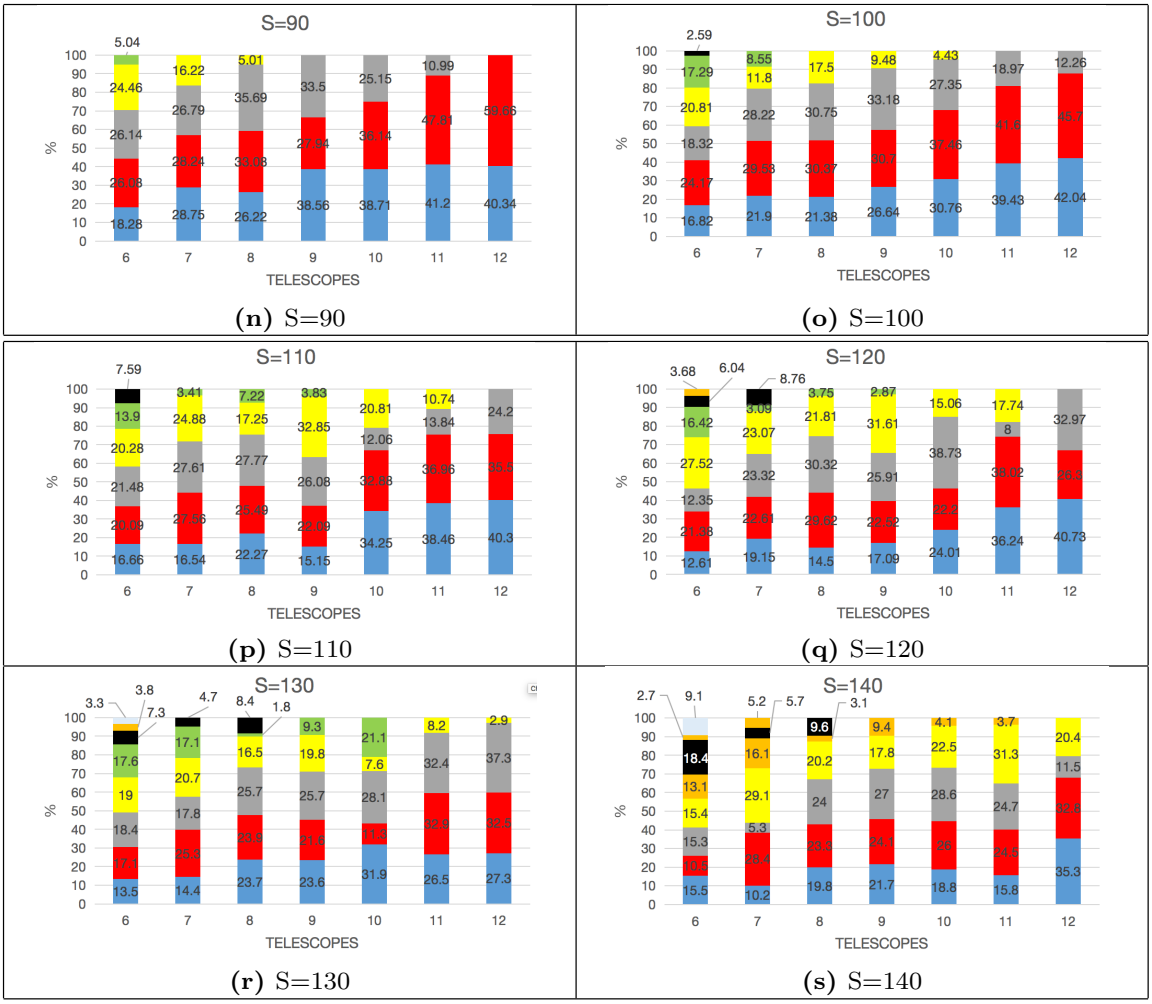

(n) S=90 **(o)** S=100

(p) S=110 **(q)** S=120

(r) S=130 **(s)** S=140

Abstract:

This thesis provides a comprehensive overview of the field of gravitational waves and multi-messenger astrophysics, with an emphasis on optimizing telescope networks for detecting transient events. The history of gravitational wave research, sources of gravitational waves, and observatories used to detect them, such as LIGO and Virgo, are discussed. Multi-messenger astrophysics is introduced as a means to combine observations from different messengers to gain a more complete understanding of astrophysical phenomena. The National Aures Observatory and its RAMSES project are presented as an example of a telescope network aimed at detecting and localizing transient events. An assignment problem solution is introduced using the branch and bound method to optimize the observatory's telescope network. Finally, simulations exploring the efficiency of telescopes, the effect of the area surveyed on the number of telescopes required, and a strategy for determining the number of telescopes needed for observation are discussed.

Key-words multi-messenger, gravitational waves, Gamma Ray Bursts, RAMSES Project, National Aures Observatory, Branch and bound Method, TAROT Telescope.

Résumé

Cette thèse offre une vue d'ensemble complète du domaine des ondes gravitationnelles et de l'astrophysique multi-messagers, avec un accent sur l'optimisation des réseaux de télescopes pour la détection d'événements transitoires. L'histoire de la recherche sur les ondes gravitationnelles, les sources d'ondes gravitationnelles et les observatoires utilisés pour les détecter, tels que LIGO et Virgo, sont discutés. L'astrophysique multi-messagers est présentée comme un moyen de combiner les observations de différents messagers pour mieux comprendre les phénomènes astrophysiques. L'Observatoire National des Aurès et son projet RAMSES sont présentés comme exemple de réseau de télescopes visant à détecter et à localiser des événements transitoires. Une solution de problème d'assignation est introduite en utilisant la méthode de branchement et de bornes pour optimiser le réseau de télescopes de l'observatoire. Enfin, des simulations explorant l'efficacité des télescopes, l'effet de la zone analysée sur le nombre de télescopes requis, et une stratégie pour déterminer le nombre de télescopes nécessaires pour l'observation sont discutées.

Mots-clés multi-messager , ondes gravitationnelles, Sursauts Gamma, Projet RAMSES, Observatoire National des Aurès, Méthode Branch and Bound, Télescope TAROT.

ملخص:

يقدم هذا البحث مرجعا شاملا عن مجال الموجات الثقالية وعلم الفلك متعدد الرسل، مع التركيز على تحسين شبكات التلسكوبات لاكتشاف الأحداث العابرة. يناقش تاريخ أبحاث الموجات الثقالية، ومصادر الموجات الثقالية، والمراصد المستخدمة لاكتشافها مثل LIGO وVIRGO. يقدم علم الفلك متعدد الرسل كوسيلة لدمج الملاحظات من رسل مختلفة للحصول على فهم أكثر اكتمالا للظواهر الفلكية. يتم عرض مرصد الأوراس الوطني ومشروع RAMSES باعتبارهما مثالا على شبكة تلسكوبات تهدف إلى اكتشاف وتحديد مواقع الأحداث العابرة. يتم تقديم حل مشكلة التعيين باستخدام طريقة الفرع والحد لتحسين شبكة التلسكوبات في المرصد. أخيرا، تتم مناقشة المحاكاة استكشاف كفاءة التلسكوبات، وتأثير المنطقة الممسوحة على عدد التلسكوبات المطلوبة، واستراتيجية لتحديد عدد التلسكوبات اللازمة للمراقبة.

الكلمات المفتاحية: متعدد الرسل، الموجات الثقالية، انفجارات أشعة جاما، مشروع RAMSES، مرصد الأوراس الوطني، طريقة الفرع والحد، تلسكوبTAROT.